Klamath River
Bioenergetics Report

Prepared For:
PacifiCorp

Photo by: Rick Kruger, Oregon Department of Fish and Wildlife

Prepared by:
R. Craig Addley
Bill Bradford
Jennifer Ludlow

Institute for Natural Systems Engineering
Utah Water Research Lab, Utah State University
Logan, Utah 84321
August 2005

Acknowledgements

We are particularly grateful to PacifiCorp contractors that were extremely responsive to our data needs and questions. Mark Allen from TRPA, Inc. was especially helpful with regard to the empirical fish collections. Tom Gast from TRPA, Inc. helped us with the PHABSIM hydraulic data and sent us a copy of the RHABSIM program. Ken Carlson at CH2MHILL was helpful in providing invertebrate and temperature data. Forrest Olson provided the size-at-age data and was prompt in replying to our queries. Linda Prendergast and Todd Olson were patient with dealing with USU contracting and were patient with the extended time it took for us to do additionally analyses (e.g., reworking the From and Rasmussen 1984 data) and complete this report. It allowed us to produce a better product. John Hayes (Cawthron Institute, New Zealand) and Nicholas Hughes (University of Alaska Fairbanks) provided valuable initial input into this project. Their work schedules and the schedule of this work were mutually exclusive, but their previous work and ideas are scattered throughout this document.

Table of Contents

List of Tables

List of Figures

Executive Summary

Utah State University conducted an analysis of rainbow/redband trout (*Oncorhynchus mykiss*) bioenergetics to assist PacifiCorp in addressing potential flow and flow fluctuation effects on fish related to PacifiCorp's Klamath Hydroelectric Project operations in the J.C. Boyle bypass and peaking reaches. The primary objectives of the analyses were:

1. Use a bioenergetics foraging model in combination with empirical data to assess the importance of considering trout "feeding stations" (i.e., velocity fields adjacent to fish focal locations) in estimates of habitat at various instream flows.
2. Assess bioenergetics and trout growth over a range of flow, food, and temperature conditions in these reaches, and predict how trout growth under Existing Conditions (with peaking operations) in the J.C. Boyle peaking reach may differ from conditions under hypothetical Without Project (assuming no hydroelectric facilities or operations) and Steady Flow (assuming hydroelectric facilities and operations, but no peaking) scenarios.

To address the first objective of the analysis, a basic trout bioenergetics foraging model was used (based on the model concepts and applications of Addley 1993, Guensch et al. 2001, Hughes and Dill 1990, and Hughes et al. 2003). The principal bioenergetics metric from the model used to address this objective was the amount of daily net energy intake (DNEI). This metric incorporates the constraints of maximum daily consumption and the losses associated with excretion, egestion, and metabolism (base metabolism + active metabolism + food digestion and processing costs). The maximum amount of daily food consumption and the energy losses due to egestion, excretion, base metabolism, and food digestion costs were determined from equations developed from a reanalysis of the laboratory experiments of From and Rasmussen (1984) on rainbow trout. The foraging model incorporates the effects of diel temperature fluctuation by including the fluctuating temperature versus steady temperature growth data developed by Hokanson (1977). Macroinvertebrate drift density and drift size data, temperature data, fish size, spawning frequency and reaction distance (modified for turbidity) are inputs to the model.

The bioenergetics foraging model was used in combination with empirical hydraulic and habitat data collected from 103 cross-sections in the J.C. Boyle bypass and peaking reaches (from a separate instream flow study conducted by PacifiCorp using the Physical Habitat Simulation System [PHABSIM] model) to quantify the availability of trout "feeding station" habitat. Feeding station habitats incorporate bioenergetically-favorable combinations of suitable water depths and velocities at a fish's feeding and focal location. This typically consists of low focal velocities and swifter adjacent velocities that efficiently deliver drifting food items to the fish's forage capture area.

Habitat versus flow relationships (aggregate of habitat at all cross-sections versus flow) derived from the bioenergetics foraging model "feeding station" approach were essentially the same as relationships derived by PacifiCorp using the PHABSIM approach. The spatial patterns of suitable habitat on each cross-section were also similar between the two approaches. Therefore, in regards to the first study objective, consideration of feeding stations in the instream flow habitat analysis did not alter conclusions regarding habitat-flow relationships derived from the PHABSIM model for the J.C. Boyle peaking reach.

As part of the analysis, the bioenergetics foraging model was used to conduct a sensitivity analysis of different adjacent velocity combinations at a fish's feeding and focal location. This analysis showed that fish could take bioenergetic advantage of various combinations of low velocity focal locations and higher adjacent velocities (and they do). However, based on the mean column hydraulic data from the PHABSIM cross-sections (e.g., pattern of mean column velocity across the cross-section) and the necessity in the analysis of having to assume a fixed vertical velocity profile, there was little difference between the results from the PHABSIM modeling and the bioenergetics foraging model approach that incorporates adjacent velocity. Better velocity field modeling (e.g., three-dimensional) than is currently standard (or perhaps practical) for instream flow analyses would need to be utilized to fully assess adjacent velocity issues in an instream flow analysis.

To validate the bioenergetics foraging model used in the analysis, modeled daily net energy intake (DNEI) was compared to measured velocities and depths at observed fish locations in the J.C. Boyle bypass reach collected as part of PacifiCorp's habitat suitability criteria (HSC) studies. In general, the observed fish locations matched the region of positive DNEI for each size class of fish. Univariate curves of velocity and depth values that correspond to maximum DNEI

also compare closely to univariate velocity and depth suitability criteria developed from the observed trout data collected as part of PacifiCorp's HSC studies. This general agreement lends confidence to the adjacent velocity/feeding station assessment using the bioenergetics foraging model (as described above) and to the quality of the empirical HSC developed in PacifiCorp's studies.

To address the second objective of the analysis, the bioenergetics foraging model was used along with a supplemental temperature-growth model based percent of maximum consumption (P value model) to assess food and water temperature effects on trout growth rates (over a nominal four-year period) under Existing Conditions, Steady Flow, and Without-Project (WOP) scenarios. Water temperatures used to portray the annual temperature regime for these three scenarios were obtained from PacifiCorp's temperature model results (hourly time step) for the year 2000. The bioenergetics foraging model and the P value model used both the mean daily temperatures and the diel temperature fluctuations predicted from PacifiCorp's temperature model. Food conditions assumed in the bioenergetics foraging model calculations were based on macroinvertebrate drift density data collected in the Keno reach, the J.C. Boyle bypass and peaking reaches, and in the Klamath River below Iron Gate dam. Macroinvertebrate drift densities were relatively high in all reaches, with the highest densities generally found in the Keno reach and lowest densities generally found in the J.C. Boyle bypass and peaking reaches. Food conditions assumed in the P value model were calculated from the observed growth of fish (size-at-age data) in the reaches based on PacifiCorp (2004) fisheries data.

A key metric from the P value temperature-growth model was the back-calculated annual percent of maximum consumption values (referred to as "P values"). Back-calculated P values were used to estimate the proportion of maximum food consumption required for trout to achieve the empirically-measured annual growth observed in the J.C. Boyle peaking, J.C. Boyle bypass, and Keno reaches. Back-calculated P values in all of the reaches were within the range of values reported in the literature for trout feeding and growth, and were highest in the Keno reach and lowest in J.C. Boyle bypass reach. In the Keno reach, P values were 0.75 in the first two years and then increased in the following two years (0.84 and 0.99, respectively). In the J.C. Boyle bypass reach, P values were 0.57, 0.41, 0.32 and 0.29 in years one through four, respectively. In the J.C. Boyle peaking reach P values were 0.73, 0.68, 0.54 and 0.36 in years one through four, respectively. Higher P values were calculated in each reach in years three and four if spawning was assumed to occur in these years.

The high P values in the Keno reach indicate these fish are acquiring more food than in the other reaches. The increasing P values in years three and four in the Keno reach may indicate that as these fish get larger they are switching to a more abundant and/or higher energy prey source than invertebrate drift (e.g., forage fish), and/or migrating and modifying their temperature regime (e.g., moving into J.C. Boyle reservoir or out of Keno reservoir). If food availability remains constant, as fish get larger and food requirements increase, it is expected that the P values would decline. In both the J.C. Boyle peaking and bypass reaches, P values declined each year with increasing fish size.

The reach-specific P values were used to compare the effects of food and water temperature on trout growth rates under Existing Conditions, Steady Flow, and WOP scenarios. Use of the reach-specific P values was assumed to represent a condition whereby food availability within each of the reaches would not be changed under the WOP and Steady Flow scenarios. Under this assumption, growth at the end of 4 years for rainbow trout in the J.C. Boyle peaking reach was predicted to be 307 mm (313 grams) for the WOP scenario and 258 mm (178 grams) for the Steady Flow scenario, compared to 275 mm (226 grams) under Existing Conditions. The WOP scenario growth is greater than Existing Conditions or Steady Flow because the combination of reduced diel temperature fluctuations and reduced mean daily temperature under the WOP scenario would slightly enhance summer growth conditions. The Steady Flow scenario growth is less than Existing Conditions or WOP because the increased mean temperatures under the Steady Flow scenario would slightly degrade summer growth conditions (even though peak daily temperatures are slightly reduced). The calculations indicate that the predicted change in growth is not as great if spawning is included. For example, if spawning is included, growth at the end of 4 years was predicted to be 301 mm (297 grams) for the WOP spawning scenario and 258 mm (186 grams) for the Steady Flow scenario, compared to 273 mm (228 grams) under Existing Conditions.

Alternative calculations were then performed in which the high P values back-calculated from the Keno reach fish during the first two years (P = 0.75) were used to assess trout growth in the J.C. Boyle peaking reach in the absence of peaking operations (i.e., WOP or Steady Flow scenarios). Use of these higher P values assumes that food availability (as assessed by P values) in the J.C. Boyle peaking reach might increase to levels observed in the Keno reach during the first two years of fish growth and remain at the same level as fish continue to get larger.

Predicted growth for both non-peaking scenarios (WOP and Steady Flow) increased significantly. The increase in growth was probably unrealistically high, however, because the P value from the Keno reach is likely high, in part, as a result of organic matter from Upper Klamath Lake and Keno reservoir flowing into the reach and increasing the productivity. Also the bioenergetics foraging model and available literature indicates as fish get larger their ability to obtain adequate rations on drifting invertebrates declines and the P value should not increase with increased size. This happens due to the higher energy requirements of large fish, the increased swimming cost of large fish and the increased gill raker spacing of large fish that reduces the amount of drift available for consumption (i.e., they can feed only on the larger drift prey sizes).

For example, in the J.C. Boyle peaking reach, the bioenergetics foraging model predicted that, due to the greater energy requirements of large fish, particularly in high summer temperatures, fish in the 400+ mm size range could not obtain a positive energy intake feeding at existing drift densities. This generally agrees with the empirical fish size data that shows relatively few fish collected above 400 mm in the J.C. Boyle peaking reach.

The foraging model accurately predicted Existing Conditions growth in the J.C. Boyle peaking reach using the observed invertebrate drift rates (assuming no spawning was occurring). This provided some measure of confidence in the foraging model's ability to accurately predict changes in growth in the J.C. Boyle peaking reach for different flow scenarios. The same foraging model under-predicted growth in the Keno reach in years three and four providing some additional evidence that fish in the Keno reach are switching to a different source of prey or modifying their temperature regime through migration. The foraging model, however, over-predicted observed growth in the J.C. Boyle bypass reach. It would be necessary to decrease the temperature and/or observed drift density inputs to the model to match the slow growth observed in the J.C. Boyle bypass reach.

The bioenergetics foraging model was used to assess a potential upper bound of growth in the J.C. Boyle peaking reach if both temperature and food change with the WOP and Steady Flow scenarios. Drift density was increased to either that observed in the Keno reach (0.139 prey/ft^3 in early September) or the highest of that observed at several sites (Tree of Heaven) below Iron Gate dam (0.094 prey/ft^3 in early September) (Hardy and Addley 2001). We chose to use the highest drift density site below Iron Gate because the drift density is approximately

midway between the high drift density found in the Keno reach and the average drift density observed at the nearest four sites below Iron Gate dam. For example, if a linear gradient of drift density occurred between the upper and lower river (Keno reach to below Iron Gate dam sites), this drift density would be the approximate mid point. It is probably the most reasonable "upper bound" estimate of drift density we can provide for the J.C. Boyle peaking reach WOP and Steady Flow scenarios based on the available information, because as mentioned earlier, the drift density in the Keno reach may be partially inflated due to organic material inflow from Upper Klamath Lake and Keno reservoir. Using the drift density assumption from below Iron Gate dam (Tree of Heaven), growth at the end of 4 years was predicted to be 355 mm (451 grams) for the WOP scenario and 320 mm (339 grams) for the Steady Flow scenario, compared to 274 mm (212 grams) under Existing Conditions.

The results of the bioenergetics foraging model and P value model indicate that food availability is more important than water temperature as a factor in trout growth in the J.C. Boyle peaking reach for the Existing Conditions, WOP and Steady Flow scenarios. There is relatively little difference in four-year growth predictions between Existing Conditions, Steady Flow, and WOP scenarios in the J.C. Boyle peaking reach when only changes in water temperature were incorporated into the modeling. This happened because there was only a relatively small difference in daily temperatures between the three scenarios relative to the temperature-related growth requirements of trout. The biggest effect on predicted growth came from the assumption that increased invertebrate drift/ food availability would occur under the WOP and Steady Flow scenarios. The most uncertainty exists in this parameter, however. Based on the literature, food would likely increase, but the amount is uncertain. The invertebrate drift densities observed below Iron Gate dam or in the Keno reach provide a reasonable upper bound on the increase that could occur in the J.C. Boyle peaking reach. Actual drift density for the WOP and Steady Flow scenarios may be somewhere between what they are now with Existing Conditions and this upper bound.

1 Introduction

The purpose of this report is to assist PacifiCorp in addressing potential flow, temperature and flow fluctuation effects on fish related to PacifiCorp's Klamath River Hydroelectric Project (Project) operations in the J.C. Boyle bypass and peaking reaches. Stakeholders were concerned that the use of "typical" suitability criteria used in instream flow studies could bias a habitat versus flow analysis by predicting flows that maximize low velocity fish holding positions, while not maintaining or accounting for the higher adjacent velocity flow fields that are important to drift-feeding fish such as rainbow trout. Also, stakeholders had concerns regarding the potential effects of flow fluctuations from peaking operations on water temperature and food availability and ultimately fish habitat and fish growth.

We used a bioenergetics approach to help address flow and flow fluctuation effects on fish and fish habitat. The primary objectives of the analyses were:

1. Use a bioenergetics foraging model in combination with empirical data to assess the importance of considering trout "feeding stations" (i.e., velocity fields adjacent to fish focal locations) in estimates of habitat at various instream flows.
2. Assess bioenergetics and trout growth over a range of flow, food, and temperature conditions in the project reaches, and predict how trout growth under Existing Conditions (with peaking operations) in the J.C. Boyle peaking reach may differ from conditions under hypothetical Without Project (assuming no hydroelectric facilities or operations) and Steady Flow (assuming hydroelectric facilities and operations, but no peaking) scenarios.

We also provide some specific resource and project background information (e.g., literature summary) that is pertinent to the objectives of this report. The background information addresses issues regarding 1) habitat suitability criteria and habitat versus flow analyses for redband trout, 2) habitat suitability versus food availability, and 3) growth versus food availability and temperature.

One of the ultimate goals of this report is to accurately predict fish growth (for a wide range of fish sizes) over a period of years directly from river reach inputs consisting of diel and seasonally fluctuating temperature, drift density and size, and depth and velocity information. We develop some of those methods here and

provide our analysis and results to date in quantifying bioenergetics habitat availability and fish growth given the different project scenarios. Methods to do this type of analysis are not readily available. Much of the work relative to this report was in developing the analysis methods.

1.1 Background

1.1.1 Habitat Suitability Criteria and Habitat Versus Flow Analyses for Redband Trout

Drift-feeding trout are known to feed across velocity differentials, from a slow – moderate focal point into faster surrounding water. They typically accomplish this by moving laterally and/or vertically in the water column to intercept drifting prey items. They also forage in slower water locations on drifting invertebrates that disperse from adjacent higher velocity habitats (Pers. Observ.). Foraging locations that provide a low velocity holding location (low swimming cost) and access to abundant drifting invertebrates (high food intake) are energetically profitable (Fausch and White 1981; Fausch 1984; Hughes and Dill 1990; Hayes and Jowett 1994, Addley 1993, Hill and Grossman 1993, Guensch et al. 2001, others).

Any quantitative analysis of habitat versus river flow should account for these known behaviors of drift-feeding trout. Typical habitat suitability criteria (e.g., used in the Physical Habitat Simulation System [PHABSIM] model), that are based on observations of mean column velocity at the holding position of drift-feeding fish, may not adequately capture the behavior of trout. These suitability criteria may underestimate the velocity field being utilized by fish because the holding or focal location of the fish is typically in water slower than the surrounding water (lateral to or above the fish). Typical mean column suitability criteria used in instream flow analyses do not account for the velocity field lateral to the holding location of fish. Mean column suitability criteria do not explicitly account for the vertical velocity profile at the fish except in the sense that the vertical velocity profile is proportional to the mean column velocity.

It is conceivable that the use of typical suitability criteria and typical habitat modeling methods could bias a habitat versus flow analysis by predicting optimal habitat occurs at low flows that maximize the amount of low velocity holding position habitat, with the unintended result that adjacent high velocity flow fields that drift-feeding fish rely on to deliver food are lost.

There have been some attempts to incorporate trout drift-feeding strategy into PHABSIM by including adjacent cell velocities and vertical velocity differentials in habitat suitability (e.g., Beecher 1987, and HABTAV in PHABSIM). More sophisticated attempts have been made with individual-based models, some using empirical estimates of foraging area and velocity differential (Clarke and Rose 1997; Crowder and Diplas 2000; Nislow *et al.* 2000; Railsback *et al*. 2002) and others using functional drift-foraging models (Van Winkle *et al*. 1998; Guensch *et al*. 2001, Addley 1993).

1.1.2 Habitat suitability versus food availability

Food availability can alter the depth and velocity habitat suitability for drift-feeding fish at a micro-habitat (e.g., Addley 1993) and at a meso-habitat scale (e.g., Hayes et al. 2003). At a micro-habitat scale (i.e., the local depths and velocities used by fish while foraging), low food availability narrows the range of suitable depths and velocities that provide profitable drift-feeding locations, whereas higher food availability increases the range of depths and velocities that provide profitable drift-feeding locations. Increasing or decreasing the overall food availability (drift density) in a river can, as a result, increase or decrease the total amount of habitat for drift-feeding fish.

At a meso-habitat scale (individual or connected habitat units—pools, runs, riffles), the discharge and the corresponding velocity and turbulence patterns can alter the area of a habitat unit that contains suitable drift densities for foraging fish (e.g., Hayes et al. 2003). In particular, low flows may cause a dramatic decline in drift density in low velocity meso-habitat (e.g., pools, runs). Longitudinal, lateral, and vertical gradients in drift density in these meso-habitats become more pronounced at low flow (Hayes et al. 2003). Also, in hydro peaking rivers, it is possible that, at high flows in some habitat types, drift is not dispersed along the margins of the channel where fry and juvenile fish are frequently located. This could happen because hydro peaking creates a varial zone (periodically dewatered margin), which is relatively devoid of benthic invertebrates (i.e., the source of drifting invertebrates)

With respect to the Klamath River, overall food availability (e.g., whole reach) is a product of nutrients, primary production, substrate, temperature and flow patterns. Rivers that have fluctuating flows due to hydropower peaking can exhibit a reduction in benthic invertebrate density/biomass, drift density, and fish biomass – depending on the magnitude of peaking (e.g., Cushman 1985, Morgan et al. 1991, Moog 1993, also see references in these articles). Local food availability (e.g.,

within habitat units) in the Klamath River could be affected by dispersal of drift as a result of daily flow patterns. For example, high daily flows can increase drift (e.g., Cushman 1985, others) and dispersal of drift (e.g., Hayes et al. 2003) whereas low daily flows can decrease both.

1.1.3 Growth versus food availability and temperature

The primary determinates of fish growth are temperature and food availability. As mentioned above, food availability in the Klamath River can be a function of the flow regime. Temperature in the Klamath River, particularly the J.C. Boyle peaking reach, is also partly a function of the flow regime. Water entering the Project is composed primarily of warm, eutrophic water from Upper Klamath Lake. In the summer, when hydro peaking in the J.C. Boyle peaking reach occurs almost daily, the daily high flows releases are composed of this warm, lower quality water; however, during the daily non-peaking periods, flows in the reach are composed primarily of cool spring water (cooler, higher quality water).

Bioenergetics analysis was used in this report to address some of the implications and interaction of temperature and food availability on trout growth (e.g., Hayes et al. 2000, Hanson et al. 1997). Bioenergetics analysis was also used to assess the habitats (e.g., depth, velocity, food availability) that provide suitable growth (Guensch *et al*. 2001, Hayes et al. 2003).

2 Methods

2.1 Habitat Suitability Criteria and Appropriate Physical Habitat Analysis Method

2.1.1 Summary of Empirical Fish Data

We summarized the empirical fish habitat data collected as part of PacifiCorp's relicensing studies (PacifiCorp 2004). Data included mean column velocity, depth, focal velocity and adjacent velocity information for rainbow trout in the J.C. Boyle bypass reach. We analyzed the velocities one and two feet to the side of each fish using three fish size categories (30-50 mm, <50-150 mm, and <150-400 mm). We summarized the change in velocity per foot away from the fish (i.e., change in velocity/distance from fish). We also summarized the velocities above the fish. We use the measured velocity profiles to do this. In the empirical data set, velocity

was measured at the focal location of the fish and at the 0.6 depth and sometimes at the 0.8 and 0.2 depth. We used this information to calculate a typical velocity profile being used by the fish using linear regression. We also compared the observed focal velocity of the fish to the expected focal velocity based on a standard logarithmic velocity profile in streams.

2.1.2 Develop Adjacent Velocity Criteria Using a Feeding Station and/or Bioenergetics Foraging Model Approach

We reviewed the Beecher (1987) and PHABSIM HABTAV feeding station modeling approaches and the 2003 empirical fish data (TRPA 2003) to determine if adjacent velocity criteria could be developed and incorporated into a PHABSIM modeling assessment.

In addition, an adjacent velocity criteria and modeling approach was developed using a bioenergetics foraging model (e.g., Addley 1993, Guensch et al. 2001, Hughes and Dill 1990, Hughes et al. 2003) to address the importance of adjacent velocity. We used a grid of depth and velocities (0-6 ft by 0-4 ft/s) in the foraging model to compare the energetic suitability of various combinations of depth and mean column velocity. Fish of sizes 30, 40, 50, 70, 100, 150, 200, 250 and 400 mm were modeled at each of the depths and velocities on the grid. Fish were placed in the foraging model at the 0.2 fraction of depth from the bottom (0.8 from the water surface) of the bed. This was the average depth obtained from the empirical fish data. The vertical velocity profile used in the foraging model was the average velocity profile observed from the empirical fish data. Various scenarios were used to test the importance of different mean column velocities adjacent to the fish (outlined below). This allowed us to compare how energetic suitability changed for a wide range of depths and velocities given different adjacent velocity assumptions. A description of how the foraging model utilizes the entire velocity field around a fish is given in Appendix A.

We used four different approaches for modeling velocities adjacent to fish: 1) we assumed mean column velocity was the same adjacent to the fish as it was at the fishes holding location (i.e., both left and right of the fish) (Scenario 0), 2) we assumed velocity increased both to the left and right of the fish over a range of different rates from (0 ft/s/ft to –1.97 ft/s/ft) (Scenario 1, note that when the rate was 0 ft/s/ft the result is the same as Scenario 0), 3) we assumed velocity increased only on one side of the fish over a range of rates from (0 ft/s/ft to –1.97 ft/s/ft) and remained the same as the focal location mean column velocity on the other side of the fish and 4) we assumed that velocity increased on one side of the fish over a

range of rates from (0 ft/s/ft to 1.97 ft/s/ft) and decreased on the other side at the same rate (Scenario 3) (note that if velocity reached zero on the declining side it remained at zero). Figure 1 shows an example of each scenario for a fish foraging at a mean column velocity of 0.5 ft/s.

In all cases we used a typical or average vertical velocity profile (developed from the fish observation data) base on mean column velocity and the empirical logarithmic velocity profile equation:

$$Vp/Vm = A(Dp/D)^B \quad (1)$$

Where:

Vp = Velocity at depth Dp in the velocity profile
Vm = The mean column velocity
A and B = Empirically derived coefficients
Dp = The depth at point
D = Total depth

The coefficients used for most of the modeling were A = 1.21817 and B = 0.229034. These were based on an analysis of the empirical velocity data at observed fish locations (see section 2.1.1 above). The typical coefficients that create the profile used by the USGS to justify using a velocity measurement at 0.6 depth from the surface to estimate mean column velocity are about A = 1.3 and B = 0.3 (see Rantz et al.1982 for the actual data). We also used this profile in some analyses.

We compared the empirical fish habitat utilization data collected in the Klamath River to the modeled bioenergetics criteria by 1) plotting observed fish locations on the grid of depths and velocities (see above) along with the modeled bioenergetics criteria and 2) by creating univariate depth and velocity suitability curves from the bioenergetics depth and velocity surfaces and comparing them to the univariate depth and velocity use curves generated from the empirical data.

The bioenergetics criteria used for this analysis was the amount of net energy intake available on a daily basis (DNEI). This includes the constraints of maximum daily consumption and the losses associated with excretion, egestion, and metabolism (base metabolism + active metabolism + food digestion and processing costs)

Net Energy Intake (daily) = Energy Available for Growth (daily)
= Daily Consumption – Wastes (egestion and excretion)
– Metabolism (basil and active)

Where, Daily Consumption is limited by the maximum consumption observed in laboratory studies. Daily consumption was calculated using the bioenergetics foraging model, the velocity and depth field, the average drift density for the site, the average size distribution of the drift, and the estimated capture velocity of each fish size at each temperature. Capture velocity was estimated as the average of the sustained maximum velocity of the fish and the most efficient swimming velocity (both are a function of fish size and temperature). See Appendix A for details of the foraging model.

The drift density and size distribution of drift was initially derived from limited (one day) drift sampling data in the J.C. Boyle peaking reach. The data were collected during PacifiCorp's macroinvertebrate sampling (PacifiCorp 2004). Subsequently, new drift data have been collected, and these were incorporated into the bioenergetics analysis.

The maximum amount of daily food consumption and the energy losses due to egestion, excretion, base metabolism, and food digestion costs were determined from equations developed from a reanalysis of the laboratory experiments of From and Rasmussen (1984) on rainbow trout. These equations are a function of fish size, temperature, and consumption level. This same data has been used by many other investigators (e.g., Rand et al. 1993 and Railsback and Rose 1999) within the framework of the Wisconsin Model (Hanson et al. 1997) for bioenergetics growth modeling of rainbow trout and steelhead. Our reanalysis of the data provided a better fit to the data at colder temperatures (e.g., J.C. Boyle bypass reach) and a more realistic approximation of the amount of food consumption on natural prey items.

Swimming cost (i.e., active metabolism) was determined from the equation in Stewart (1980):

Ra (J*hr^-1) = 1.4905W^0.784*e^(0.068*T)*e^((0.0259-0.0005T)*U) (2)

Where: Ra = Active metabolism
W = Wet weight (g)
T = Temperature (C)
U = Swimming velocity or focal velocity of the fish

2.1.3 Habitat Analysis on Cross-sections and/or 2D Modeling Site

We used the data from 103 cross-sections collected during PacifiCorp's instream flow study to assess the effect of using or not using adjacent velocities in the habitat analysis (PacifiCorp 2004). Cross-section data were collected in the J.C. Boyle bypass and peaking reaches and modeled over the range of flows from 350 to 7,500 cfs. Cross-section data (transects) were collected in three main areas of the peaking reach: Upper J.C. Boyle peaking reach (referred to in this report as the Oregon portion of the J.C. Boyle peaking reach), Frain Ranch reach, and the Lower J.C. Boyle peaking reach (referred to in this report as the California portion of J.C. Boyle peaking reach).

Depth and velocity data for each of the cross-sections and for each flow were input into a spreadsheet where various analyses could be performed. Typically, the distance between velocity/depth measurements on the cross-sections was 2 ft. We linearly interpolated all velocity and depth data to a spacing of 1 ft to facilitate the various analyses.

The initial plan was to compare and contrast habitat results of the bioenergetics foraging model, typical PHABSIM model, and adjacent velocity PHABSIM analysis model. We reviewed the adjacent velocity method in the PHABSIM HABTAV adjacent velocity program to understand how it is implemented. Based on these results we were not able to determine a meaningful way to implement the program concepts into a rational physical habitat analysis (a review of the method is provided in the Results section). Therefore, we used the bioenergetics foraging model analysis to incorporate the "adjacent velocity concept" into the habitat analysis and compared the results to standard PHABSIM results.

We compared the results by 1) comparing the habitat versus flow relationships for each of the methods and 2) comparing the spatial pattern of suitable habitat on each cross-section. Comparison of the spatial pattern of suitable habitat was done using visual comparison methods.

2.2 Assess Potential Food Availability and Temperature Ranges Over a Reasonable Range of Flow Scenarios (Existing Peaking to Stable Flows) in the Klamath River.

2.2.1 Summarize Various Temperature and Flow Regimes

We used PacifiCorp's temperature model results (hourly time step) for the year 2000 as an example of the annual temperature regime for various reaches of the Klamath River (PacifiCorp 2004). We used the temperature data in the Keno reach, in the lower J.C. Boyle bypass reach, and in the J.C. Boyle peaking reach at Stateline to assess bioenergetic growth in the Keno reach, the J.C. Boyle bypass reach and the J.C. Boyle peaking reach of river, respectively. We used three of the temperature scenarios: Existing Conditions (with peaking operations), Steady Flows (assuming hydroelectric facilities and operations, but no peaking) and Without Project (WOP). The WOP scenario assumes conditions without the hydropower facilities and operations.

The hourly temperature data were used to address maximum temperature tolerance with relation to short-term acute temperature impacts in a cursory manner and to modify the mean daily temperature for growth modeling (see below). Mean daily temperature (modified by diel fluctuations) was calculated and used for daily growth modeling over a four-year period. Mean daily temperature for 2000 was replicated for four years for the growth modeling.

The laboratory fish growth data that were used for bioenergetics growth modeling was derived from constant temperature experiments (From and Rasmussen 1984). Using mean daily temperature and constant temperature growth data provides a good first approximation to growth in fluctuating temperature environments.

Elliott (1975) found that a growth model developed from constant temperature experimental data predicted brown trout growth in daily fluctuating temperature environments fairly accurately when the mean daily value of the fluctuating temperature was used as input to the growth model. Some well-done growth experiments in constant and fluctuating temperature regimes, however, have shown that fish in fluctuating temperatures biologically respond to a temperature somewhat higher than the mean of the fluctuating temperature. Hokanson et al. (1977) found that fish feed at maximum ration and subjected to a ±3.8°C fluctuating temperature regime grew similar to fish in constant temperature

regimes, but with a mean temperature 1.5°C greater than the mean of the fluctuating regime (mean plus 39% of the fluctuation above the mean).

For example, fish grown in a fluctuating temperature regime with a mean of 17°C grew similar to fish in a constant temperature regime of 18.5°C. Other investigators have found similar results (Cox and Coutant 1981; Spigarelli et al. 1982), while some investigators have found little difference between constant and fluctuating temperature regimes (Thomas et al. 1986, Dickerson and Vinyanrd 1999). Experimental methods, temperature regimes, and food levels likely contribute to the observed differences.

We incorporated the results of Hokanson et al. (1977) into this analysis because the fish and temperature fluctuations were very similar to the fish and diel temperature fluctuations in the Klamath River. We modified the mean daily temperature by adding 39% of the daily fluctuation above the mean to the mean temperature. During cool periods of the year the mean temperature was only slightly modified because daily temperature fluctuations were small. During the summer, daily fluctuations were very similar to those in Hokanson et al. (1977). Daily fluctuations above the mean averaged 3.7°C under Existing Conditions, 2.6°C in the WOP scenario, and 2.4°C in the Steady Flow scenario.

To assess daily flow fluctuations on local habitat availability we selected two representative days during the summer (August 14-15, 2000) to assess daily flow fluctuations. The first day shows typical flow fluctuations with one hydropower unit (e.g., 350 to 1,500 cfs) and the second day shows flow fluctuations with two units (e.g., 350 to about 3,000 cfs). These data were derived from the calibrated hydraulic RMA-2 model runs at the powerhouse and at Stateline (PacifiCorp 2004).

2.2.2 Assess Food Availability (Invertebrate Drift) and the Potential Range of Variation Between Peaking and Stable Flows

For bioenergetics analysis we used drift density and size data collected as part of this work (see below) and an existing, but limited set of drift data that was collected in the J.C. Boyle peaking reach at a riffle near the BLM campground (PacifiCorp 2004). These existing data were collected over a partial peaking cycle (high flows dropping to low flows). We summarized these data and, after obtaining the invertebrate samples, measured and quantified the sizes of the invertebrates in 2 mm intervals.

We compared the observed drift invertebrate densities in the Project reaches to values developed from a literature review to assess the amount of food available in the project reaches compared to other rivers and to determine the potential change in drift and benthic invertebrate densities if existing hydro peaking operations were modified (e.g., more stable flow conditions). We also compared the observed drift to data collected in the lower river below Iron Gate dam (Hardy and Addley 2001). The purpose was to "bound" the analysis and provide information for conducting a sensitivity analysis regarding the bioenergetic impact to fishes of alternative flow scenarios.

2.2.3 2004 Summer Drift Density and Size Collection

During the summer of 2004 drift data were collected as part of this work. We sampled drift at four sites in the J.C. Boyle peaking reach. Two of the sites were in the upper (Oregon) part of the reach and two sites were in the lower (California) part of the reach. We sampled drift at three sites in the Keno reach and two sites in the J.C. Boyle bypass reach. Sample locations were located near the downstream segment of representative riffle habitats.

Drift was sampled once in late June / early July and once in early-September, 2004. Drift nets consisted of three 0.5 mm mesh drift samplers (modified from Field-Dodgson 1985) stacked vertically in the water column at 0.1 m above the bed, at 0.4 x water depth, and at the surface (only two nets in shallow water). Three sets of nets were placed across the stream at each site: near mid-channel (or as close as possible depending on flows), mid-way between shore and mid-channel, and near shore.

Water velocity flowing into each of the stacked drift nets was measured at the start and end of each drift sample collection period. Drift was sample once at mid-morning (~ 8-10 AM) and once at mid afternoon (~ 1-3 PM). Duration of each sample period was approximately one hour. Samples were sorted and quantified by subsampling. Organisms were measured for length and counted into 2 mm length size classes. Results were summarized in tables of mean drift density (#/ft^3) and size frequency at each location (Keno reach, J.C. Boyle bypass reach, J.C. Boyle upper peaking and lower peaking reaches).

2.3 Sensitivity Analysis of Bioenergetics Habitat and Growth Over a Range of Temperature, Potential Food Availability, and Flow Scenarios

2.3.1 Bioenergetic Habitat Assessment Over a Daily Time Series of Peaking

Using the foraging model (Appendix A) and the cross-sections in the California portion of the J.C. Boyle peaking reach and the available drift information (sections 2.2.2 and 2.2.3), the spatial availability of suitable bioenergetics habitat over a daily cycle of peaking was assessed. We assumed for simplicity that drift would be evenly dispersed in the cross-sections.

2.3.2 Bioenergetic Growth Assessment

We used both the temperature-growth relationship (developed from data in From and Rasmussen (1984)) and the bioenergetics foraging model to integrate food and temperature to predict growth rates for four years for the Existing Conditions, Steady Flow, and WOP scenarios. The alternative temperature and flow regimes for these three scenarios were used to predict growth rates and these were compared to existing age versus size data for Klamath River trout. Age versus size data for redband trout in the J.C. Boyle peaking reach, J.C. Boyle bypass reach, and Keno reach were provided by PacifiCorp and are reported in PacifiCorp (2004).

Two annual drift density regimes were used for inputs to the foraging model to predict growth under Existing Conditions and alternative project scenarios (see Section 2.2.2 above). We used the reach specific drift densities observed in this work to predict existing growth. In the J.C. Boyle peaking reach we also used the highest drift density that likely could occur if flows were released in a more natural pattern without peaking (e.g., WOP or Steady Flow scenarios) to predict growth. The drift density observed in reaches without peaking, Keno reach and below Iron Gate reservoir (collected previously by Hardy and Addley (2002)) were used to develop a without peaking drift density (see Results Section 3.2.2.1 below).
We developed a seasonal drift density pattern in each reach using the reach specific data collected at two different months in the Klamath River and superimposing a "typical" seasonal pattern onto this data from information gathered in the literature review (see Results Section 3.2.2.1)

We also modeled growth by using just the temperature-growth relationship (From and Rasmussen 1984). To do this we calculated the annual percent of maximum consumption (P value) required to produce the observed growth in the Keno reach, J.C. Boyle bypass reach, and J.C. Boyle peaking reach (using the Existing Conditions temperature regime). We refer to this model as the P value model. We used these observed P values to estimate the changes in growth given different Steady Flow and WOP temperature regimes (assuming the P values remained constant) in the J.C. Boyle peaking reach. We also used the highest observed P values in the Keno reach to estimate an "upper bound" of potential growth in the J.C. Boyle peaking reach if food levels increased due to elimination of peaking under the WOP and Steady Flow scenarios.

3 Results

3.1 Habitat Suitability Criteria and Appropriate Physical Habitat Analysis Method

3.1.1 Summary of Empirical Fish Data

3.1.1.1 Horizontal (Lateral) Shear Used by Fish

An example of the lateral adjacent velocity data collected in 2003 is shown in Figure 2. Figure 2 shows only the data for fish from 200 to 400 mm and is shown to provide an example of what the individual fish data looks like. Data for each fish was reversed, if needed, so that the highest adjacent velocity (1 foot from the fish) is on the left side of the plot (at distance –1) (this was done to make the data easier to view). Figures 3, 4 and 5 show aggregated data for fish in the 30-50, >50-150, >150-400 mm size range. The data were plotted in a slightly different format to facilitate viewing (i.e., the velocity points for each individual fish are not connected with a line). Again the individual fish data were rotated if needed so the highest adjacent velocity was on the left side of the plot. Average values for each velocity group (focal location and adjacent velocity 1 or 2 feet from the fish) are shown. A regression between the focal location mean column velocity and the one foot adjacent mean column velocity shows the typical maximum positive velocity gradient. Fish 30-50 mm had an average focal mean column velocity of 0.4 ft/s and the average highest velocity 1 foot away was 0.2 ft/s faster; on the "other side" of the fish the velocity was 0.1 ft/s slower. Fish >50-150 mm had an average focal mean column velocity of 0.8 ft/s and the average highest velocity 1 foot away was 0.24 ft/s faster; on the "other side" of the fish the velocity was 0.23 ft/s slower.

Fish >150-400 mm had an average focal mean column velocity of 1.25 ft/s and the highest velocity 1 foot away was 0.49 ft/s faster; on the "other side" of the fish the velocity was 0.32 ft/s slower.

3.1.1.2 Vertical Shear Used by Fish

Vertical velocity shears are typical in rivers (see Methods 2.1.2) and the shape of the vertical shear affects fish foraging and holding behavior and affects the results of the bioenergetics foraging model. The vertical velocity data collected in 2003 are shown in Figure 6. These data include 0.6, 0.2, and 0.8 depth velocity measurements at the fish location and at adjacent velocity locations (also velocity measurements were taken at the fish focal point). A regression line using equation 2 is shown in Figure 6 along with the "typical" USGS vertical velocity profile and the vertical velocity profile used later in this report for bioenergetics modeling. All of these velocity profiles are very similar. The USGS profile provides a useful reference. The velocity data are relatively noisy (typical of rivers with large substrates). The coefficients for the regression line (see equation 2) are A = 1.189 and B = 0.259. The observed vertical velocity profile is only slightly different than the "average USGS" profile. Velocity measurements at 0.6 of the depth are not equal to the average velocity in the water column as is typically assumed (not equal based on the regression); the 0.6 depth mean column velocity for the profile is about 7% too low. Thus the "mean column velocities" measured in the field from 0.6 depth measurements were 7% too low. This happens when, for instance, large substrates cause the velocity at the 0.6 depth to be less than the average (i.e., the velocity profile is more "s" shaped—higher than normal at the top of the water column and lower than normal at the bottom of the water column).

For use in bioenergetics foraging modeling (below) we created a velocity profile with a similar shape to the observed profile, but that also has the mean column velocity at 0.6 depth (see Addley 1993) and has a dimensionless mean column velocity equal to unity (i.e., if you sum up the velocities in the vertical on the dimensionless plots, e.g., Figure 6, the mean velocity will be 1). Coefficients for "our" profile are A = 1.21817 and B = 0.229034. The use of this vertical velocity profile instead of the exact profile measured was mostly an "aesthetics" decision so that bioenergetics analysis results (below) would be based on mean column velocity. Using the actual regression vertical velocity profile generated nearly identical results.

On average the focal depth for the 2003 fish data was 0.8 of the depth from the surface of the water (n=709).

A comparison of predicted focal point velocities of fish (from our theoretical velocity profiles) and measured focal point velocities of fish (based on the observed focal depths) is shown in Figure 7. We compared predicted versus measured focal velocities using (1) the observed regression coefficients and equation 1, (2) the "typical USGS" profile, and (3) our coefficients for equation 1 that provide a similar shaped profile. Each comparison was nearly identical and Figure 7 shows the results for only the "USGS" profile (the "USGS" profile is shown as a reference for a typical river velocity profile). Figure 7 shows that fish are using focal velocities that are equal to or, often times, much slower than would be expected from a "typical" velocity profile. These low focal velocity locations are typically created by wakes from upstream substrates (Pres. Observ.). Deviations between "expected" focal velocity (using the mean velocity profile) and actual focal velocities used by fish sampled in the field affect the accuracy of the position holding costs in the bioenergetics foraging model.

We also compared the vertical velocity profiles in different habitat types and in different depths of water using the 2003 empirical fish data. Vertical velocity profiles in deep water were steeper (relative change in velocity/relative change in depth). On average, deep-water "mean column" velocities measured in the field from 0.6 or 0.8 and 0.2 point measurements were about 10% too low compared to the regression of all points in the water column (this can be observed from the amount that the relationships are shifted too far to the left in the dimensionless plots). Figure 8 shows the data. A similar relationship occurs for different habitat types. Deep pools have steeper velocity profiles than shallow riffles. The measured "mean column" velocity data from 0.6 or 0.8 and 0.2 point measurements in the field are too low (about 7% too low for all the deep pool data) (Figure 9). Discrepancies between the velocity profiles in different habitat types or depths of water and the single velocity profile used for most of the bioenergetics foraging model calculations will cause some limited error in the bioenergetics model results. Section 3.1.2.2 provides a small sensitivity analysis of the affects of different velocity profiles.

3.1.1.3 Empirical Depth and Velocity Locations of Fish

For the 2003 data we plotted the depth and velocity locations for each size class of fish (30-50, >50-150, >150-400) (Figure 10). As fish get bigger they use deeper and faster water. Average depth and velocity for each size class is shown in Table 1.

3.1.1.4 Vertical and Horizontal Velocity Shear Comparison
The vertical velocity shear above fish can be compared in magnitude to the horizontal velocity shear. We used the depth specific average velocity profile relationships (Figure 8) and the average depths and mean column velocities measured for each fish size class (see above) to calculate the vertical velocity shear one foot above the fish. Table 1 shows the results. Vertical shear and horizontal shear on the high velocity side of the fish are approximately the same magnitude

3.1.2 Adjacent Velocity Criteria

3.1.2.1 Beecher Style Feeding Station Adjacent Velocity Criteria and Analysis
The concept proposed by Beecher (1987) and partially implemented in PHABSIM for feeding station analysis is to use the velocity at a point location and the surrounding velocity (lateral and vertical) to determine if the point location is a suitable feeding station. We view this fundamental concept as a sound basis for determining habitat suitability for drift feeding salmonids. Implementing the approach, however, with existing data and the PHABSIM algorithm is problematic.

The PHABSIM feeding station analysis method is ultimately based on having an adequate empirical suitability data set that consists of data for 1) fish focal velocity (for fish of a given size), 2) water depth (again fish size dependent) and 3) velocity difference (delta velocity) some distance (delta distance) from the fish. The mechanics of implementing the analysis in PHABSIM is based on scanning a cross-section laterally some user specified distance from the point location to determine if a suitable delta mean column velocity is available. Vertical delta velocity cannot be analyzed.

Two problems exist for the analysis. One is obtaining an adequate empirical data set that consists of four and possibly five or six dimensions. These dimensions are suitability for (1) focal location depth, (2) focal location velocity, (3) delta velocity difference (lateral and/or vertical), (4) delta distance for the velocity difference, and with all of these variables as a function of (5) fish size and possibly (6) temperature. This is an impossibly large empirical data set. The second problem is to obtain sufficiently detailed hydraulics and develop appropriate habitat algorithms to assess velocities laterally and vertically.

We reviewed the 2003 fish data with the first problem (adequate empirical data set) in mind. While the data set is a very useful data set it appears to us inadequate to address the immense combination of focal depths, focal velocities, velocity differences (lateral and vertical), and velocity difference distances (delta distance)

potentially used by different sized fish. Additionally, it is impossible from the data set to determine which velocity difference (lateral or vertical) and what velocity difference distance (0.5, 1.0, 1.5, 2.0 feet, etc.) is actually being used by the fish. Clearly some assumptions can be made; however, it appears that a partially mechanistic approach instead of a purely empirical approach is needed to assess the potentially large combination of conditions that provide suitable conditions for drift feeding fish.

We reviewed the PHABSIM HABTAV program with the second problem in mind (having sufficiently detailed velocity information and appropriate habitat algorithms). The PHABSIM HABTAV program is limited in its ability to interpolate velocity horizontally at a specified distance (the algorithm just works, as far as we can tell, based on the point velocities in adjacent cells). In addition, the algorithm has no ability to compute vertical velocity differences (even though it has velocity profile algorithm to calculate nose velocities).

Based on our review and the problems discussed above regarding the near impossibility of collecting an adequate 5 dimensional empirical adjacent velocity data set and the limitation of the PHABSIM hydraulics and HABTAV algorithms, we could not envision an adequate way to use the empirical fish observation data and the existing PHABSIM HABTAV program to make a competent feeding station analysis. Further, the PHABSIM feeding station analysis as currently implemented in PHABSIM is not a recommended modeling approach (Instream Flow Council 2002). The Instream Flow Council (2002) discussion of the feeding station method is contained in Appendix C.

3.1.2.2 Adjacent Velocity Criteria Using a Bioenergetics Foraging Model

The feeding station approach addressed in section 3.1.2.1 (e.g., Beecher 1987) has been implemented in a detailed mechanistic manner in several bioenergetics foraging models (Addley 1993, Guensch et al. 2001, Hughes and Dill 1990, Hughes et al. 2003, Hill and Grossman 1993). The bioenergetic foraging model detailed in Appendix A is used in this report. The model uses empirically derived vertical velocity profiles, mean water column velocity measurements, and depths. Velocity is interpolated on as fine of a grid as needed (e.g., every few centimeters) based on the empirical velocity profile(s) and mean column velocities (e.g., Figure 2A). This data is used in combination with invertebrate drift density (and size distribution) and several fish size and temperature dependent relationships for swimming velocity, swimming cost, maximum consumption, reaction distance (distance fish can see and recognize prey of a given size) and turbidity to mechanistically assess the daily energy intake (suitability) of foraging locations.

Daily Net Energy Intake vs. Klamath River Fish Location
Using the foraging model we compared observed fish locations to modeled daily net energy intake (DNEI) to determine if the foraging model approach adequately represented the feeding stations used by Klamath trout. We assumed the length of time fish would forage in a day was only as long as it took to reach maximum consumption at the best depth and velocity combination. The length of time it took fish of 30, 50, 70, 100 and 250 mm to reach maximum consumption was 2.7, 3.6, 3.7, 5.1, and 7.4 hours, respectively. Figures 11, 12, 13, 14 and 15 show the foraging model DNEI for these fish sizes compared to the 2002 and 2003 (TRPA 2003) fish observations. Each depth and velocity combination on the grid was modeled as a short cross-section (11 feet) composed only of that specific depth and velocity. The foraging model calculates the DNEI at the center of the cross-section for the specific fish size, water temperature (14.75 C measured during fish data collection) and drift density (0.06 prey/ft^3) (measured in the J.C. Boyle bypass reach in 2004). The fish was placed at the specified depth in the center of the cross-section (0.8 depth from the surface).

A small number of fish observations were excluded *a priori* from the analysis because the observed focal velocity varied greatly from the modeled velocity profile (i.e., the fish were using a location where the velocity profile differed greatly from the average velocity profile).

In general, the observed fish locations match the modeled daily net energy intake very well. There are a few scattered outliers, particularly for the larger fish, that appear to be using "too fast" of water to be energetically profitable (Figures 13, 14, and 15). We investigated these fish (e.g., what habitat types, focal velocities, etc., they were using), but could see no unusual pattern to explain their "fast water" location. It is possible these fish were actually using the high velocity locations long-term or it is possible they were scared to these locations temporarily during snorkeling (snorkeling conditions are difficult on the Klamath River due to low visibility). Other explanations may exist for these high velocity locations, such as higher drift densities than we modeled actually existing in the river at the time of fish data collections (i.e., making unsuitable locations suitable).

Univariate Foraging Model Suitability Criteria vs. Fish Observations
We also compared the univariate depth and velocity suitability criteria developed from the 2002-2003 empirical trout data to univariate depth and velocity criteria derived from cutting "slices" through the DNEI surfaces. Surfaces were sliced at the velocity that provided maximum energy to derive a depth suitability curve.

The surfaces were sliced at a depth approximately equal to the average depth being utilized by each size class of fish to derive a velocity suitability curve. We grouped the fish into the three size classes currently being used for PHABSIM modeling (20-40, >50-150, >150). Figures 16, 17, and 18 show the frequency histograms for the fish (i.e., un-smoothed utilization curves) and the DNEI curves. These figures also show the scaled (between 0 and 1) velocity suitability criteria from the foraging model. We used a foraging model fish size that was approximately the median size of the fish in each size class. Because we only modeled a few discrete sizes of fish in the foraging model (30, 40, 50, 70, 100, 150, 200, 250, and 400 mm), we used the 30 mm foraging model results to represent fish from 20 to 40 mm, the 100 mm foraging model results to represent fish from 50 to 150 mm, and the 250 mm foraging model results to represent fish from 160 to 400 mm (fish were placed in 10 mm bin size classes).

For the small fish the foraging model curves require some discussion. The smaller size classes of fish (Figure 16 and 17) can reach maximum consumption relatively quickly and there is a relatively broad range of velocity that allows for high-energy consumption. For 30-40 mm fish (Figure 16) the range is from just over zero to just less than 1.0 ft/s. The energetic curve suitability increases rapidly on the low velocity side and peaks at about 0.16 ft/s. At higher velocity there is a gradual decline because swimming cost increases with increased velocity (i.e., some of the acquired energy is being used to pay swimming cost). At about 0.82 ft/s (mean column velocity) the velocity becomes greater than the fish can continually capture prey in (sustained maximum swimming speed) and suitability (energy capture) drops rapidly.

The match between the energetic curve and the fish frequency data is fair in the sense that most of the fish are within the energetic curve, but the fish are using the lower velocity side much more than the higher velocity side. This makes sense because there is more energy to be gained (i.e., less swimming cost paid to acquire maximum gross energy consumption) and less effort required. The energetic curve also shows this pattern but it is not very obvious. One way to show this pattern more clearly is to scale only the “top portion” of the energetics curve or the portion of the curve that provides maximum consumption. If only the portion of the curve that provides maximum consumption is scaled to create a suitability curve, there is an excellent match between the observations and the foraging model.

Larger fish, greater than about 250 mm (see section below), could not reach maximum consumption (i.e., laboratory feeding maximum consumption) at the observed drift density. The shape of the energetics versus velocity curve for 250

mm fish is more bell shaped because these fish can only reach maximum consumption in a small range of depth and velocity combinations (Figure 18). On the left side of the curve velocity is too slow to deliver enough food and on the right side velocity is too fast to capture food and swimming costs are higher. Figure 19 shows the observed depth suitability curves versus the scaled energetics depth suitability curves. The match is good.

Gross Energy Intake and Energetics Habitat at Different Food Levels

The amount of laboratory derived daily gross energy intake for fish 30, 40, 50, 70, 100, 250, and 400 mm is compared in Figures 1B-4B (Appendix B) to foraging model estimates of gross energy intake at the estimated drift density of 0.06 prey/ft^3 (based on 2004 drift density measurements in the J.C. Boyle bypass reach) and the average temperature (14.73 C), and average day length (13 hrs) that occurred during the 2002-3 fish observations. The laboratory daily gross energy intake is based on the equations derived below from data in From and Rasmussen (1984). These comparisons provide a snapshot (specific temperature and drift density) estimate of the ability of different sized fish to fill their gut on a daily basis. Small fish up to 250 mm could fill their gut on a daily basis. Larger fish could not. A drift density of nearly 0.20 prey/ft^3 was needed for 400 mm fish to fill their gut.

DNEI was shown previously (Figures 11-14) for fish 250 mm or less. The 250 mm modeled fish were able to reach "maximum" consumption and showed a positive DNEI over a wide range of depths and velocities. For 400 mm fish, however, the range of depths and velocities that provide positive DNEI is very narrow (Figure 20). If drift density was increased, for example, 1.67 times to 0.1 prey/ft^3, 400 mm fish had a large (and positive) DNEI over a broad range of depths and velocities (Figure 21).

Adjacent Velocity Effects on Habitat Suitability

We used the foraging model to investigate the effect of adjacent velocity on the suitability for different depth and velocity habitats. Many different habitat-modeling runs were produced. Here we use only the results from 250 mm fish to illustrate the general results. We do this by comparing adjacent velocity foraging model DNEI results to DNEI results for no adjacent velocity modification. In all of the analyses, little change occurs in the DNEI surfaces in the depth direction due to adjacent velocity changes. As a result, we show only the change that occurs in the velocity direction. This is done using 1D slices cut through the DNEI surfaces at 3.1 ft of depth (the average depth the >150 to 400 mm fish were using).

The four adjacent velocity patterns we used were 1) no change in adjacent velocity (Scenario 0), 2) increased velocity on both sides of the fish (Scenario 1), 3) increased velocity one side of the fish (Scenario 2), and 4) increased velocity on one side of the fish and decreased on the other (Scenario 3) (Figure 1). Scenario 0 was used previously to compare fish locations (e.g., Figures 11-14) and the DNEI surface for a 250 mm fish is shown in Figure 15 (top). If Scenario 1 is compared to Scenario 0 for different adjacent velocities the modeling shows that by increasing the adjacent velocity on both sides of a fish DNEI increases and the mean column velocity that provides maximum DNEI decreases (Figure 22). This pattern happens because of increased delivery of prey close to the fish with no increase in swimming cost.

When Scenario 2 (increased velocity on just one side) is compared to Scenario 0 DNEI increases slightly for small increases in adjacent velocity up to about 0.048 ft/ft/s and the best mean column velocity decreases slightly (similar to Scenario 1), but at higher adjacent velocities DNEI begins to decrease. This occurs because capture window on the high velocity side gets smaller (velocity too high) and less food capture occurs (Figure 23).

Scenario 3 (increased velocity on one side and decreased on the other) compared to Scenario 0 shows no change in the optimal velocity and a steady decrease in DNEI with increases in adjacent velocity (corresponding decreases on the opposite side) (Figure 24). This occurs because the corresponding decrease in velocity on the one side of the fish rapidly approaches zero (no delivery of food) in a large part of the capture window and the increase on the other side cannot compensate.

The observed average lateral velocity pattern for fish sampled in 2003 shows that on average fish were using lateral velocities similar to Scenario 2 or 3 (increase on one side and either a slight decrease or corresponding decrease on the other side) (Figures 3-5). Fish >150 to 400 mm were using an average pattern similar to Scenario 2 with an average increased adjacent velocity on one side of 0.49 ft/ft/s. Figure 22 shows that this lateral velocity use pattern provides slightly higher DNEI and allows for fish to reside in a slightly lower mean column velocity than if no increase in lateral velocity occurred.

Based on the modeling, it appears that the best option for fish is to use locations with increased lateral velocity on both sides. Generally this is relatively rare in the field (mostly only behind boulders without too much turbulence) and likely the reason few fish were observed using this pattern.

Fish can also potentially take advantage of greater than average vertical velocity shears to reduce costs and increase food intake. In our previous modeling we used the average vertical velocity profile. Here we compare those results to three different runs with vertical velocity profiles that have greater shear for 250 mm fish. A vertical velocity profile with greater shear allows modeled fish to obtain greater DNEI (Figure 25). The optimum velocity stays about the same in these model results.

3.1.3 Habitat Analysis on Cross-sections

To assess differences in habitat modeling results if adjacent velocities are accounted for in the analysis versus just using a static mean column velocity suitability curve (typical PHABSIM), we compared the weighted usable area versus flow relationships at the Frain Ranch reach, J.C. Boyle bypass reach, California portion of the J.C. Boyle peaking reach, and Oregon portion of the J.C. Boyle peaking reach (based on the adult use suitability curve) to "energetic" habitat using the foraging model. The foraging model takes into account the velocities (measured/modeled) adjacent to the fish location. Velocity and depth across each cross-section are based on the PHABSIM simulations (TRPA 2003), but the energetics model interpolates the mean column velocity at any location across the cross-section and generates a vertical velocity profile at any location (see Appendix A). Figures 26, 27, 28, and 29 show the weighted usable area versus energetics habitat. Energetics habitat was calculated similar to weighted usable area in the sense that joules/hr NEI calculated at each point (every 1 ft across the cross-section) was multiplied by the "area of the cell" if the NEI was positive (we multiplied by zero if energetics was 0 or negative). The area of the cell for every point was 1 ft^2 or a unit area. We weighted all cross-sections equally by spacing them 1 ft apart. The scale for the energetics habitat was not normalized like the suitability curves at the initial computation stage, but was later "normalized" on the comparison figures by putting it on a different axis. It can be seen from the figures that there is, as a practical matter, very little difference between the shapes of the habitat versus flow functions.

To see if there was a difference at the individual cell level in the analysis we created animated movie files of the "use curve" suitability's compared to the energetics suitability's at each cross-section (positive energetics habitat was scaled between 0 and 1 to compare with the use suitability). Movie file links for the Frain Ranch reach, J.C. Boyle bypass reach, California portion of the J.C. Boyle peaking reach, and Oregon portion of the J.C. Boyle peaking reach are provided. Figures 30, 31, 32, and 33 show images for the same sites for a 1000 cfs flow. The figures

and movie files show each cross-section. Each horizontal row of cells is a cross-section. The cells are 1 foot interpolated velocity/depth verticals along the cross-section. The top part of the figure is the energetic suitability and the bottom part is the suitability derived from the use suitability curve. The general pattern of suitability can be viewed for each cross-section and/or each cell. The general patterns are the same at each site. For the adult use curve there are many more cells that have low suitability (red), but the general pattern between the high suitability cells for both methods is very similar. Some individual cells are clearly different, most likely due to adjacent velocity issues. The exact reasons for the differences were not investigated in detail.

3.2 Potential Food Availability and Temperature Ranges

3.2.1 Temperature and Flow Regimes

Plots of daily average temperature for the year 2000 in the Keno reach, J.C. Boyle peaking reach at Stateline, and the J.C. Boyle bypass reach above the J.C. Boyle powerhouse for Existing Conditions, Steady Flow, and WOP scenarios are shown in Figure 34. The J.C. Boyle bypass reach node has higher winter temperatures and lower summer temperatures than the other locations. The Stateline node shows similar temperatures for all of the scenarios. Mean daily temperature exceeds 20 °C in the summer at this node. The Keno reach has the highest temperatures (summer temperatures several degrees greater than at Stateline).

Figure 35 shows hourly plots of temperature for year 2000 at Stateline for Existing Conditions, Steady Flow, and WOP scenarios. Peak daily temperatures are roughly similar for Existing Conditions and Steady Flow scenarios with summer peaks near 25°C. The Steady Flow temperatures have slightly lower peaks and slightly smaller diel fluctuations. Daily minimums are lower for Existing Conditions. WOP flow conditions produce lower summer peaks (maximums are about 24 °C) and less diel variation.

A “typical” summer peaking flow hydrograph over a 24-hour period for one hydropower unit and two hydropower unit peaking, and the corresponding steady flow hydrograph for the Stateline node, is shown in Figure 36.

3.2.2 Assessment of Food Availability (Invertebrate Drift) and the Potential Range of Variation Between Peaking and Stable Flows

3.2.2.1 2004 Klamath River Drift Data

Drift data recently collected in the Klamath River are shown in Table 4 (drift density) and Table 5 (drift size). Table 4 shows that the late June / early July drift density was relatively high (e.g., 0.629 prey/ft^3 in the Keno reach, 0.183 prey/ft^3 in the upper J.C. Boyle peaking reach) (see literature drift densities in Section 3.2.2.3 below). Even the later September samples show good drift densities, albeit much smaller than the earlier samples (e.g., 0.139 prey/ft^3 in the Keno reach, 0.025 prey/ft^3 in the upper J.C. Boyle peaking reach).

For the foraging model runs based on Existing Conditions we used the measured drift densities in each reach. For the J.C. Boyle peaking reach modeling at Stateline we used the average of the California and Oregon peaking reach drift densities. For an estimate of the highest potential drift density in the J.C. Boyle peaking reach, if peaking were eliminated, we used the drift density in the Keno reach and the drift density in the river below Iron Gate dam. Drift density in the Keno reach was the highest measured and flows are relatively stable in this reach. Drift density measured in the river below Iron Gate dam (relatively stable flows) during late August / early September was about 0.68 times that measured in the Keno reach (see section 3.2.2.3 below). We used the highest drift density in the four closest sites below Iron Gate dam. The highest drift density was about midway between the Keno drift density and the average density of the four sites below Iron Gate dam.

Because we measured drift on only two dates, we created a seasonal drift density by using the late June / early July drift density as the peak annual drift density and linearly interpolating drift density to the early September samples. We used literature data from Allan (1987), Clifford (1972), and Cellot (1996) to estimate that drift reached a minimum in the fall about November 1st and stayed low until approximately April 1st. After April 1st we linearly interpolated drift from the low winter densities to the high densities in late June. For drift density in the winter months, we used a drift density of 0.01 prey/ft^3 from data collected previously in the lower river (Hardy and Addley 2002) (see section 3.2.2.3 below). Table 6 shows the assumed seasonal drift density pattern. Linear interpolation was used to estimate drift density on days not shown.

There was very little difference in the size frequency distribution of drift between reaches. We averaged the size distribution in Table 5 to obtain a drift size distribution for input to the foraging model.

3.2.2.2 PacifiCorp Drift Data Over a Partial Peaking Cycle

Drift data collected in the J.C. Boyle peaking reach by PacifiCorp during Sept. 12, 2002 over part of a peaking cycle (PacifiCorp 2004) are shown in Figure 36 for a location in the Klamath River that was permanently wetted, only wetted at high flow, and for a mid channel location. The size frequency of drift prey items (length) is shown in Table 2.

3.2.2.3 Literature Review of Drift Density

Drift density and size frequency data collected downstream of the J.C. Boyle peaking reach below Iron Gate dam by Hardy and Addley (2002) are shown in Table 3 and Table 2.

Temperature, water current (stream hydraulics) and substrate are the most fundamental physical variables defining aquatic invertebrate habitat (Allen 1995). Appendix D contains a literature review of food (e.g., drift) and space regulation of fish production. The reported literature generally shows that large frequent flow fluctuations from peaking can have a negative impact on benthic invertebrate density and can alter species composition depending on the magnitude of the flow fluctuations. It appears that the larger the difference between peak flows and base flows the larger the affect (e.g., Moog 1993). In addition, benthic invertebrate biomass is affected most strongly near the flow release point and less farther downstream (i.e., flow impacts are attenuated downstream). The literature generally shows that drift density is a proportion of benthic density and the proportion of the benthos in the drift varies depending on the specific taxa in the benthos. Different taxa have different propensities to drift. As a result, drift density can be affected by changes in benthic density and composition.

Daytime drift densities in the literature span a very wide range depending on the river (physical and chemical characteristics), season, and sampling methods (e.g., net size). Drift densities are the highest in the summer and decrease into winter. Excluding some of the very high drift densities, most of the reported densities are between about 0.005 and 0.3 per ft^3. The drift densities in the project reaches easily fall within this range (Table 4) .

Because of the large number of variables affecting drift density (temperature, water quality, flow, season, substrate, sampling design, etc.) and the lack of a good

control reach for the J.C. Boyle peaking reach, it is impossible to determine drift densities if there was no peaking. We were not able to find enough good literature-based drift studies prior to and after initiation of peaking or above and within peaking reaches to address this issue quantitatively. The best way to estimate bounds for drift density in the J.C. Boyle peaking reach seems to be to assume the measured drift density is the lower bound and use the high drift density in the Keno reach (no peaking) as the upper bound. Drift density in the Klamath River below Iron Gate dam (no peaking) was lower than drift density in the Keno reach (0.139 prey/ft^3 versus 0.094 prey/ft^3, late summer/early fall) and this can be included as an alternative (additional) upper bound. Note that of the several sites with available drift data in the Klamath River below Iron Gate dam (Table 3), we elected to use the site (Tree of Heaven) with the highest drift density in order to represent the alternative upper bound.

3.3 Sensitivity Analysis of Bioenergetics Habitat and Growth Over a Range of Temperature, Potential Food Availability, and Flow Scenarios

3.3.1 Bioenergetic Habitat Assessment Over a Daily Time Series of Peaking

Using the "typical" daily peaking sequence in Figure 36 we calculated WUA over the daylight hours from 6:00 to 21:00. Figure 37 shows the WUA using the adult use curves and the NEI foraging model. Both WUA and NEI decrease in the afternoon as flow peaks to 1,500 cfs or 3,000 cfs depending on whether one or two units are used. The largest amount of habitat occurs at the low flow portion of the cycle. Corresponding steady daily flows (same amount of flow, but spread out evenly over a day) provide less habitat than occurs at the low flow portion of the peaking cycle and more habitat than occurs during the high flow portion of the cycle. How the habitat moves around as flows change is available in a movie file for the One Unit Peaking (August 14th) and the Two Unit Peaking. Habitat moves from the center of the channel at low flows to the edges of the channel at high flow.

3.3.2 Bioenergetic Growth Assessment

3.3.2.1 Rainbow trout data model (From and Rasmussen 1984)

The rainbow trout growth data from From and Rasmussen (1984) were reanalyzed to provide equations for maximum daily consumption of natural prey items as a function of temperature and fish size and for total daily energy losses as a function

of amount of consumption, temperature and fish size. This information is needed to limit daily consumption and account for all energy losses except swimming cost in a growth model (also used above in the DNEI foraging model).

From and Rasmussen (1984) fed rainbow trout high-energy content moist pellets on an hourly feeding schedule (hourly feeding only for fish used to measure maximum consumption). They found that for brown trout fed in a similar manner to the rainbow trout their estimates of maximum consumption were almost exactly double the maximum consumption estimates Elliott (1975a) observed for brown trout feed on natural prey items (amphipods). We fit equations to the maximum consumption data of From and Rasmussen (1984), but in the final application we reduced the maximum consumption by 50% to account for the difference in food type (artificial versus natural) and feeding regimes and we also reduced the energy consumption an additional 6% to account for the chitin content of natural prey (e.g., amphipods) which is indigestible energy (Higgs et al. 1995). We fit equations to the From and Rasmussen (1984) data using non-linear least squares regression.

Maximum consumption (Cmax) of moist pellet food versus fish size at each temperature is shown in Figure 38. The best-fit equation used for regression was

$$Cmax = A \bullet W^{B} \qquad (3)$$

where W is fish wet weight grams, B=0.7292, and A varies by temperature (Table 7). Moist pellet food is converted to gram chemical oxygen demand (g COD) by multiplying it by 0.935573. Figure 39 shows the maximum consumption data after being corrected to a standard weight of 1 g. Equation 3 was used to calculate Cmax at each measured temperature using the A coefficient values in Table 7 and linear interpolation of those values for intermediate temperatures. Figure 40 shows the predicted maximum consumption for all of the From and Rasmussen (1984) data versus that predicted using Equation 3.

Energy loss (Eloss) in g COD that consists of faeces, excretion, basil metabolism, and food digestion/processing costs versus fish size at each temperature (fish feed at Cmax) is shown in Figure 41. The best-fit equation used for regression was

$$Eloss\ (g\ COD) = A \bullet W^{B} \qquad (4)$$

where W is fish wet weight grams, B=0.7403, and A varied by temperature and by the fraction of maximum consumption (P). The equation for A is

$$A=a' + a'' \bullet P^{b'} \quad (5)$$

where the values for a', a'', and b' are shown in Table 8. Figure 42 shows the regression of Equation 5 versus the fish data. Figure 43 shows the temperature relationship of modeled maximum consumption (P value of 1) against maximum consumption data standardized to a 1 g fish. We used Equation 5 to generate a table of values for A at the measured temperatures (5, 10, 15, 20, 22, and 24.3 C) and over a range of P values from 0 to 2 (Table 9). We then simply used a two-way interpolation to estimate A at any other temperature or P value. Figure 44 shows predicted energy loss (Equation 5) versus measured energy loss.

Maximum consumption and energy loss (Eloss) were converted from grams COD to calories using the relationship 3,420 calories/ g COD (see From and Rasmussen 1984). Figure 45 shows a comparison of maximum energy intake, energy loss, and remaining energy for growth of a 50 g rainbow. A 50 g brown trout based on the equation of Elliott and Hurley (1999) is shown for comparison. Note that the rainbow trout maximum consumption was reduced in this example 56% to account for natural food versus pellets (see discussion above). The curves of energy available for growth are similarly shaped, but the rainbow trout shows growth up to 20 C and a sharp decline in growth rate thereafter. This is consistent with other rainbow trout growth data (Myrick and Cech 2000). Myrick and Cech (2000) compared the growth rates of two strains of rainbow trout at temperatures of 10 to 25 C. Growth rates increased with temperature to a maximum of 19 C and declined rapidly at temperatures higher than 19 C.

3.3.2.1 Klamath River Rainbow Trout Growth Modeling (Bioenergetics Foraging Model and P Value Model)

Foraging Model Versus Observed Data

For fish 30, 40, 50, 70, 100, 150, 250 and 400 mm and drift densities from 0.01 to 0.6 prey/ft^3 we calculated DNEI for temperatures ranging from 2 to 22 C. Figure 46 shows DNEI for two different drift densities, 0.02 and 0.1 prey/ft^3, that are applicable to the J.C. Boyle peaking reach (early September drift and late June drift, respectively). DNEI was calculated from the foraging model based on "allowing" fish to use the best depth and velocity combination (i.e., highest daily NEI). Maximum energy intake was constrained by the maximum energy intake relations developed above as a function of fish size and temperature. Energy losses were calculated from the relationships above as a function of temperature, fish

size, and foraging ration (P). Energy costs for swimming were calculated using Equation 2.

Modeled 250 and 400 mm fish were limited in terms of DNEI at high temperatures (i.e., energy costs exceed energy intake) for the 0.02 drift density (Figure 46). The 400 mm fish could not achieve positive growth. At the higher drift density all fish sizes (except the 400 mm fish) had positive growth potential up to a temperature just over 20C (above this, temperature is excessive and growth declines rapidly irregardless of the amount of food available) (Figure 46). The 400 mm fish show a precipitous decline in growth after temperature reaches 15°C.

The data illustrated in Figure 46 (for the entire range of drift densities) were used in the foraging model to predict growth in the Keno reach, J.C. Boyle bypass reach, and J.C. Boyle peaking reach given existing temperatures (year 2000 model results). Fish were assumed to start growing beginning May 5 at 1 gram. DNEI was summed each day. Energy content was converted to grams wet weight using the relationship in Rasmussen and From (1991; see Table 7). Figure 47 shows modeled growth to the size-at-age data collected in the Keno reach, J.C. Boyle bypass reach, and J.C. Boyle peaking reach (Forrest Olson, CH2M HILL, Pers. Comm.). The foraging model growth matches the measured growth for the J.C. Boyle peaking reach surprisingly good. The foraging model matches the Keno reach fish accurately for the first two years, but then predicts much too low of growth for years 3 and 4. Predicted growth for the J.C. Boyle bypass reach is also much higher than the observed growth.

Assuming the foraging model is formulated properly, the results suggest that some other source of food is available for the larger Keno reach fish rather than drifting invertebrates (e.g., forage fish) and/or the temperature regime used is not what the larger fish are experiencing (e.g., moving into the downstream reservoir or out of the upstream reservoir during some periods). The results also suggest that the drift density measured and modeled in the J.C. Boyle bypass reach is either too high or the temperature regime used for the reach is not the temperature the fish are using. Either lower drift density or colder temperatures in the model would produce the observed lower growth in the J.C. Boyle bypass reach (it is also possible that not including energy losses due to spawning may be part of the problem in this reach as spawning has been observed here).

The observed decline in the growth rate exhibited by the foraging model growth predictions as fish get larger (in each reach) is a direct result of the fact that as fish get larger they need more food, and as they get larger their swimming costs

increase and their the ability to utilize the smaller size fractions of the drift are decreased (e.g., gill raker spacing increases). The observed weight losses in the modeled summer weight (e.g., Keno reach) are due to high summer temperatures.

P Value Model Versus Observed Data

The back-calculated annual percent of maximum consumption (P value) required to reach the observed growth (using the temperature–growth relationship from the From and Rasmussen data) in the Keno reach, J.C. Boyle bypass reach, and J.C. Boyle peaking reach is shown in Table 10. Figure 48 shows the growth generated from the temperature-growth relationship using the calculated P values. Growth and P values were calculated for both the assumption that no spawning occurs and the assumption that spawning occurs in years 3 and 4 (46% decrease in energy at spawning). These data show that P values gradually decline each year for the J.C. Boyle bypass and peaking reaches. P values in the J.C. Boyle bypass reach are lower than the other reaches. P values increase in the Keno reach in years three and four. These data in combination may suggest that there is less food available in the J.C. Boyle bypass reach (or alternatively the temperature regime used for modeling is not what the fish are experiencing) and that fish in the Keno reach either increase their ability to obtain food (begin eating prey fish) or modify their temperature regime somehow (e.g., movement).

P Value Model Growth Predictions for the WOP and Steady Flow Scenarios

The back-calculated P values for the J.C. Boyle peaking reach were used in the P value growth model to determine the effect temperature regime differences associated with the Steady Flow and WOP scenarios would have on growth (Figure 49 and Table 11). Using the observed P values in the J.C. Boyle peaking reach the predicted growth at the end of 4 years is 307 mm (313 grams) for the WOP scenario and 258 mm (178 grams) for the Steady Flow scenario, compared to 275 mm (226 grams) under Existing Conditions. If spawning is included, growth at the end of 4 years is predicted to be 301 mm (297 grams) for the WOP spawning scenario and 258 mm (186 grams) for the Steady Flow scenario, compared to 273 mm (228 grams) under Existing Conditions. The growth changes are smaller when spawning is included due to the associated reproductive energy demands. The WOP scenario shows higher growth because the peak daily temperatures are lower. The Steady Flow scenario shows lower growth because the mean daily temperatures are higher (less favorable for growth) even though the diel fluctuations are somewhat reduced.

Similar alternative calculations were performed using back-calculated P values from the Keno reach to estimate a possible upper bound of trout growth effects in

the J.C. Boyle peaking reach in the absence of peaking operations (i.e., WOP or Steady Flow scenarios) (Figure 50 and Table 11). Assuming that the alternative flow regimes (no peaking) increase food consumption to a constant P value of 0.75 as was calculated in the Keno reach for the first two years of fish growth, predicted growth of trout in the J.C. Boyle peaking reach at the end of 4 years is 440 mm (868 grams) for the WOP scenario and 381 mm (576 grams) for the Steady Flow scenario, compared to 275 mm (226 grams) under Existing Conditions. Again the growth changes for the spawning alternative are smaller (see Figure 50 and Table 11).

Because the assumed change in food availability (P value) is much larger than the change in temperature regime between Existing Conditions and the flow scenarios, the change in food caused most of the change in predicted growth. However, application of the Keno reach P value to the J.C. Boyle peaking reach, as done here, may not be realistic (see Discussion).

Foraging Model Growth Predictions for the WOP and Steady Flow Scenarios
The foraging model predictions of changes in growth for the WOP and Steady Flow scenarios, assuming drift densities increase to the level observed in the Keno reach or the level below Iron Gate dam, are shown in Figure 51 and Table 11. Using the Keno reach observed drift density, predicted growth of trout in the J.C. Boyle peaking reach at the end of 4 years is 371 mm (511 grams) for the WOP scenario and 332 mm (376 grams) for the Steady Flow scenario, compared to 274 mm (212 grams) under Existing Conditions. If drift density is assumed to increase to the level found below Iron Gate Reservoir (Table 3, Trees of Heaven) or 67% of the increase assumed using the Keno reach drift density, growth of trout in the J.C. Boyle peaking reach at the end of 4 years is 355 mm (451 grams) for the WOP scenario and 320 mm (339 grams) for the Steady Flow scenario, compared to 274 mm (212 grams) under Existing Conditions.

4 Discussion and Summary

On average, trout observed in the Klamath River were using depth and velocity combinations similar to those that would be expected for drift feeding salmonids. They typically used microhabitats where there was a higher velocity on one side and a slightly lower velocity on the other side (Figures 3-5). With respect to vertical velocity, fish were using focal velocities that were lower than the mean column velocity and their focal velocities were typically lower than would be expected from an average vertical velocity profile (e.g., using focal locations where velocity was sheltered by an upstream object) (Figure 7).

The bioenergetics foraging model predictions (a priori) of depth and velocity suitability, based on daily net energy intake (DNEI) for different sizes of fish, matched the observed depth and velocity use patterns accurately (Figures 11-15 and Figure 16-19). Because the bioenergetics foraging model is based on the mechanisms of drift feeding and laboratory derived bioenergetics data, and because the results match the observed fish locations, it can be used with reasonable confidence to assess issues related to the affect of adjacent velocities on habitat suitability modeling.

A sensitivity analysis of different adjacent velocity combinations showed that one of the initial concerns of this report, potential biases in habitat modeling due to using mean column velocity criteria, could not be detected. Fish can and do take advantage of adjacent velocity (lateral and vertical) to enhance foraging (Figure 22-25). These velocity fields are not accounted for in typical PHABSIM modeling except via an implicit correlation between mean column velocity and the vertical velocity profile. However, given the hydraulic data available (mean column velocity on cross-sections), we could ascertain no biologically significant difference between model results using standard PHABSIM analysis and applying a foraging model that accounts for the adjacent velocity field and vertical velocity profiles (Figures 26-29 and Figures 30-33). For modeling an overall habitat versus flow relationship, essentially the same results were obtained using either the measured suitability curves and standard PHABSIM modeling, or using a more sophisticated adjacent velocity modeling approach like the bioenergetics foraging model.

At an individual fish location level we are relatively confident that if better velocity data were available (e.g., full 3D velocity field which is not practical at the present) that some locations that were assumed to be suitable using standard

PHABSIM modeling would not be suitable to fish and vice versa. Thus, given better velocity data a more sophisticated analysis method like the foraging model would likely do a better job of predicting habitat. However, we are uncertain whether in the aggregate (summation of all suitable habitat) the habitat versus flow relationships would be appreciably different. Irregardless, full 3D modeling of velocity fields is not standard practice in instream flow modeling and at the present is only practical on a small-scale research basis.

It appears from the foraging modeling results and the empirical fish size data collected in the project reaches that large fish growth (e.g., 400+ mm) in the Klamath River is limited by the combination of high temperature and drifting food availability. This is in spite of the fact that drift density information indicates that drift density is relatively high in the Project reaches. The high temperatures in the Klamath River require large fish to maintain very high consumption rates to maintain weight. A review (Appendix D) of invertebrate drift density literature suggests that daytime drift density for many rivers is in the range of 0.005 to 0.3 prey/ft^3. Drift density measured in the Keno reach was particularly high (0.63 and 0.14 prey/ft^3, July and September, respectively), and drift densities were lower, but still well within the range reported in the literature in the J.C. Boyle bypass and peaking reaches (Bypass Reach 0.068 and 0.059 prey/ft^3, Upper Peaking Reach 0.183 and 0.025 prey/ft^3, Lower Peaking Reach 0.059 and 0.018 prey/ft^3, July and September, respectively).

In all of the Klamath River reaches drift density declined in the late summer and early fall. This is typical of temperate streams. The reason for consistently higher drift density in the Keno reach is uncertain, but may partially be due to more stable flows (i.e., no peaking) and/or more productive (eutrophic) water quality from organic matter moving in a downstream direction from Upper Klamath Lake and Keno reservoir (K. Carlson, CH2M HILL, pers. comm., observations based on information from water quality monitoring and modeling conducted by PacifiCorp).

Using the rainbow trout temperature-growth relationship developed in this report (laboratory data of From and Gorm (1984)) and the temperature regimes from the Existing Conditions temperature modeling, we calculated the annual percent of maximum consumption (P value) required to meet observed four-year growth in the Keno reach, J.C. Boyle bypass reach, and J.C. Boyle peaking reach. Modeling was based on both the assumption that no spawning was occurring and the assumption that spawning was occurring (Table 10). The amount of spawning occurring in these reaches is uncertain. Overall, P values were generally highest in

the Keno reach and lowest in the J.C. Boyle bypass reach. P values in the J.C. Boyle peaking and bypass reaches decreased with fish size, suggesting that there is likely a limitation on food availability for larger trout in the existing temperature regime. While there is a paucity of P value data available for river fish, a recent study of 16 rivers in Minnesota showed nearly an identical decline in summer P values for brown trout as they increased in size (years one through four) (Dieterman et al. 2004, see Table 3). In contrast, P values for the Keno trout increased significantly for years three and four.

The high P values in the Keno reach indicate these fish are acquiring more food than trout in the other reaches. The increasing P values in years three and four in the Keno reach may indicate that as these fish get larger they are switching to a more abundant and/or higher energy prey source than invertebrate drift (e.g., forage fish) and/or migrating and modifying their temperature regime (e.g., moving into J.C. Boyle reservoir or out of Keno reservoir). Migratory behavior was recently inferred as the reason some trout in a New Zealand river are much larger than others (Young and Hayes 1999). The foraging model for drift feeding fish (discussed below) also suggests that larger fish in the Keno reach likely cannot be sustained on the observed drift rates in the existing temperature regime.

Using the P value temperature-growth model and the calculated P values based on Existing Conditions to predict growth in the J.C. Boyle peaking reach (i.e., assuming food availability does not change), we estimated increased growth for the WOP scenario and decreased growth for the Steady Flow scenario (Figure 49). Results, when spawning costs were included, were similar, but with smaller changes. The WOP scenario showed more growth because the peak daily temperatures were predicted to be lower. The Steady Flow scenario showed less growth because the mean daily temperatures were predicted to be higher even though the diel fluctuations were reduced.

Based on the assumption that a no-peaking scenario would increase food levels in the J.C. Boyle peaking reach so that P values would match those observed in the Keno reach (0.75) (where peaking does not occur), the temperature-growth relationship predicted appreciably more growth for the Steady Flow and WOP scenarios than the Existing Conditions scenario. Again, growth increases based on the assumption that fish spawn in years three and four were less than when spawning was not included because the fish had to make up for an annual loss of 46% of their energy each year they spawned.

It is important to note that while the application of Keno-reach P value to the J.C. Boyle peaking reach seems to be a rational approach to modeling growth, it may not provide realistic results. The high P values in the Keno reach may be partially a product of organic matter inflows to the reach from Upper Klamath Lake and Keno Reservoir, which may increase the productivity of the reach. In addition, keeping the P value constant as fish get larger may not be realistic. For the Keno reach trout, the P value increased in years three and four. As mentioned above, this may be due a diet switch to forage fish and/or migratory behavior. The foraging model based on invertebrate drift could not replicate year three and four growth in the Keno reach and indicated decreased growth potential as fish got larger.

The foraging model accurately predicted Existing Conditions growth in the J.C. Boyle peaking reach using the observed invertebrate drift density (assuming no spawning was occurring). This provides some measure of confidence in the foraging model's ability to accurately predict changes in growth in the J.C. Boyle peaking reach for different flow scenarios. The same foraging model accurately predicted growth of Keno reach trout in years one and two using the observed drift density, but under-predicted growth in the Keno reach in years three and four. This provides some additional evidence that fish in the Keno reach may be switching to a different source of prey or modifying their temperature regime through migration. The foraging model, however, over-predicted observed growth in the J.C. Boyle bypass reach. It would be necessary to decrease the temperature and/or observed drift density inputs to the model to match the slow growth observed in the J.C. Boyle bypass reach.

The bioenergetics foraging model was used to provide our best assessment of the potential upper bound of growth in the J.C. Boyle peaking reach if both temperature and food change with the WOP and Steady Flow scenarios. Drift density was increased in the peaking reach to either that observed in the Keno reach (0.139 prey/ft^3 in early September) or the highest of that observed at several sites (Tree of Heaven) below Iron Gate dam (0.094 prey/ft^3 in early September) (Hardy and Addley 2001). We chose to use the highest drift density site below Iron Gate because the drift density is approximately midway between the high drift density found in the Keno reach and the average drift density observed at the nearest four sites below Iron Gate dam. For example, if a linear gradient of drift density occurred between the upper and lower river (Keno reach to below Iron Gate dam sites), this drift density would be the approximate mid point. It is probably the most reasonable "upper bound" estimate of drift density we could provide for the J.C. Boyle peaking reach WOP and Steady Flow scenarios based on

the available information. Using the drift density assumption from below Iron Gate dam (Tree of Heaven), growth at the end of 4 years was predicted to be 355 mm (451 grams) for the WOP scenario and 320 mm (339 grams) for the Steady Flow scenario, compared to 274 mm (212 grams) under Existing Conditions (Figure 51).

The results of the bioenergetics foraging model and P value model runs indicate that food availability is more important than water temperature as a factor in trout growth in the J.C. Boyle peaking reach for the WOP and Steady Flow scenarios. There is relatively little difference in four-year growth predictions between Existing Conditions, Steady Flow, and WOP scenarios in the J.C. Boyle peaking reach when only changes in water temperature were incorporated into the modeling. This happened because there was only a relatively small difference in daily temperatures between the three scenarios relative to the temperature-related growth requirements of trout. The biggest effect on predicted growth came from the assumption that increased invertebrate drift/ food availability would occur under the WOP and Steady Flow scenarios. The most uncertainty exists in this parameter, however. Based on the literature, food would likely increase, but the amount is uncertain. The invertebrate drift densities observed below Iron Gate dam or in the Keno reach provide a reasonable upper bound on the increase that could occur in the J.C. Boyle peaking reach. Actual drift density and growth for the WOP and Steady Flow scenarios may be somewhere between what they are now with Existing Conditions and this upper bound.

It is important to note that it was not our task to address acute temperature tolerance, and growth was modeled irrespective of any potential acute (short duration) temperature affects on fish. Peak daily summer temperatures, particularly those in the Keno reach, are in the range where research literature has indicated acute affects can occur (e.g., Hokanson et al. 1977; Rodnick et al. 2004).

In diel fluctuating temperature regimes, it has been shown that fish react to a temperature somewhat higher than the mean daily temperature (i.e., they acclimate to the higher temperatures faster than the lower temperatures). The temperature they react to is somewhere between the mean and maximum daily temperature (e.g., Hokanson 1977, Cox and Coutant 1981). We incorporated the findings of Hokanson et al. (1977) into both the foraging model and the P value growth model used in this analysis. The result was that fluctuating daily temperature produced lower growth at high temperature than the equivalent mean daily temperature regime. As a result, a lower maximum daily temperature, such as occurs for the WOP scenario, causes the models to predict more growth during the summer when

temperatures are too high for good fish growth even if the mean daily temperature is nearly the same (actually for the WOP scenario the mean daily temperature also declined slightly). Conversely, for the Steady Flow scenario, daily temperature fluctuations during the summer are predicted to be less than Existing Conditions, but the mean daily temperatures during the summer are higher for the Steady Flow scenario, which outweighs the benefit of slightly decreased peak temperatures and the model predicts less growth (if only temperature and not food increases are assumed for the scenario).

5 References

Addley, R.C. 1993. A mechanistic approach to modeling habitat needs of drift-feeding salmonids. Masters Thesis. Utah State University, Logan.

Alan, J.D. 1987. Macroinvertebrate drift in a Rocky Mountain stream. *Hydrobiologia,* 144:261-268.

Beecher, H.A. 1987. Simulating trout feeding stations in instream flow models. In *Regulated Streams — Advances in Ecology* (Kemper, J.B., J. Craig, ed.) pp. 71-82. Plenum Press, New York.

Cellot, B. 1996. Influence of side-arms on aquatic macroinvertebrate drift in the main channel of a large river. *Freshwater Biology*, 35:149-164.

Clarke, M.E., K.A. Rose. 1997. Individual-based model of stream-resident rainbow trout and brook char: model description, corroboration, and effects of sympatry and spawning season duration. *Ecological Modeling*, 94: 157-175.
Clifford, H. F. 1972. A years' study of the drifting organisms in a brown-water stream of Alberta, *Canadian Journal of Fisheries and Aquatic Sciences,* 50:975-983.

Cox, D.K. and C. C. Coutant. 1981. Growth dynamics of juvenile striped bass as functions of temperature and ration. *Transactions of the American Fisheries Society*, 110:226-238.

Crowder, D.W., P. Diplas. 2000. Evaluating spatially explicit metrics of stream energy gradients using hydrodynamic model simulations. *Canadian Journal of Fisheries and Aquatic Sciences*, 57: 1497-1507.

Cushman, R.M. 1985. Review of ecological effects of rapidly varying flows downstream from hydroelectric facilities. *North American Journal of Fisheries Management,* Vol.5: 330-339.

Dickerson, B.R. and G.L. Vinyard. 1999. Effects of high chronic temperatures and diel temperatures cycles on the survival and growth of Lahontan cutthroat trout. *Transactions of the American Fisheries Society,* 128:516-521.

Dieterman, D.J., W.C. Thorn, and C.S. Anderson. 2004. Application of a bioenergetics model for brown trout to evaluate growth in Southeast Minnesota streams. *Minnesota Department of Natural Resources Investigational Report 513.*

Elliott, J.M. 1975a. The growth rate of brown trout (Salmo trutta L.) fed on maximum rations. *Journal of Animal Ecology,* 44:805-821.

Elliott, J.M. and M.A. Hurley. 1999. Anew energetics model for brown trout, Salmo trutta. *Freshwater Biology*, 42:235-246.

Fausch, K.D. 1984. Profitable stream positions for salmonids: relating specific growth rate to net energy gain. *Canadian Journal of Fisheries and Aquatic Sciences*, 62: 441-451.

Fausch, K.D., R.J. White. 1981. Competition between brook trout (*Salvelinus fontinalis*) and brown trout (*Salmo trutta*) for positions in a Michigan stream. *Canadian Journal of Fisheries and Aquatic Sciences*. 38: 1220-1227.

Field-Dodgson, M. S. 1985. A simple and efficient drift sampler. *New Zealand Journal of Freshwater Research,* 19: 167–172.

From, J. and G. Rasmussen. 1984. A growth model, gastric evacuation, and body composition in rainbow trout, *Salmo gairdneri* Richardson, 1836. *Dana*, 3:61-139.

Guensch, G.R., T.B. Hardy, R.C. Addley. 2001. Examining feeding strategies and position choice of drift-feeding salmonids using an individual-based, mechanistic foraging model. *Canadian Journal of Fisheries and Aquatic Sciences*. 58: 446-457.

Hanson, P.C., T.B. Johnson, D. E. Schindler and J. F. Kitchell. 1997. Fish bioenergetics 3.0 for Windows. University of Wisconsin Sea Grant Institute, Madison.

Hardy, T.B., and R.C. Addley. 2001. Evaluation of Interim Instream Flow Needs in the Klamath River Phase II Draft Final Report. Report prepared for US Dept. Interior by Institute of Natural Systems Engineering, Utah State University, Logan, Utah.

Hayes, J.W., I.G. Jowett. 1994. Microhabitat models of large brown trout in three New Zealand rivers. *North American Journal of Fisheries Management*. 14: 710-725.

Hayes, J.W., J.D. Stark, K.A. Shearer. 2000. Development and test of a whole-lifetime foraging and bioenergetics growth model for drift-feeding brown trout. *Transactions of the American Fisheries Society*, 129: 315-332.

Hayes, J.W.; Hughes, N.F.; Kelly, L.H. 2003. Overview of a process-based model relating stream discharge to the quantity and quality of brown trout habitat. Proceedings of the International IFIM Workshop. Fort Collins, Colorado, June 2003.

Hokanson, K.E.F., C.F. Kleiner, and T.W. Thorslund. 1977. Effects of constant temperatures and diel temperature fluctuations on specific growth and mortality rates and yield of juvenile rainbow trout, *Salmo gairdneri*. *Journal of the Fisheries Research Board of Canada*, 34:639-648.

Hughes, N.H. and L. Dill. 2005. The geometry, dynamics, and energetics of prey interception by drift-feeding fish: a model and test using Arctic grayling *Thyumallus arcticus*. *Canadian Journal of Fisheries and Aquatic Sciences*, (accepted).

Hughes, N.H., J.W. Hayes, K.A. Shearer, and R.G. Young. 2003. Testing a Model of drift-feeding using three-dimensional videography of wild brown trout, *Salmo trutta*, in a New Zealand river. *Canadian Journal of Fisheries and Aquatic Sciences*, 60:1462-1476.

Hill, J., G.D. Grossman. 1993. An energetic model of microhabitat use for rainbow trout and rosyside dace *Ecology*, 74: 685-698.

Higgs, D.A., J.S. Macdonald, C.D. Levings, and B.S. Dosanjh. 1995. Nutrition and feeding habits in relation to life history stage. Pp. 159-316. *In:* C. Groot, L. Margolis, and W.C. Clarke [Editors]. Physiological ecology of Pacific Salmon. UBC Press, Vancouver, B.C.

Hughes, N.F. 1998. A model of habitat selection by drift-feeding stream salmonids at different scales. *Ecology*, 79(1):281-294.

Hughes, N.F., L.M. Dill. 1990. Position choice by drift-feeding salmonids: model and test for Arctic grayling (*Thymallus arcticus*) in subarctic streams, interior Alaska. *Canadian Journal of Fisheries and Aquatic Sciences*, 47: 2039-2048.

Hughes, N.F. 1992. Selection of positions by drift feeding salmonids in dominance hierarchies: model and test for Arctic grayling (*Thymallus arcticus*) in subarctic mountain streams, interior Alaska. *Canadian Journal of Fisheries and Aquatic Sciences*, 49: 1999-2008.

Instream Flow Council, 2002. Instream flows for riverine Resources stewardship: Instream Flow Council, 411 p.

Kelly, L. H. 2003. 3 d patterns of invertebrate drift density: a model and test in a New Zealand trout stream. Proceedings of the IFIM Users Workshop 1- 5 June, Fort Collins, Colorado.

Moog, O. 1993. Quantification of daily peak hydropower effects on aquatic fauna and management to minimize environmental impacts. *Regulated rivers: Research and Management,* Vol.8: 5-14.

Morgan, R.P.II, R.E. Jacobsen, S.B. Weisberg, L.A. McDowell, H.T. Wilson. 1991. Effects of flow alteration on benthic macroinvertebrate communities below the Brighton hydroelectric dam. *Journal of Freshwater Ecology,* Vol.6(4): 418-429.

Myrick, C.A. and J.J. Cech. 2000. Temperature influences on California rainbow trout physiological performance. *Fish Physiology and biochemistry*, 22:245-254.

Nislow, K.H., C.L. Folt, D.L. Parrish. 2000. Spatially explicit bioenergetics analysis of habitat quality for age-0 Atlantic salmon. *Transactions of the American Fisheries Society*. 129: 1067-1081.

PacifiCorp. 2004. Fish Resources. Final Technical Report. Klamath Hydroelectric Project (FERC Project No. 2082). February 2004.

Railsback, S.F., B.C. Harvey, R.H. Lamberson, D.E. Lee, N.J. Claasen, S. Yoshihara. 2002. Population-level analysis and validation of an individual-based cutthroat trout model. *Natural Resource Modeling*. 15: 83-110.

Railsback, S.F., and K.A. Rose. 1999. Bioenergetics modeling of stream trout growth: Temperature and food consumption effects. *Transactions of the American Fisheries Society*,128:241-256.

Rand, P.S, D.J. Stewart, P.W. Seelbach, M.L. Jones, and L.R. Wedge. 1993. Modeling steelhead population energetics in Lakes Michigan and Ontario. *Transactions of the American Fisheries Society*, 122:977-1001.

Rantz, S.E. and others. 1982. Measurement and computation of streamflow: Volume1. measurement of stage and discharge. US Geological Survey Water-Supply Paper 2175.

Rasmussen, G. and J. From.1991. Improved estimates of a growth model and body composition of rainbow trout, Oncorhynchus mykiss (Walbaum, 1792) as function of feeding level, temperature and body size. *Dana*, 9:15-30.

Rodnick K.J., A.K. Gamperl, K.R. Lizars, M.T. Bennett, R.N. Rausch and E.R. Keeley. 2004. Thermal tolerance and metabolic physiology among redband trout populations in south-eastern Oregon. *Journal of Fish Biology*, 64:310-335.

Spigarelli, S.A., M.M. Thommes and W. Prepejchal. 1982. Feeding, growth, and fat deposition by brown trout in constant and fluctuating temperatures. *Transactions of the American Fisheries Society*,111:199-209.

Stewart, D.J. 1980. Salmonid predators and their forage base in Lake Michigan: a bioenergetics-modeling synthesis. Ph.D. dissertation, University of Wisconsin, Madison, Wis.

Thomas, R.E., J.A. Gharrett, M.G. Carls, S.D. Rice, A. Moles, and S. Korn. 1986. Effects of fluctuating temperature on mortality, stress, and energy reserves of juvenile coho salmon. *Transactions of the American Fisheries Society*,115:52-59.

Van Winkle, W., H.I. Jager, S.F. Railsback, B.D. Holcomb, T.K. Studley, J.E. Baldrige. 1998. Individual-based model of sympatric populations of brown and rainbow trout for instream flow assessment: model description and calibration. *Ecological Modeling*. 110: 175-207.

Young, R. G., and J.W. Hayes. 1999. Trout energetics and effects of agricultural land use on the Pomahaka trout fishery. *Cawthron Institute, Cawthron Report 455, Nelson, New Zealand.*

6 Tables

Table 1. Comparison of the approximate vertical shear above fish and lateral shear to the side of fish from data measured in 2003. Calculated vertical shear is based on the depth specific velocity profiles Figure 8 and the mean depth and velocity in this table.

Fish Size	Mean Depth Observed (ft)	Mean Velocity observed (ft/s)	Calculated Vertical Shear 1 ft Above Fish (ft/s/ft)	Measured Lateral Shear 1 ft Lateral to the Fish* (ft/s/ft)
30-50 mm	1.3	0.4	0.17	0.20
>50-150 mm	1.7	0.8	0.22	0.24
>150-400 mm	3.3	1.3	0.35	0.49

Note: the measured lateral shear is calculated in section 3.1.1.1 and is based on mean column velocity.

Table 2. Percentage of prey in each size class based on data collected in the J.C. Boyle peaking reach in September of 2002 (PacifiCorp 2004) (limited sampling) and data collected by Hardy and Addley (2001) in the lower river below Iron Gate Dam (R-Ranch).

Length (mm)	Peaking Reach	R-Ranch
11	0.0%	1.8%
9	0.7%	0.9%
7	3.1%	1.4%
5	17.4%	21.3%
3	52.3%	50.2%
1	26.4%	24.4%

Table 3. Drift density (prey/ft^3), number of samples (n) and standard deviation for sites below Iron Gate Dam (Hardy and Addley 2002). For a map of the sampling locations see Appendix E.

	Aug-Sep			Nov			Mar-Apr		
Site	Mean	n	Std dev	Mean	n	Std dev	Mean	n	Std dev
R-Ranch	0.074	8	0.055				0.012	9	0.014
Tree of Heaven	0.094	15	0.048				0.011	9	0.007
Brown Bear	0.023	8	0.010				0.004	9	0.004
Seiad	0.050	9	0.038	0.010	5	0.010	0.010	9	0.004
Rodgers Cr.	0.023	9	0.018						
Orleans							0.001	9	0.002
Weitchpec	0.028	9	0.020				0.004	9	0.004
Youngs Bar	0.024	6	0.021				0.002	9	0.001

Table 4. 2004 drift data collected in the Klamath River in the Keno Reach, J.C. Boyle Bypass Reach, J.C. Boyle Upper Peaking Reach and Lower Peaking Reach.

	Late June/ Early July 2004				Early September 2004			
			Upper	Lower			Upper	Lower
	Keno	Bypass	Peaking	Peaking	Keno	Bypass	Peaking	Peaking
Avg # / ft^3	0.629	0.068	0.183	0.059	0.139	0.059	0.025	0.018
# Samples	18	12	12	18	18	12	12	12
Std Dev.	0.497	0.035	0.223	0.019	0.085	0.027	0.011	0.009
Avg Size mm	3.444	2.746	3.336	3.230	3.207	2.956	3.246	3.359

Table 5. Size of 2004 drift data collected in the Klamath River in the Keno Reach, J.C. Boyle Bypass Reach, J.C. Boyle Upper Peaking Reach and Lower Peaking Reach.

	Total Number of Organisms per Class size for June/July												
June/July	**< 1**	**1-2mm**	**2-4mm**	**4-6mm**	**6-8mm**	**8-10mm**	**10-12mm**	**12-14mm**	**14-16mm**	**16-18mm**	**20-22mm**	**26-28mm**	**Total number of bugs**
Bypass	264	118	701	252	14	1	1	0	1	0	1	0	1353
Keno	221	1245	11986	4814	1064	50	0	4	0	0	0	4	19388
Lower Peaking	56	48	1283	267	14	4	1	1	0	0	0	0	1674
Upper Peaking	40	608	858	324	25	7	3	0	0	1	0	0	1866
	Fraction of Total by Size Class												
Bypass J	0.195	0.087	0.518	0.186	0.010	0.001	0.001	0.000	0.001	0.000	0.001	0.000	
Keno J	0.011	0.064	0.618	0.248	0.055	0.003	0.000	0.000	0.000	0.000	0.000	0.000	
Lower Peaking J	0.033	0.029	0.766	0.159	0.008	0.002	0.001	0.001	0.000	0.000	0.000	0.000	
Upper Peaking J	0.021	0.326	0.460	0.174	0.013	0.004	0.002	0.000	0.000	0.001	0.000	0.000	
	Total Number of Organisms per Class size for September												
September													
Bypass	38	291	763	214	29	3	0	0	0	1	0	0	1339
Keno	18	157	1901	311	31	5	0	0	0	0	0	0	2423
Lower Peaking	6	21	266	140	22	5	2	0	0	0	0	0	462
Upper Peaking	22	38	290	99	26	6	0	0	0	0	0	0	481
	Fraction of Total by Size Class												
Bypass S	0.028	0.217	0.570	0.160	0.022	0.002	0.000	0.000	0.000	0.001	0.000	0.000	
Keno S	0.007	0.065	0.785	0.128	0.013	0.002	0.000	0.000	0.000	0.000	0.000	0.000	
Lower Peaking S	0.013	0.045	0.576	0.303	0.048	0.011	0.004	0.000	0.000	0.000	0.000	0.000	
Upper Peaking S	0.046	0.079	0.603	0.206	0.054	0.012	0.000	0.000	0.000	0.000	0.000	0.000	
	Combined Reaches Fraction of Total by Size Class												
AVG Sept. and July	0.0445	0.1141	0.6120	0.1956	0.0279	0.0046	0.0009	0.0001	0.0001	0.0002	0.0001	0.0000	
AVG Sept.	0.0236	0.1016	0.6333	0.1993	0.0340	0.0069	0.0011	0.0000	0.0000	0.0002	0.0000	0.0000	
AVG July	0.0654	0.1265	0.5906	0.1919	0.0217	0.0024	0.0007	0.0002	0.0002	0.0001	0.0002	0.0001	

Table 6. Seasonal drift density (Prey/ft^3) at the Keno Reach, J.C. Boyle Bypass Reach, J.C. Boyle Upper (Oregon) Peaking, and Lower (California) Peaking reaches. Only the drift density at day 181 (late June) and 247 (early September) are from measured data (see Table 4). The other drift densities are assumed (see text for discussion). Drift density at days not show can be estimated by linear interpolation.

Day of The Year	Keno Reach	Bypass Reach	Oregon Peaking	California Peaking	Average Oregon & California
1	0.010	0.010	0.010	0.010	0.010
91	0.010	0.010	0.010	0.010	0.010
181	0.629	0.068	0.183	0.059	0.121
247	0.139	0.059	0.025	0.018	0.021
305	0.010	0.010	0.010	0.010	0.010
365	0.010	0.010	0.010	0.010	0.010

Table 7. Consumption of moist pellets versus temperature. Calculated from From and Rasmussen (1984) data.

Temperature	Consumption of Moist Pellets=aW^b. W=gram wet weight fish, b=0.7292, a is g consumption/g fish. Fraction Max Consumption	a (Consumption g/g fish)
0	0.06164	0.01000
5	0.30454	0.04940
10	0.57375	0.09307
15	0.78470	0.12730
20.05	1.00000	0.16222
22	0.82754	0.13425
24.3	0.25110	0.04073
25.3	0.00047	0.00008

Table 8. Non-linear regression values for the energy loss (g COD) at measured temperatures. Eloss=a'+a''•P^b', where P is the fraction of maximum consumption.

Coefficient	Temperature C 5	10	15	20	22	24.3
a"	0.002087	0.003503	0.004969	0.007049	0.008107	0.009521
a"	0.032533	0.055308	0.076386	0.103408	0.081724	0.027922
b'	1.257459	1.045704	1.062975	1.064971	0.802816	0.812245

Table 9. Calculated values for A in Equation 4 (Eloss (g COD) =A•W^B) based on Equation 5. Values are for use in 2-way interpolation. The values for 0 C are based on extrapolation of the maximum consumption (P=1) and no consumption (P=0.0) data. Between and beyond P= 1 or 0 the values are linearly interpolated or extrapolated.

P value	Temperature C 0	5	10	15	20	22	24.3
2	0.028200	0.079865	0.117678	0.164557	0.223391	0.150674	0.058551
1.75	0.024790	0.067843	0.102799	0.143439	0.194713	0.136181	0.053511
1.5	0.021381	0.056256	0.088016	0.122511	0.166301	0.121273	0.048334
1.25	0.017971	0.045158	0.073346	0.101802	0.138196	0.105864	0.042992
1	0.014561	0.034620	0.058810	0.081355	0.110457	0.089830	0.037443
0.9	0.013197	0.030583	0.053040	0.073261	0.099481	0.083202	0.035153
0.8	0.011833	0.026661	0.047300	0.065225	0.088584	0.076427	0.032815
0.7	0.010470	0.022862	0.041592	0.057251	0.077776	0.069482	0.030421
0.6	0.009106	0.019201	0.035921	0.049349	0.067068	0.062337	0.027961
0.5	0.007742	0.015695	0.030294	0.041530	0.056476	0.054953	0.025423
0.4	0.006378	0.012366	0.024718	0.033810	0.046021	0.047270	0.022787
0.3	0.005014	0.009246	0.019207	0.026211	0.035737	0.039193	0.020023
0.2	0.003650	0.006386	0.013780	0.018773	0.025677	0.030556	0.017076
0.1	0.002286	0.003885	0.008481	0.011576	0.015953	0.020975	0.013824
0	0.000922	0.002087	0.003503	0.004969	0.007049	0.008107	0.009521

Table 10. Percent of maximum consumption (P values) for the observed fish growth in the J.C. Boyle Peaking, Keno and J.C. Boyle Bypass reaches. The top table is calculated without the assumption that spawning occurs and the bottom table is calculated assuming spawning occurs (annual energy loss of 46% in years 3 and 4).

	Reach (no spawning)		
P Value	Peaking	Keno	Bypass
Yr 1	0.73	0.75	0.57
Yr 2	0.68	0.75	0.41
Yr 3	0.54	0.84	0.32
Yr 4	0.36	0.99	0.29

	Reach (with spawning)		
P Value	Peaking	Keno	Bypass
Yr 1	0.73	0.75	0.57
Yr 2	0.68	0.75	0.41
Yr 3	0.73	1.04	0.45
Yr 4	0.58	1.31	0.44

Table 11. Four-year growth results for the Prey Capture growth model and for the P Value growth model for the Existing, Steady Flow and WOP scenarios. Model assumptions for the Prey Capture model are that drift density with the Steady Flow or WOP scenarios could increase to a maximum of either the drift rate observed in the Keno Reach or the drift rate observed below Iron Gate Reservoir. Model assumptions for the P value growth model (either with or without spawning included) are that either no change in food availability occurs (only temperature changes) or that food availability changes and the P values increase to a constant 0.75 as observed for the fish in the Keno Reach for the first two years.

		Four Year Growth	
Model	Flow Scenario	Weight (gram)	Length (mm)
Foraging Model	Existing	212	274
Keno Reach Drift Rate	Steady Flow	376	332
Sept 4 = 0.139 prey/ft^3	WOP	511	371
*Bl Iron Gate Drift Rate	Steady Flow	339	320
Sept 4 = 0.094 prey/ft^3	WOP	451	355
***P Value Model	Existing	226	275
Temp Change Only	Steady Flow	178	258
	WOP	313	307
**P Value Model	Steady Flow	576	381
Temp and Food Change	WOP	868	440
***P Value Model w/	Existing	228	273
Spawning Temp	Steady Flow	186	258
Change Only	WOP	297	301
**P Value Model w/ Spawning	Steady Flow	296	301
Temp and Food Change	WOP	445	347

* Our best estimate of the upper bound on growth for the WOP and Steady Flow scena

**This is a rational method to estimate the upper bound on growth, but it likely over estimates growth. The P value used (0.75) comes from the Keno reach fish where the productivity may be inflated due to organic material inflow from upstream Klamath Lake. Also the P value remains fixed as fish get larger, when it likely would decline for fish feeding on drift. The results are different depending on whether or not spawning

*** This assumes food availability does not change, only temperature. It is our best estimate of the lower bound of growth for the WOP and Steady Flow scenarios. The results are different depending on whether or not spawning is assumed.

7 Figures

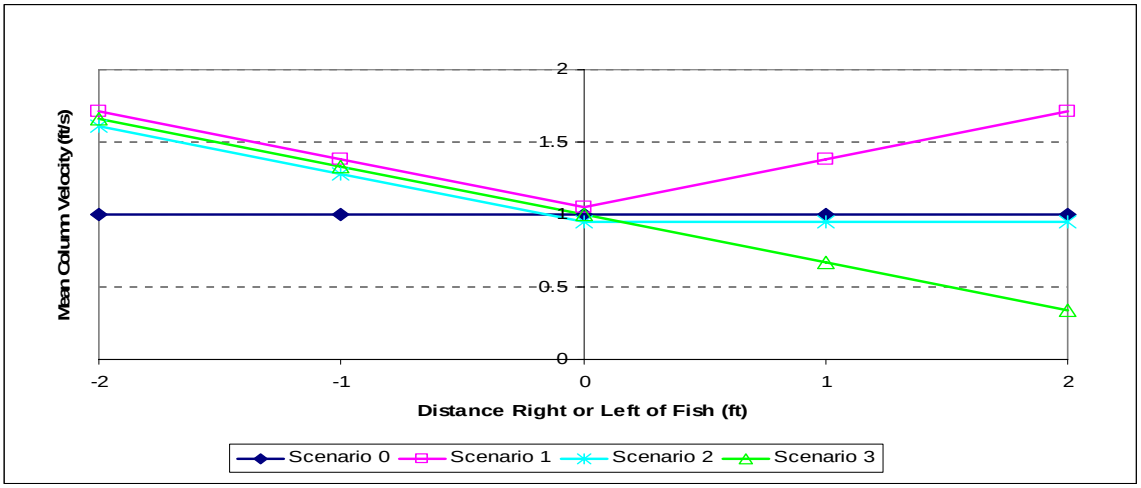

Figure 1. Example of adjacent velocity Scenarios 0, 1, 2, and 3. Scenario 0 has the same mean column velocity adjacent as at the holding location. Scenario 1 has the mean column velocity higher (or lower) on both sides by different fixed rates (ft/s/ft) of 0 – 1.97 ft in 0.164 ft increments). In this case the rate of increase in 0.164 ft/s/ft (5 cm/ft/ft). Scenario 2 has increased mean column velocity on one side but the same velocity as the holding location on the other. Scenario 3 has velocity increasing on one side and declining on the other. Note that the lines were separated in this figure a small amount for visual clarity. (Enlarge to view)

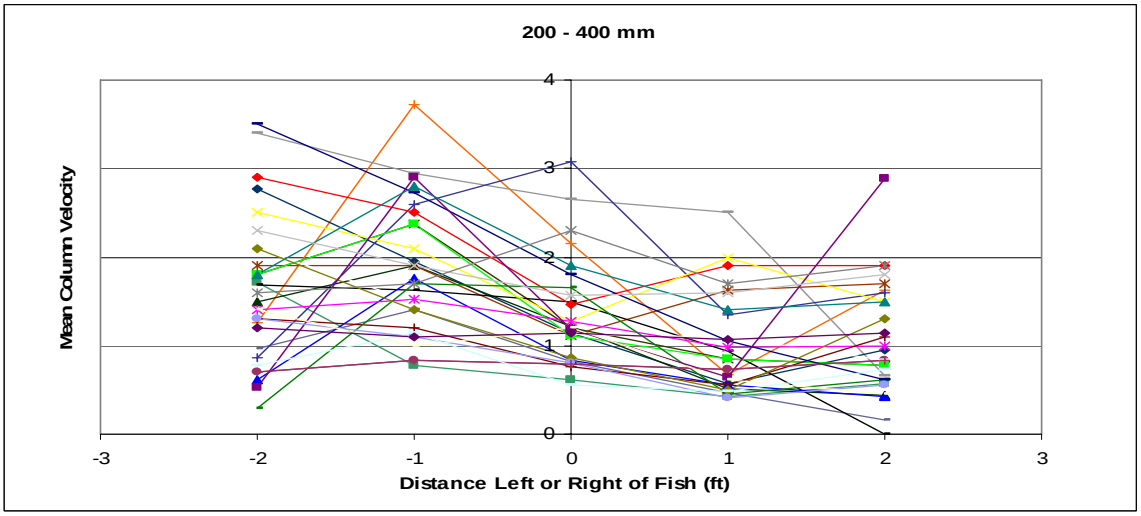

Figure 2. Example plot of collected mean column velocity for fish. Mean velocities are at the fish focal location (distance = 0) and one and two feet from the fish (200 – 400 mm fish). Note that all measurements were rotated so that the highest velocity one foot from the fish plots on the left side (i.e., distance = -1).

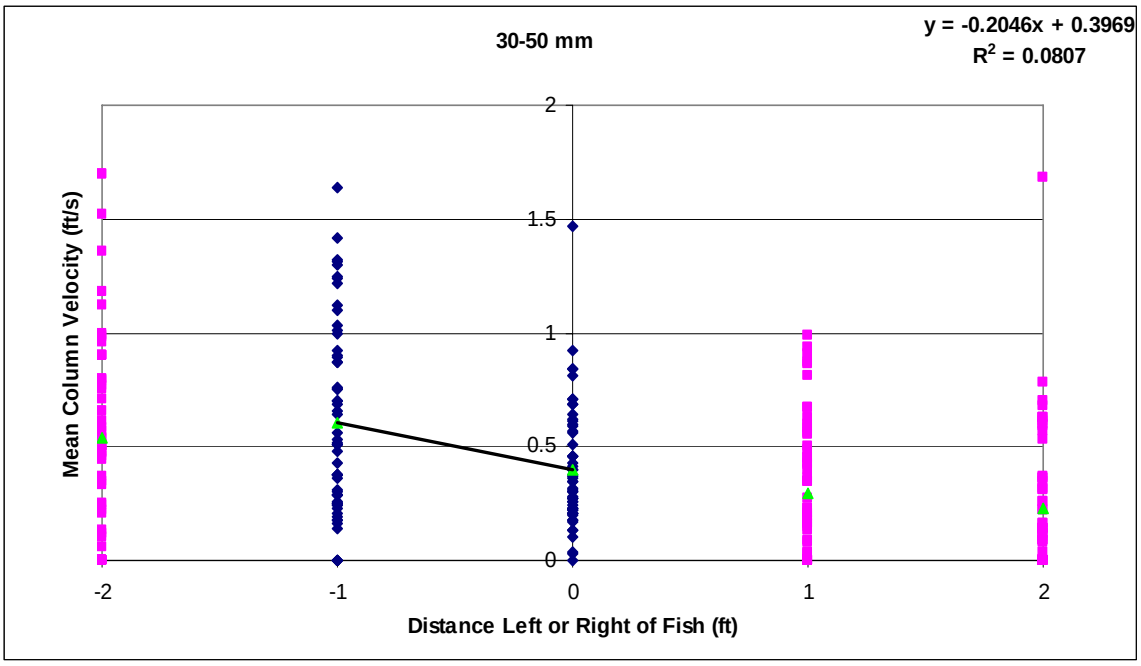

Figure 3. 30-50 mm fish mean column and adjacent mean column velocities. Green triangles are the mean values. The regression line is between velocities at the fish location and one foot from the fish (high velocity side).

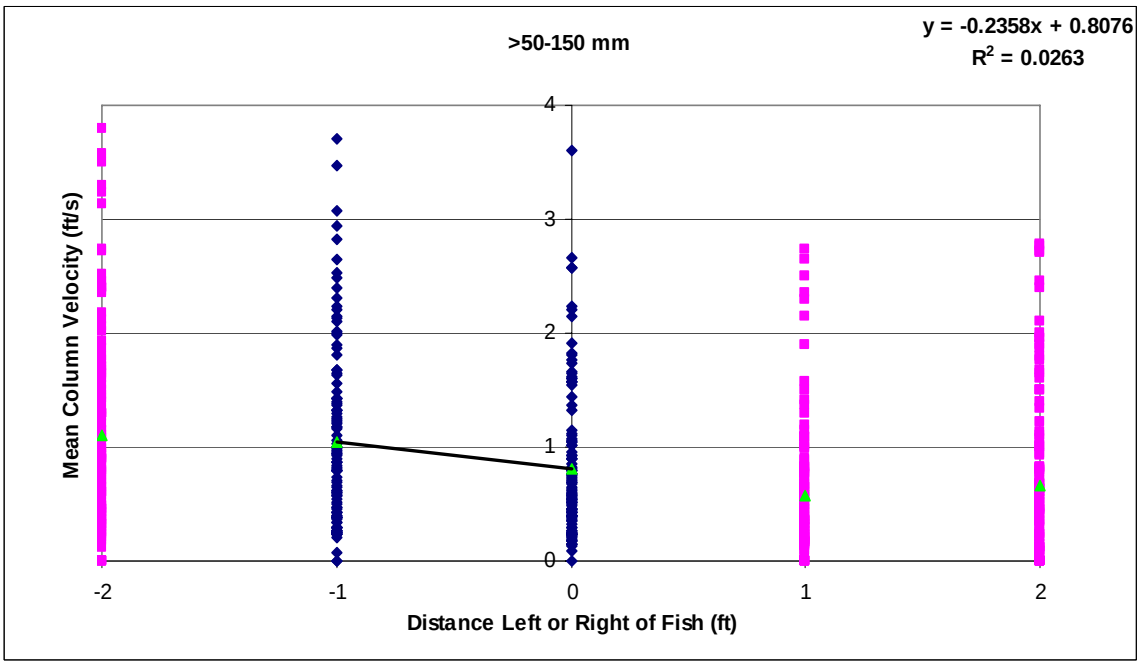

Figure 4. Fish >50-150 mm mean column and adjacent mean column velocities. Green triangles are the mean values. The regression line is between velocities at the fish location and one foot from the fish (high velocity side).

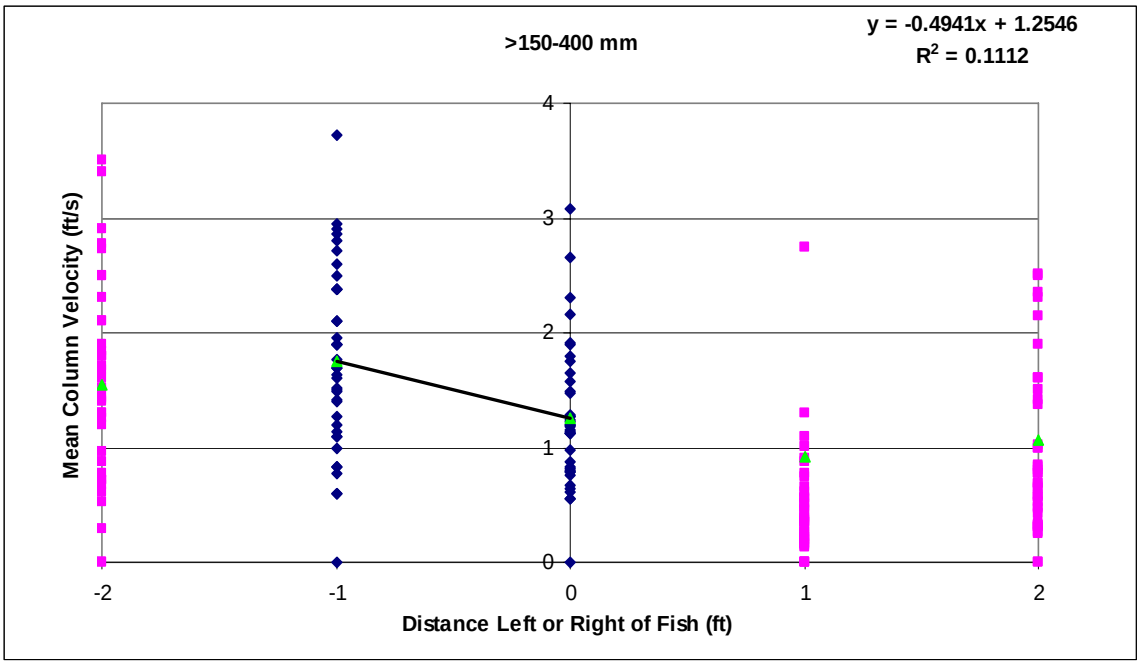

Figure 5. Fish >150-400 mm mean column and adjacent mean column velocities. Green triangles are the mean values. The regression line is between velocities at the fish location and one foot from the fish (high velocity side).

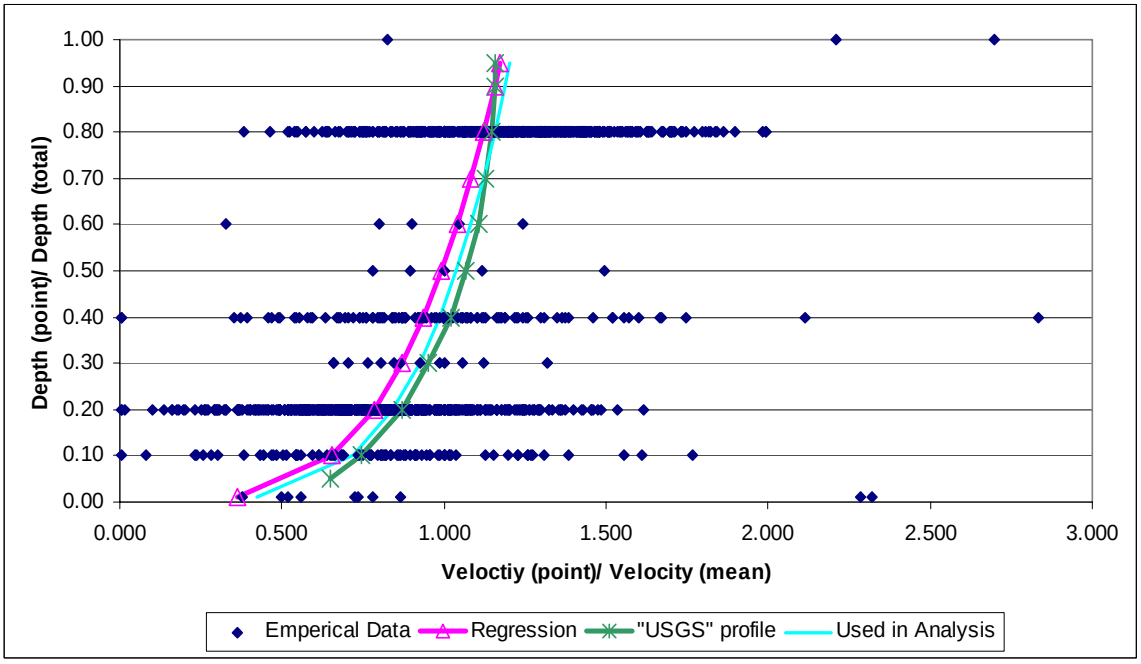

Figure 6. Observed vertical velocity profile data at fish locations along with a regression of the data using equation 1. Also shown are a typical "USGS" profile and the profile we used in the bioenergetics foraging model analysis.

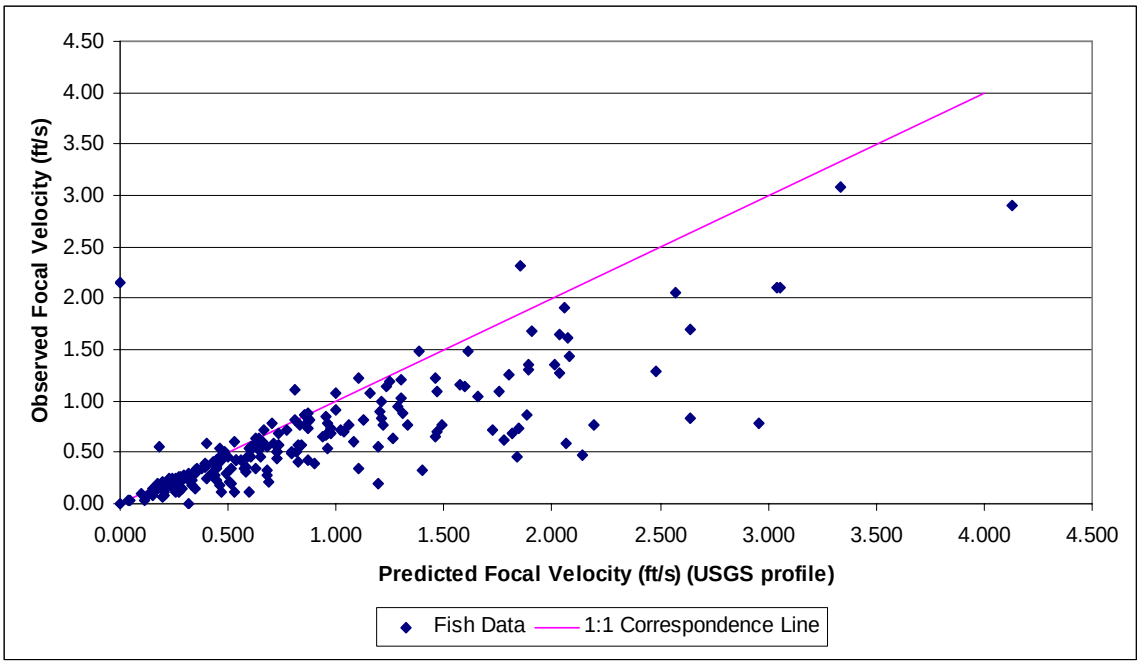

Figure 7. Predicted focal velocity using a typical "USGS" vertical velocity profile versus measured focal velocity for fish. Note that fish are using focal velocities equal to or less (sometimes much less) than would be predicted from a typical velocity profile.

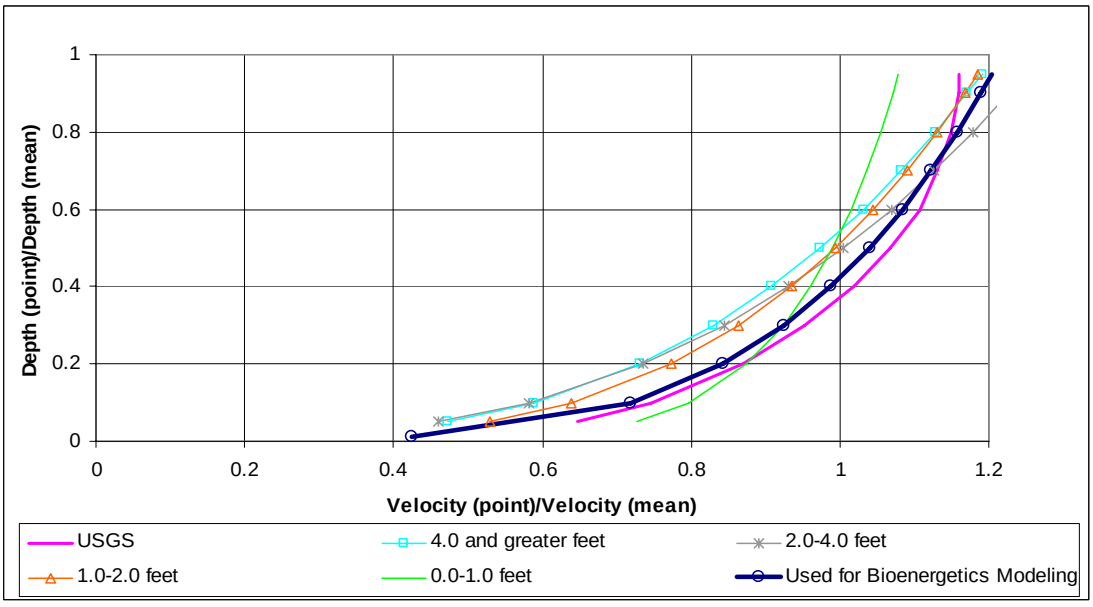

Figure 8. Average vertical velocity profiles in shallow (0.0- 1.0 ft) and deeper water (e.g., 4.0 ft and greater). Velocity gradients are flatter in the deep water and the profiles in deep water are shifted to the left because the average velocities measured in the field are about 10% too low.

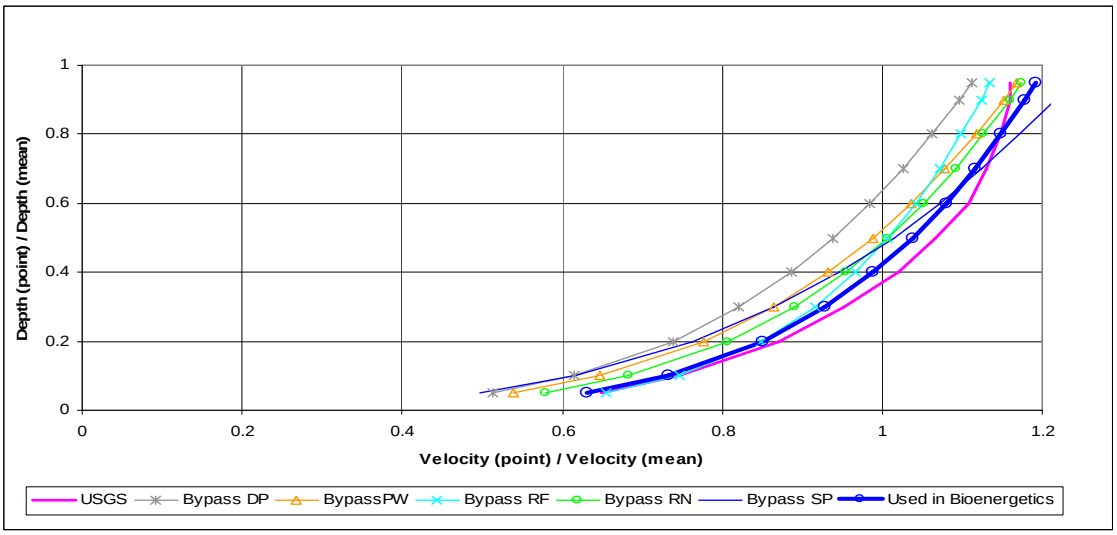

Figure 9. Average vertical velocity profiles in different habitat types in the J.C. Boyle Bypass reach (most of the velocity data were collected in the J.C. Boyle Bypass reach). Habitat types are DP=deep pool, PW=pocket water, SP=shallow pool, RF=riffle, RN=run, and SP=shallow pool. Velocity gradients are flatter in the deep water habitat types and the velocity profiles in deep water habitat types are shifted to the left because the average velocities measured in the field are about 7% too low (for deep pools).

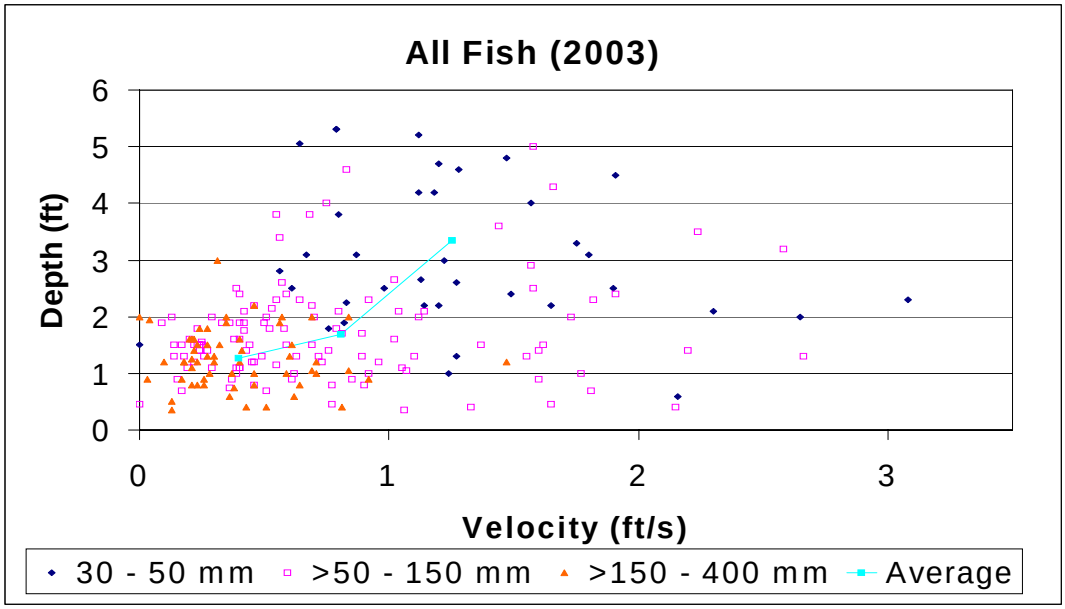

Figure 10. Depth and velocity locations for each 2003 fish grouped by fish size. Fish sizes are 30-50, >50-150, >150-400 mm. Mean velocity for the small, medium and large fish is 0.4, 0.8, and 1.3 ft/s, respectively. Mean depth for the small, medium and large fish is 1.3, 1.7, and 3.3 ft, respectively. The average line connects these mean depths and velocities.

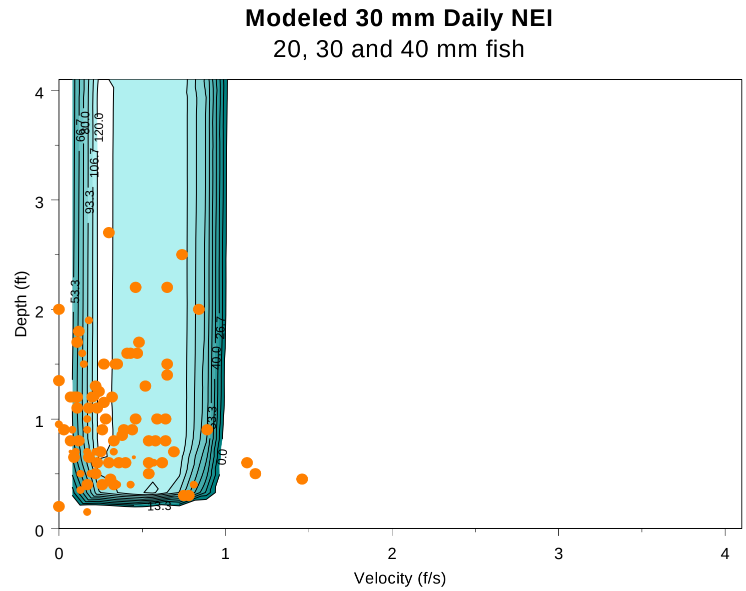

Figure 11. Modeled daily net energy intake for a 30 mm fish overlain with 2002-3 fish locations for 20-40 mm fish (small dots are smaller fish, big dots are bigger fish). Contours are in joules/day. The maximum daily net energy intake is light blue and about 120 joules/day.

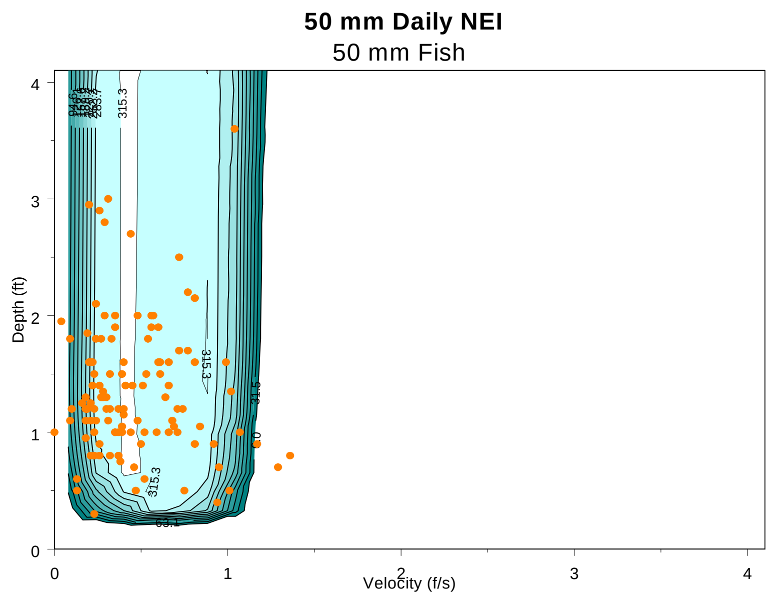

Figure 12. Modeled daily net energy intake for a 50 mm fish overlain with 2002-3 fish locations for 50 mm fish (small dots are smaller fish, big dots are bigger fish). Contours are in joules/day. The maximum daily net energy intake is light blue and about 315 joules/day.

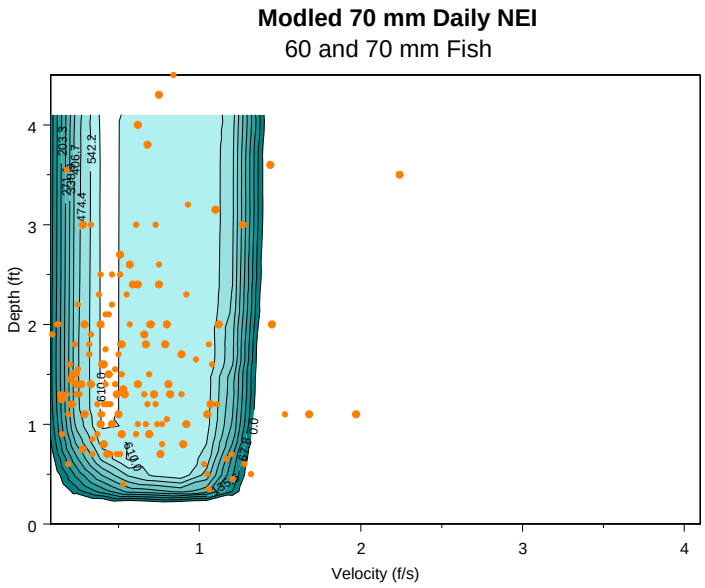

Figure 13. Modeled daily net energy intake for a 70 mm fish overlain with 2002-3 fish locations for 60-70 mm fish (small dots are smaller fish, big dots are bigger fish). Contours are in joules/day. The maximum daily net energy intake is light blue and about 610 joules/day

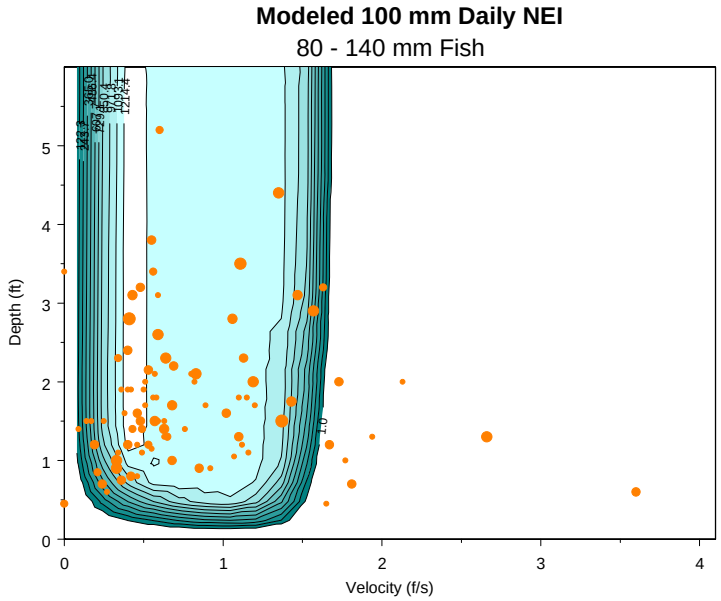

Figure 14. Modeled daily net energy intake for a 100 mm fish overlain with 2002-3 fish locations for 80-140 mm fish (small dots are smaller fish, big dots are bigger fish). Contours are in joules/day. The maximum daily net energy intake is light blue and about 1214 joules/day.

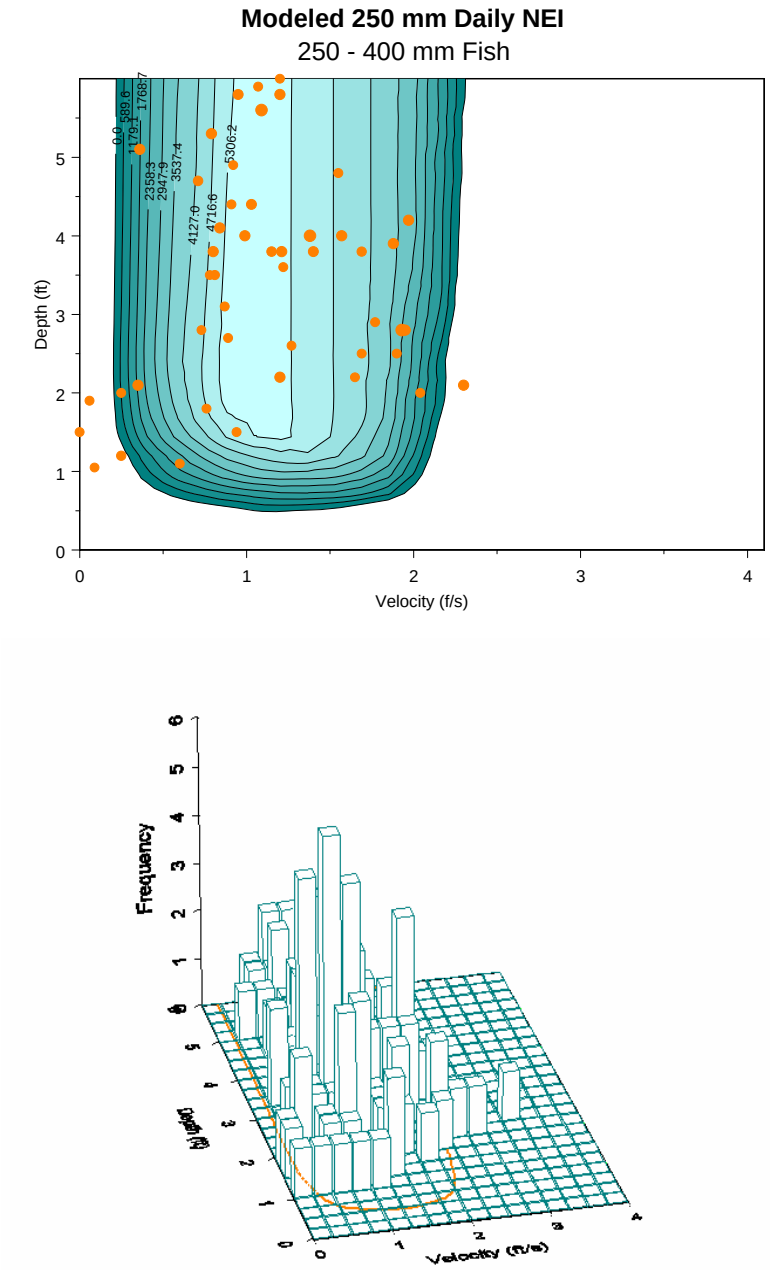

Figure 15. (Top) Modeled daily net energy intake for a 250 mm fish overlain with 2002-3 fish locations for 150-400 mm fish (small dots are smaller fish, big dots are bigger fish). Contours are in joules/day. The maximum daily net energy intake is light blue and about 5,306 joules/day. (Bottom) Histogram of fish frequencies and 250 mm fish positive daily net energy intake (orange line).

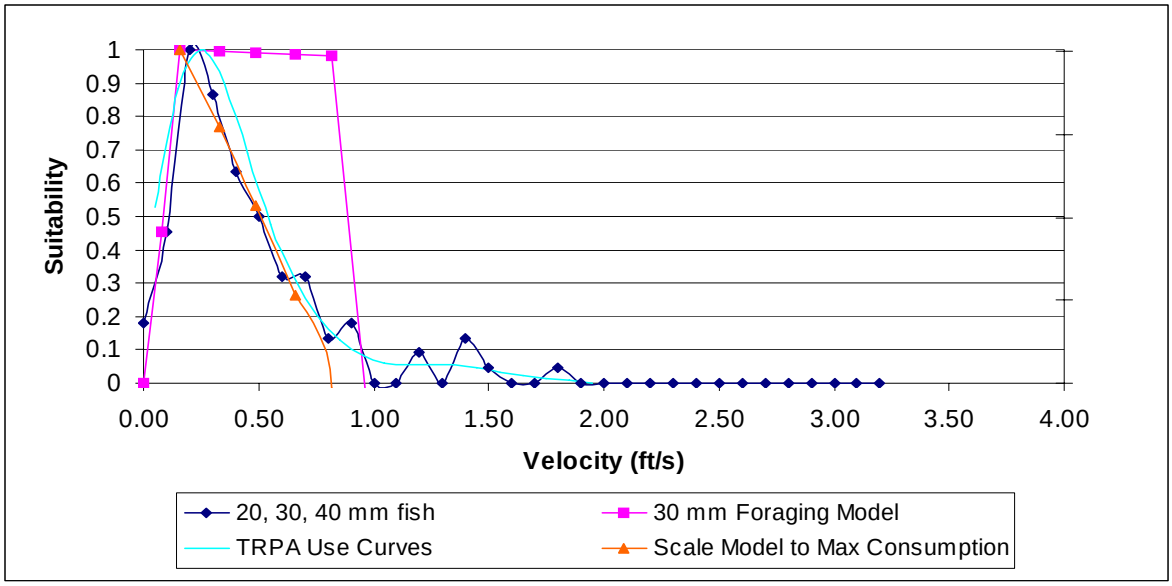

Figure 16. Scaled (between 0 and 1) frequency distribution of velocity use by 20 – 40 mm fish (average 37 mm) (dark blue), scaled 30 mm foraging model velocity relationship at a depth of 0.98 ft (average of fish observations) (magenta), re-scaled 30 mm foraging model velocity relationship for only velocities that provide maximum consumption (orange), and TRPA velocity use curves for 20-40 mm fish (cyan).

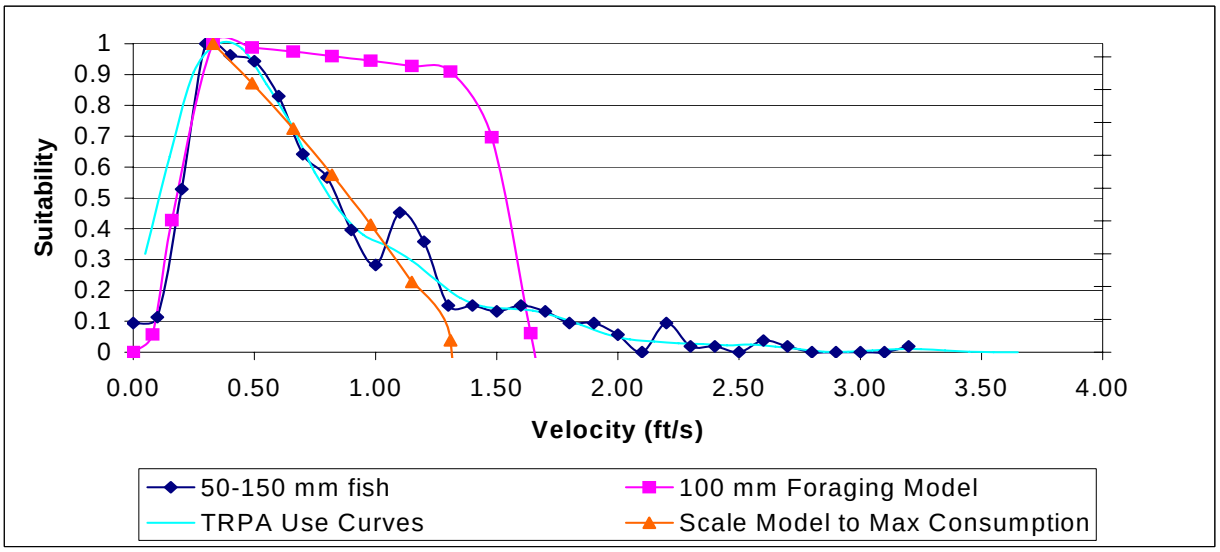

Figure 17. Scaled (between 0 and 1) frequency distribution of velocity use by 50 – 150 mm fish (average 71 mm) (dark blue), scaled 100 mm foraging model velocity relationship at a depth of 1.68 ft (average of fish observations)(magenta), re-scaled 100 mm foraging model velocity relationship for only velocities that provide maximum consumption (orange), and TRPA velocity use curves for 50-150 mm fish (cyan).

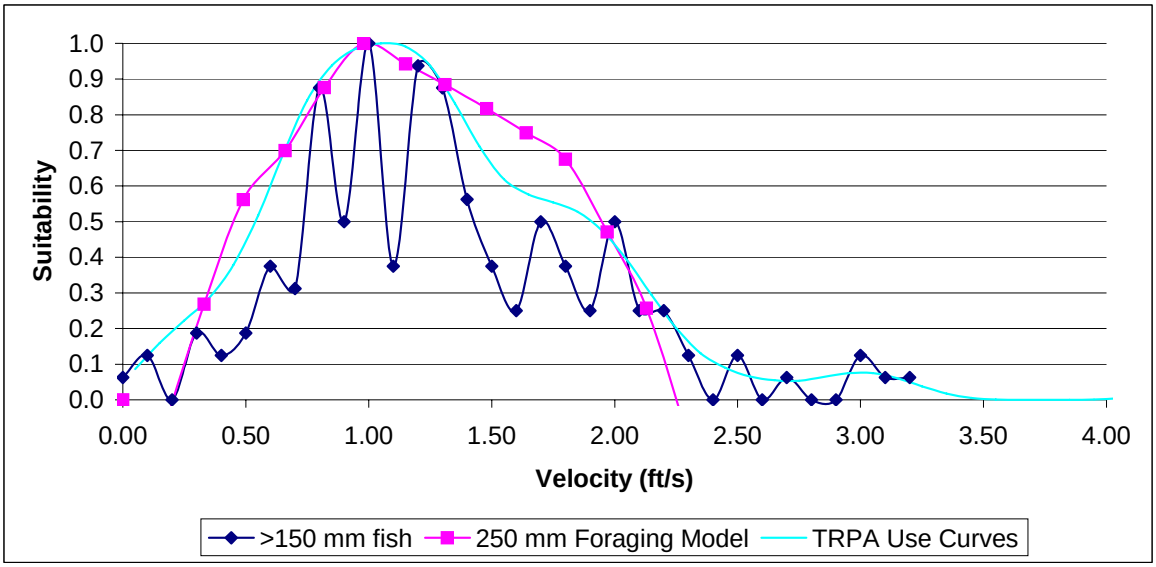

Figure 18. Scaled (between 0 and 1) frequency distribution of velocity use by >150-400 mm fish (average 228 mm) (dark blue), scaled 250 mm foraging model velocity relationship at a depth of 3.1 ft (average of fish observations)(magenta), and TRPA velocity use curves for >150-400 mm fish (cyan). Note some fish are in "fast" water outside the "energetics window."

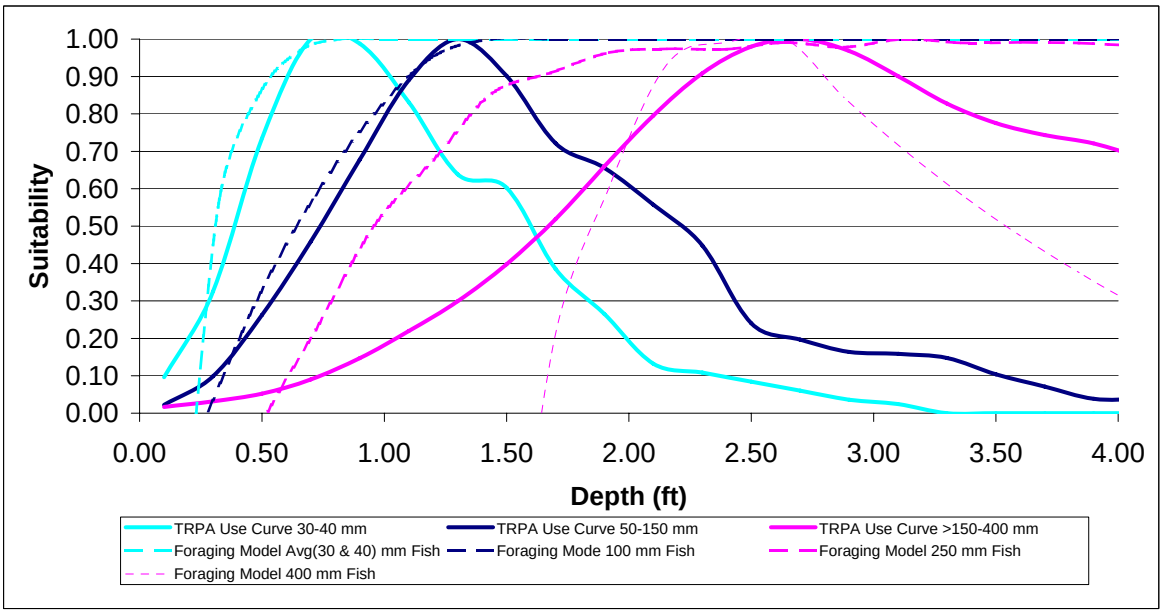

Figure 19. Scaled (between 0 and 1) frequency distribution of depth use by 20-40 mm (average 37 mm), 50-150 mm (average 71 mm) and >150-400 mm fish (average 228) compared to foraging model scaled depth suitability for fish of approximately the median fish size class. For the small fish the 30 mm foraging relationship was used, for the medium fish the 100 mm foraging relationship was used and for the larger fish both the 250 and 400 mm foraging relationships are shown. Note that the smaller fish appear to "behaviorally" be avoiding deeper water (e.g., predation) even though it appears to be energetically profitable.

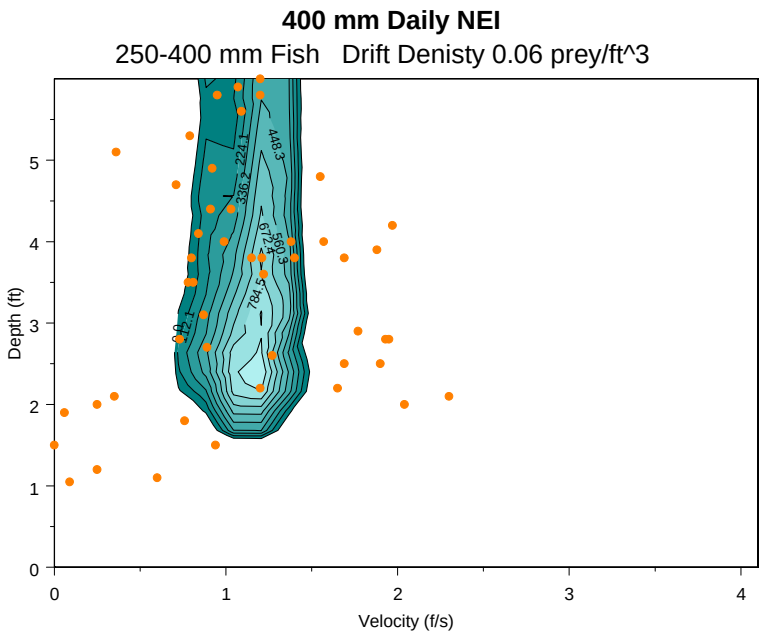

Figure 20. Modeled daily NEI for 400 mm trout for a drift density of 0.06 prey/ft^3. 400 mm daily NEI is negative at many depths and velocities.

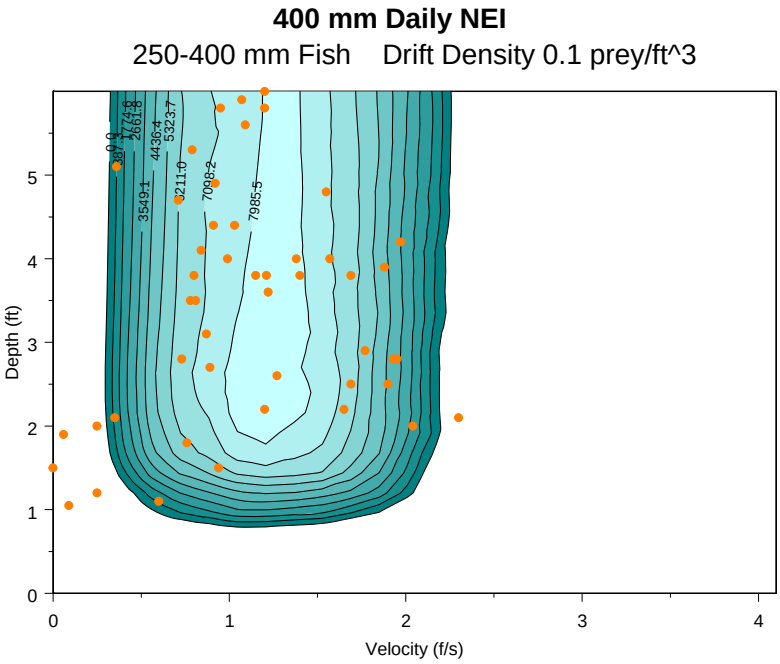

Figure 21. Modeled daily NEI for 400 mm trout for a drift density of 0.10 prey/ft^3. Note that a wide range of depths and velocities provide positive daily NEI compared to the lower drift density shown in Figure 20.

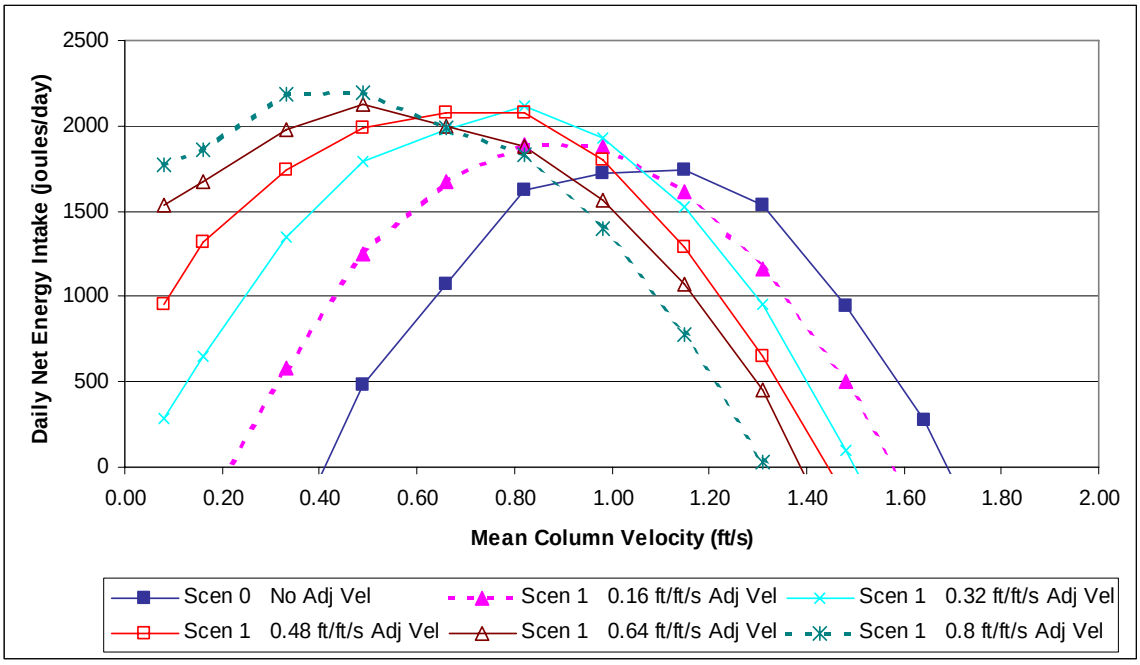

Figure 22. DNEI for a 250 mm trout with no adjacent velocity (Scenario 0) and with varying increases of velocity on both sides of the fish (Scenario 1).

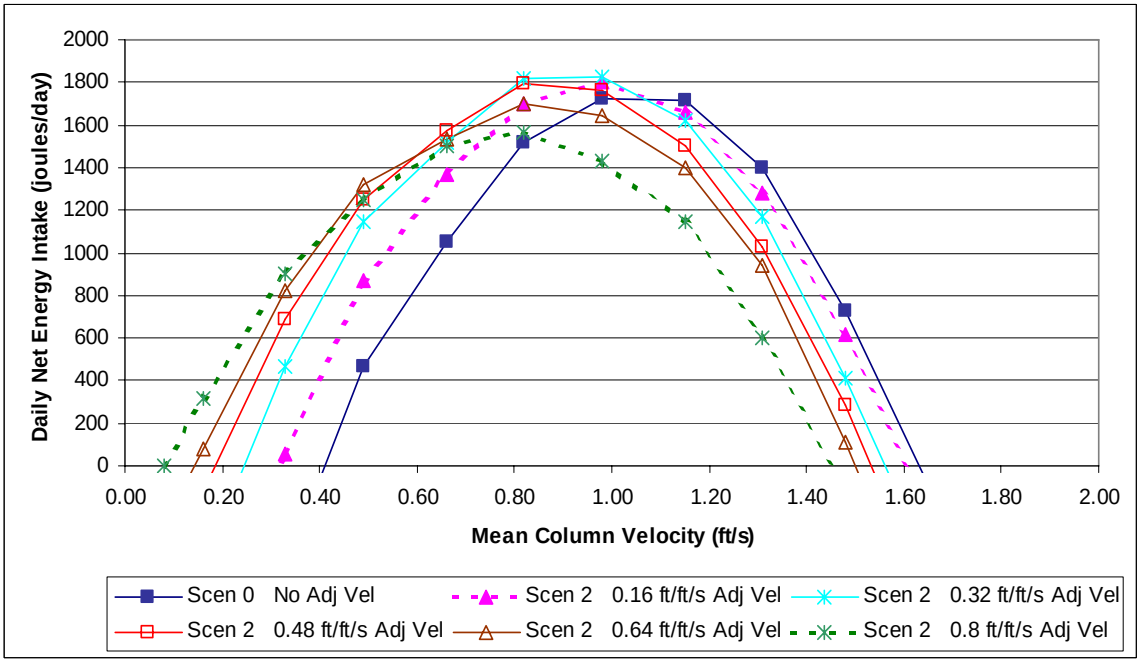

Figure 23. DNEI for a 250 mm trout with no adjacent velocity (Scenario 0) and with varying increases (0.16 to 0.8 ft/ft/s) of velocity on one side of the fish (Scenario 2).

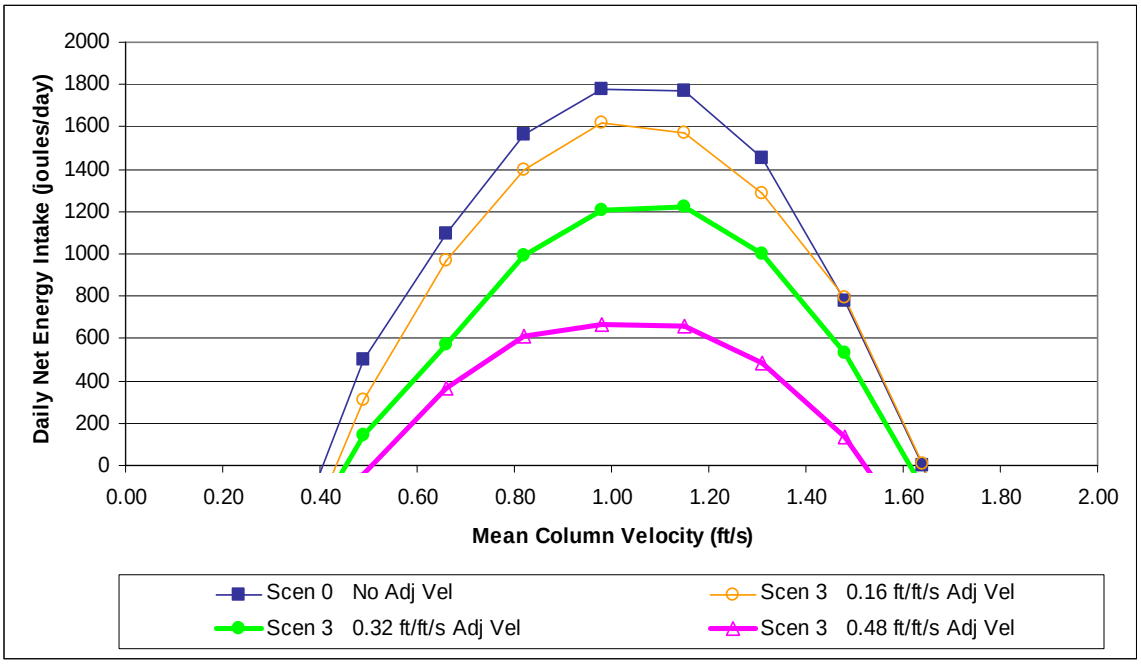

Figure 24. DNEI for a 250 mm trout with no adjacent velocity (Scenario 0) and with varying increases (0.16 to 0.48 ft/ft/s) of velocity on one side of the fish and corresponding decreases on the other side (Scenario 3).

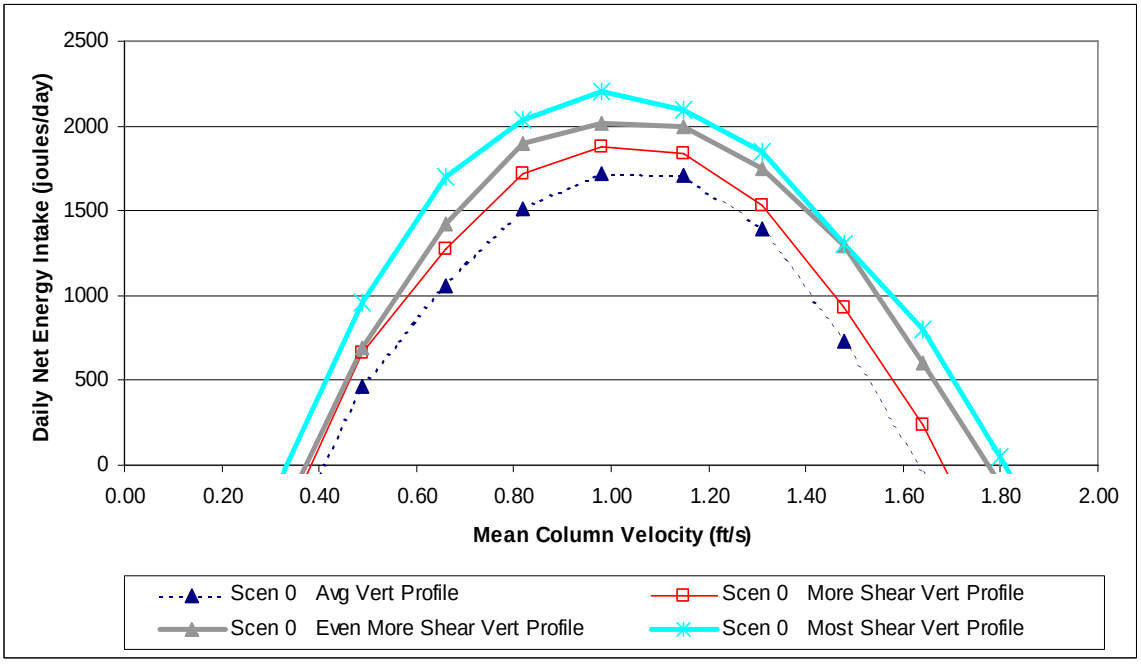

Figure 25. DNEI for a 250 mm trout using the average vertical velocity profile and three other vertical profiles with greater shear (i.e., lower velocity at the bottom of the channel and higher at the water surface).

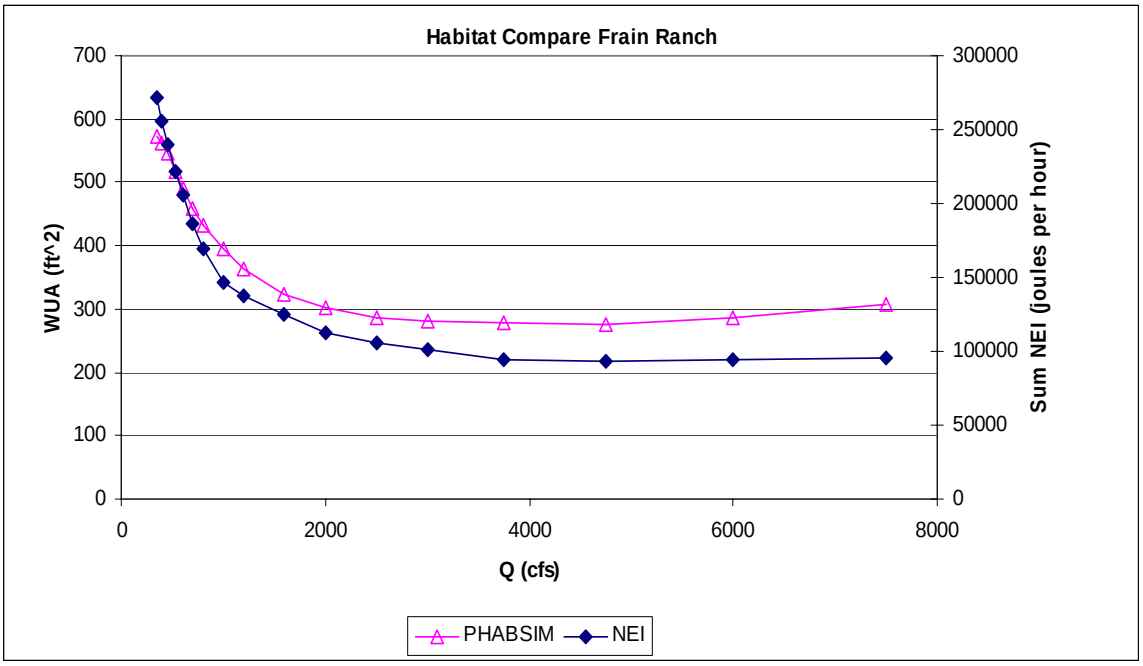

Figure 26. Frain Ranch comparison of the shape of the habitat versus flow relationship for typical PHABSIM (WUA) and for the Sum of Net Energy Intake (i.e., using the foraging model and the full velocity field).

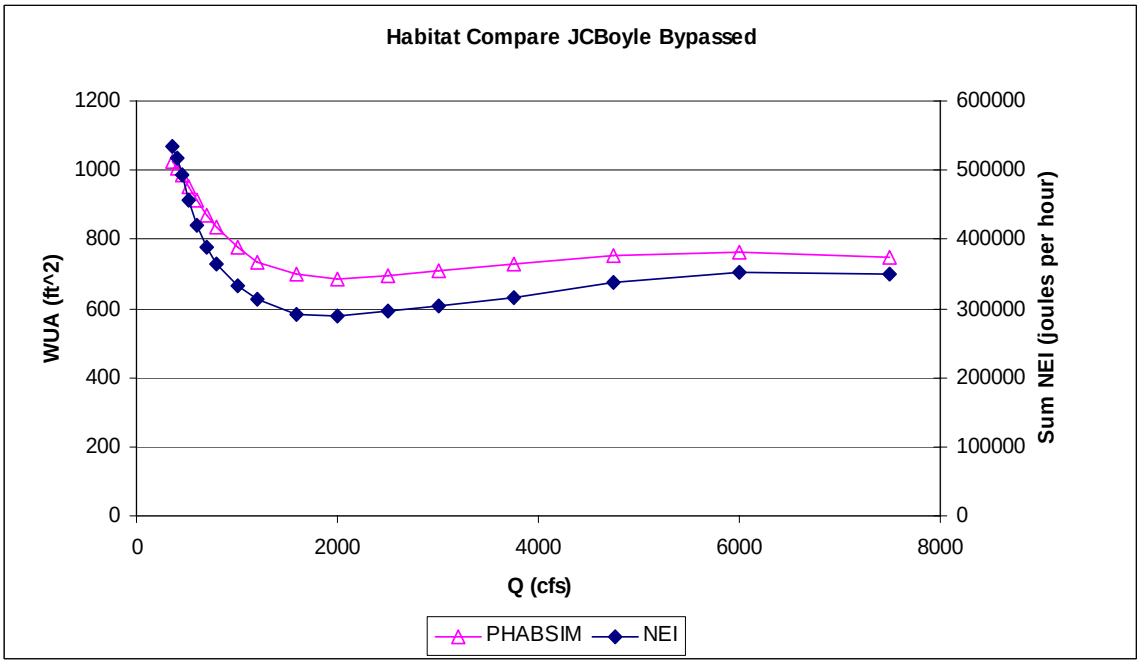

Figure 27. J.C. Boyle Bypass Reach comparison of the shape of the habitat versus flow relationship for typical PHABSIM (WUA) and for the Sum of Net Energy Intake (i.e., using the foraging model and the full velocity field).

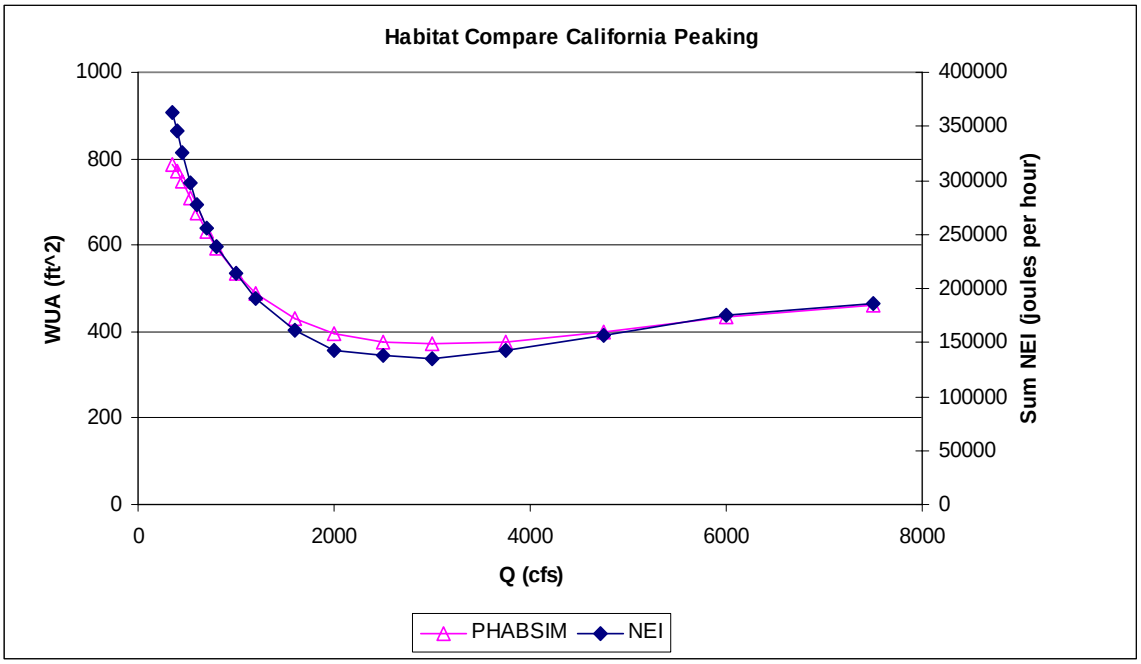

Figure 28. J.C. Boyle Lower (California) Peaking Reach comparison of the shape of the habitat versus flow relationship for typical PHABSIM (WUA) and for the Sum of Net Energy Intake (i.e., using the foraging model and the full velocity field).

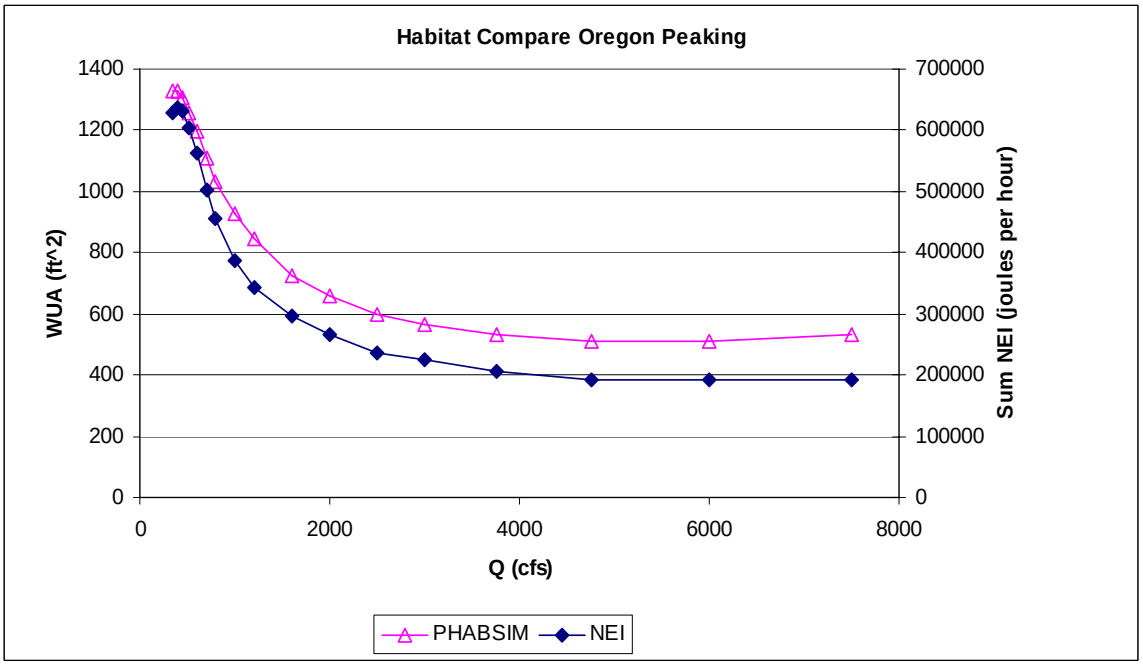

Figure 29. J.C. Boyle Upper (Oregon) Peaking Reach comparison of the shape of the habitat versus flow relationship for typical PHABSIM (WUA) and for the Sum of Net Energy Intake (i.e., using the foraging model and the full velocity field).

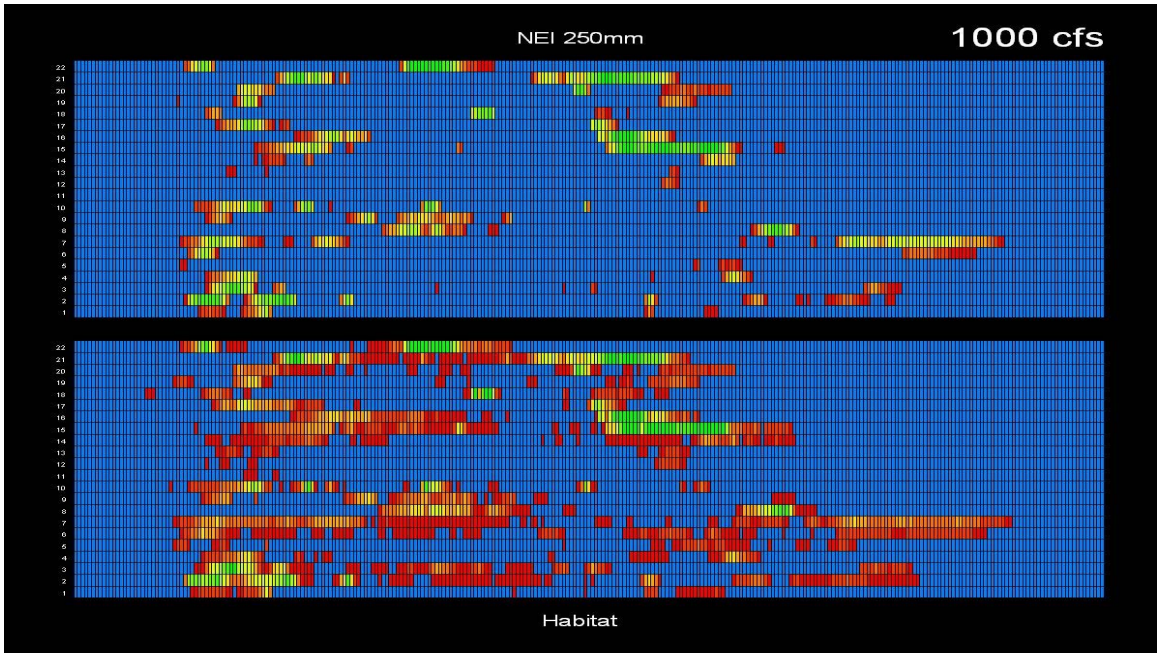

Figure 30. Frain Ranch reach all cross-sections relative suitability (green to red = maximum to least suitable, blue = not suitable) by cell for 250 mm trout NEI (joules/hr) (top half of figure) and adult use suitability curve (bottom half of figure). Each horizontal block of cells is a cross-section. The flow visualized is 1000 cfs. (enlarge to view)

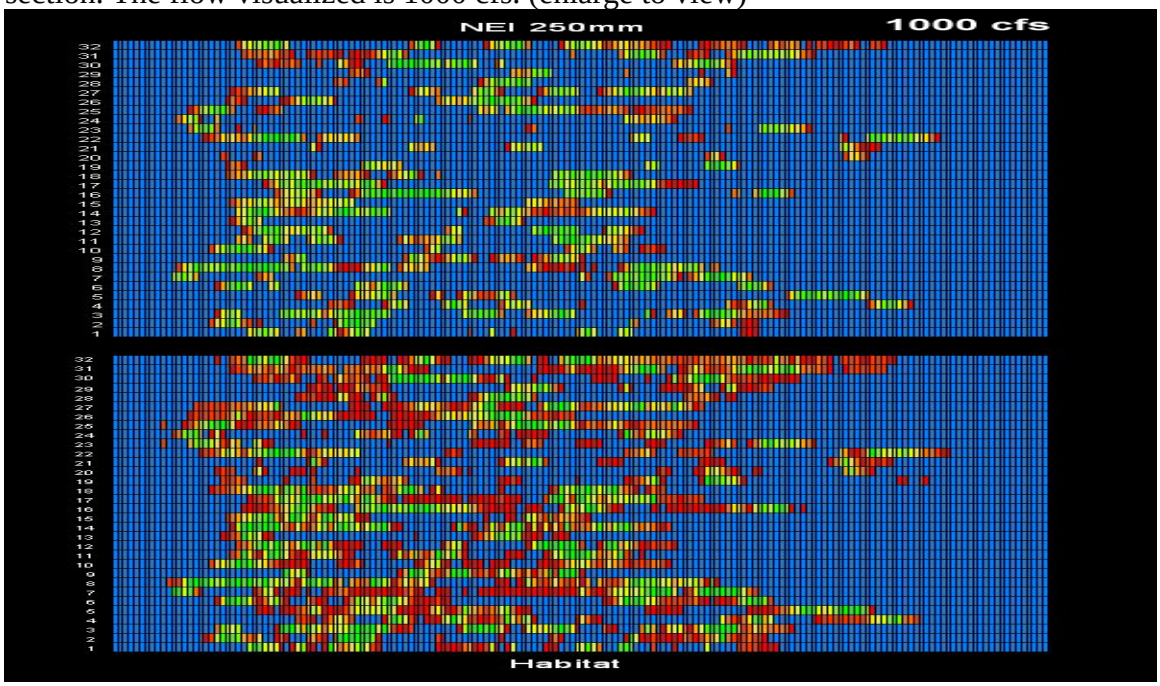

Figure 31. J.C. Boyle Bypass reach all cross-sections relative suitability (green to red = maximum to least suitable, blue = not suitable) by cell for 250 mm trout NEI (joules/hr) (top half of figure) and adult use suitability curve (bottom half of figure). Each horizontal block of cells is a cross-section. The flow visualized is 1000 cfs. (enlarge to view)

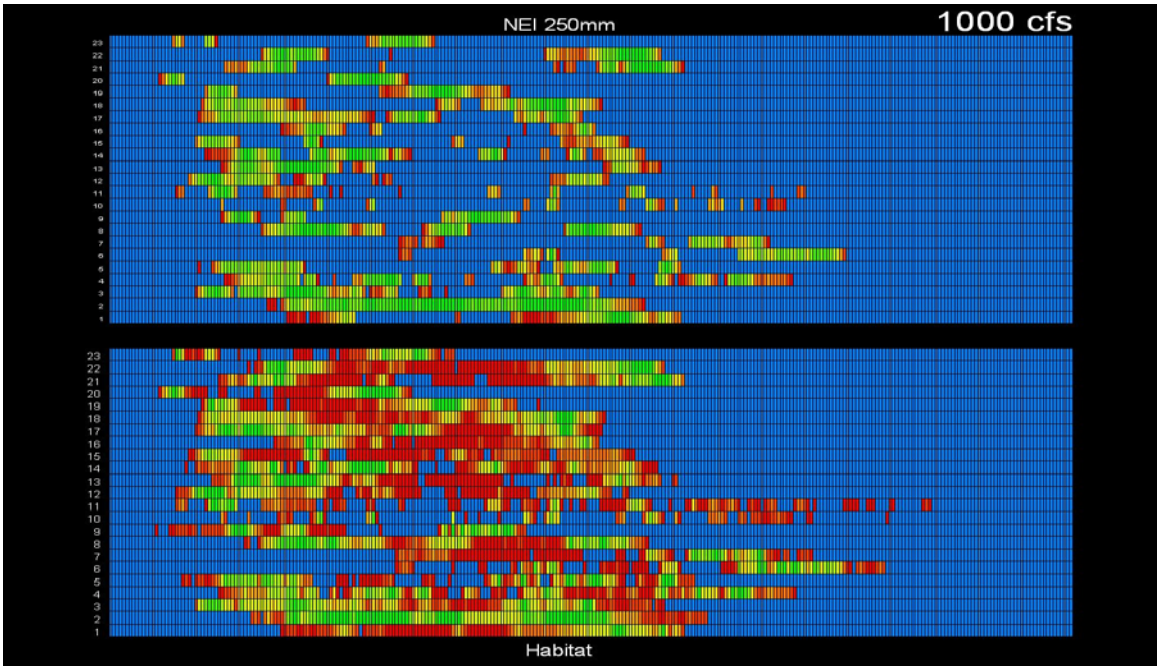

Figure 32. J.C. Boyle Lower (California) Peaking reach all cross-section relative suitability (green to red = maximum to least suitable, blue = not suitable) by cell for 250 mm trout NEI (joules/hr) (top half of figure) and adult use suitability curve (bottom half of figure). Each horizontal block of cells is a cross-section. The flow visualized is 1000 cfs. (enlarge to view)

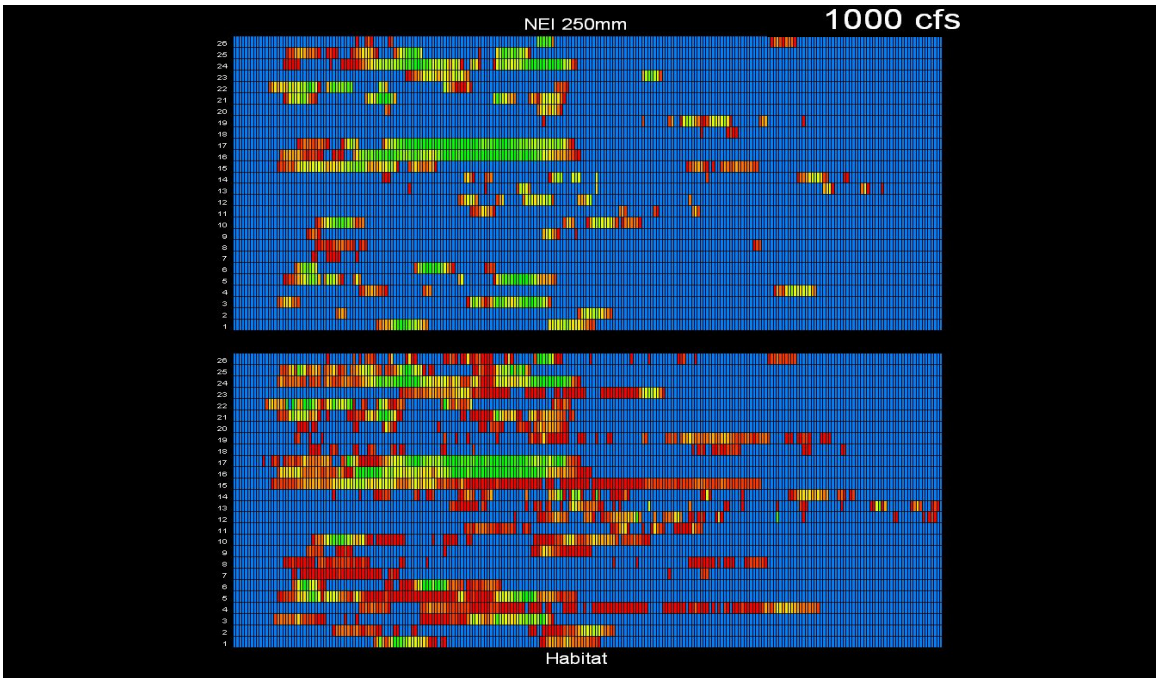

Figure 33. J.C. Boyle Upper (Oregon) Peaking reach all cross-section relative suitability (green to red = maximum to least suitable, blue = not suitable) by cell for 250 mm trout NEI (joules/hr) (top half of figure) and adult use suitability curve (bottom half of figure). Each horizontal block of cells is a cross-section. The flow visualized is 1000 cfs. (enlarge to view)

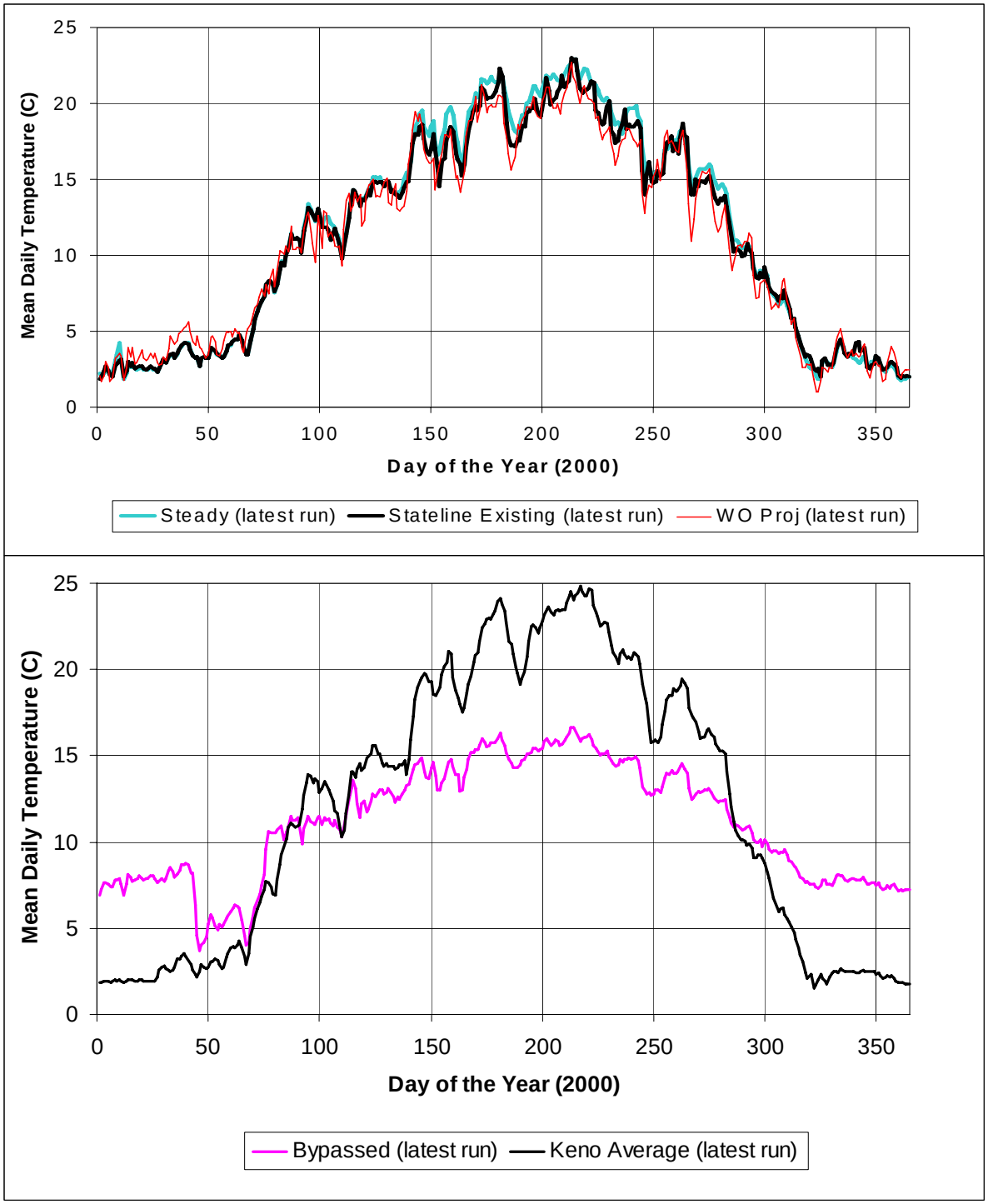

Figure 34. Mean daily temperature for the year 2000 for Stateline under Existing Conditions, Stateline under Steady Flow conditions, and Stateline Without Project (upper graph) and for the J.C. Boyle Bypass Reach (Above the J.C. Boyle Powerhouse) under Existing Conditions and the Keno Reach under Existing Conditions (lower graph).

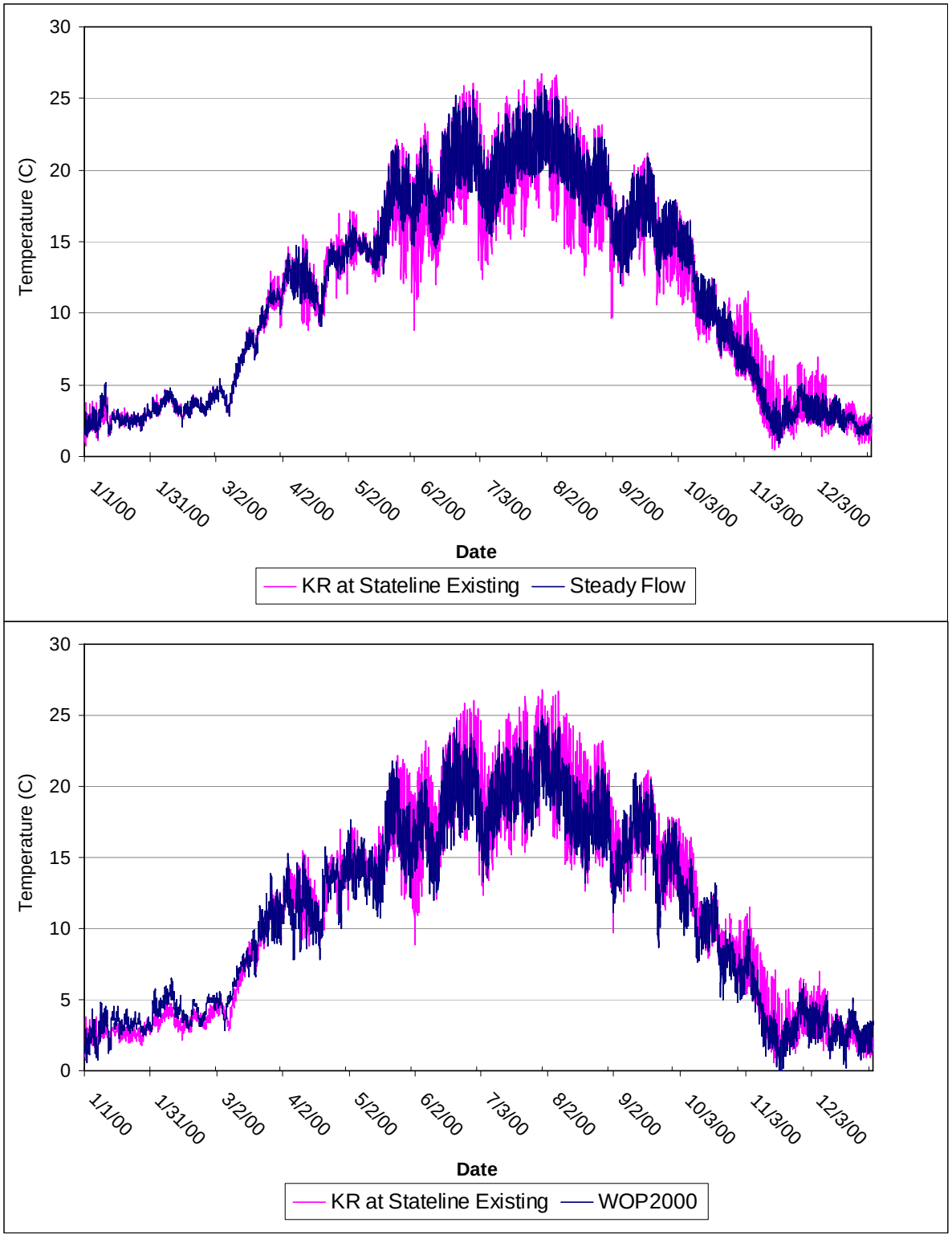

Figure 35. Comparison of hourly temperatures (year 2000) at the Stateline node for Existing Conditions (magenta), Steady Flow (blue line, top), and Without Project scenarios (blue line, bottom).

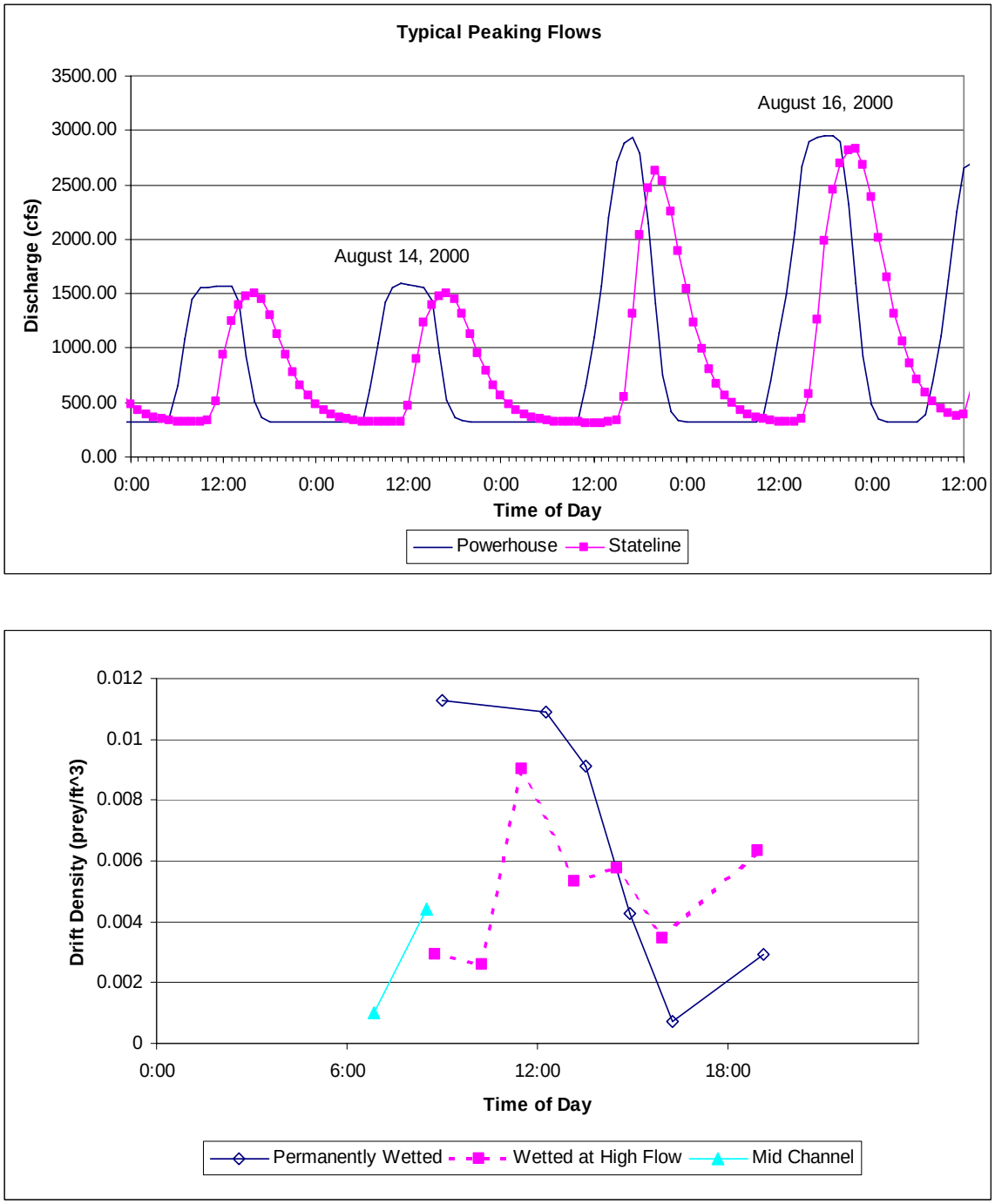

Figure 36. Typical summer peaking flows at Stateline and corresponding steady flows (July 1, 200) (above). Drift data collected during Sept. 12, 2002 (PacifiCorp 2004) near the BLM campground in the J.C. Boyle Peaking reach in the Klamath River that was permanently wetted, only wetted at high flow, and for a mid channel location (below).

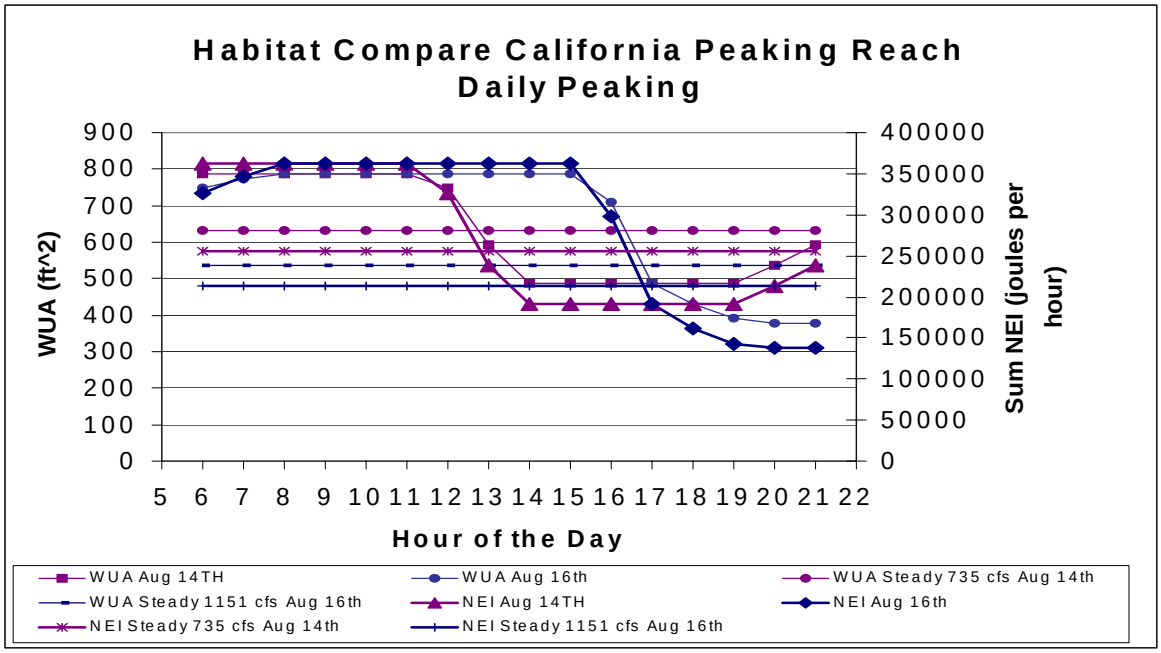

Figure 37. WUA and NEI habitat for one unit peaking (Aug 14th) and two unit peaking (Aug 15th). See Figure 36A for the hourly flows. Low flows in the early part of the day are about 350 cfs and peak flows in the afternoon are about 1,500 and 3,000 cfs for the one and two unit peaking cycles, respectively. The most habitat occurs at the low flow portion of the cycle and the least at the peak portion of the cycle. WUA and NEI at the corresponding steady flows of 735 cfs (one unit peaking) and 1,151 cfs (two unit peaking) are also shown.

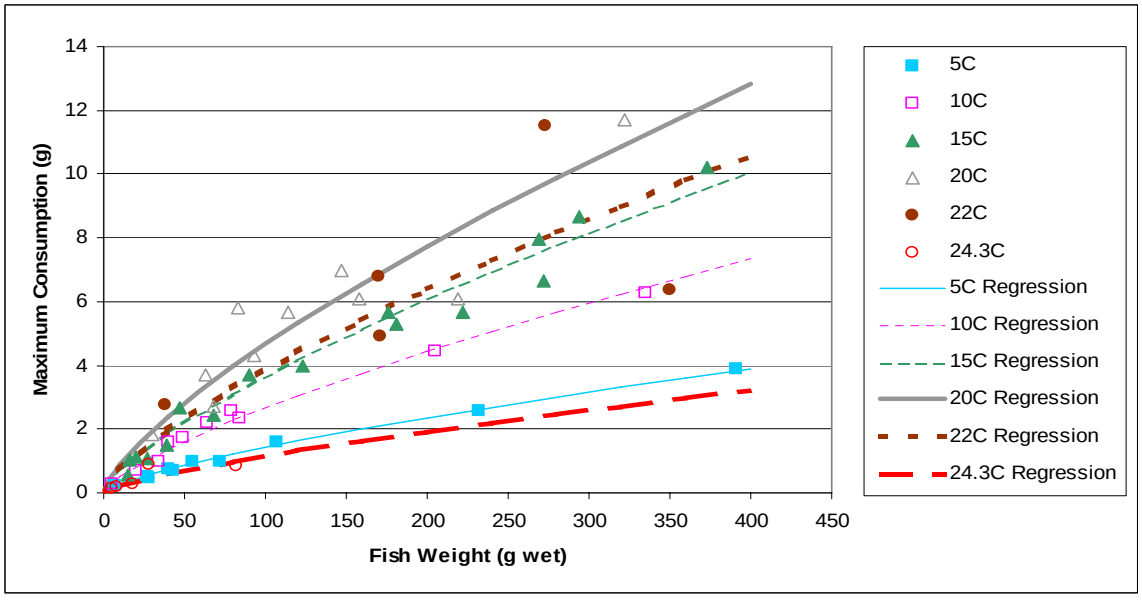

Figure 38. Comparison of new rainbow trout maximum consumption versus fish weight equations and data from From and Rasmussen 1984. Consumption is in grams moist pellets (0.935575 X grams moist pellets = grams chemical oxygen demand (COD))

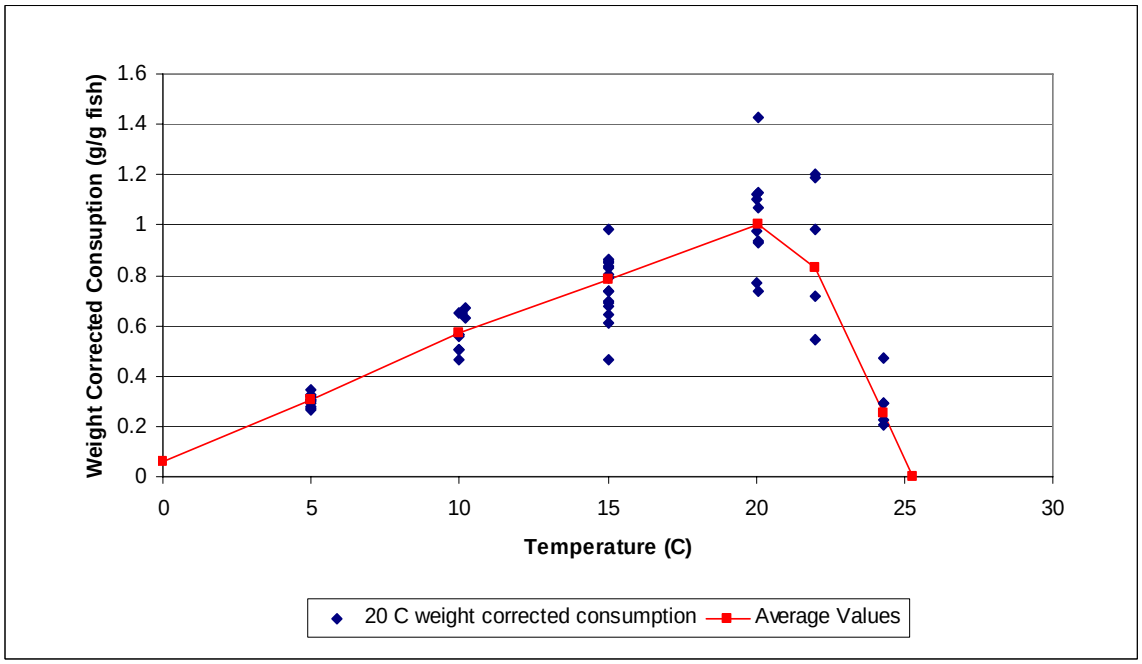

Figure 39. Comparison of new rainbow trout maximum consumption versus temperature equations and data from From and Rasmussen 1984. Data standardized for fish weight (g/ g fish). Consumption is in grams moist pellets (0.935575 X grams moist pellets = grams chemical oxygen demand (COD))

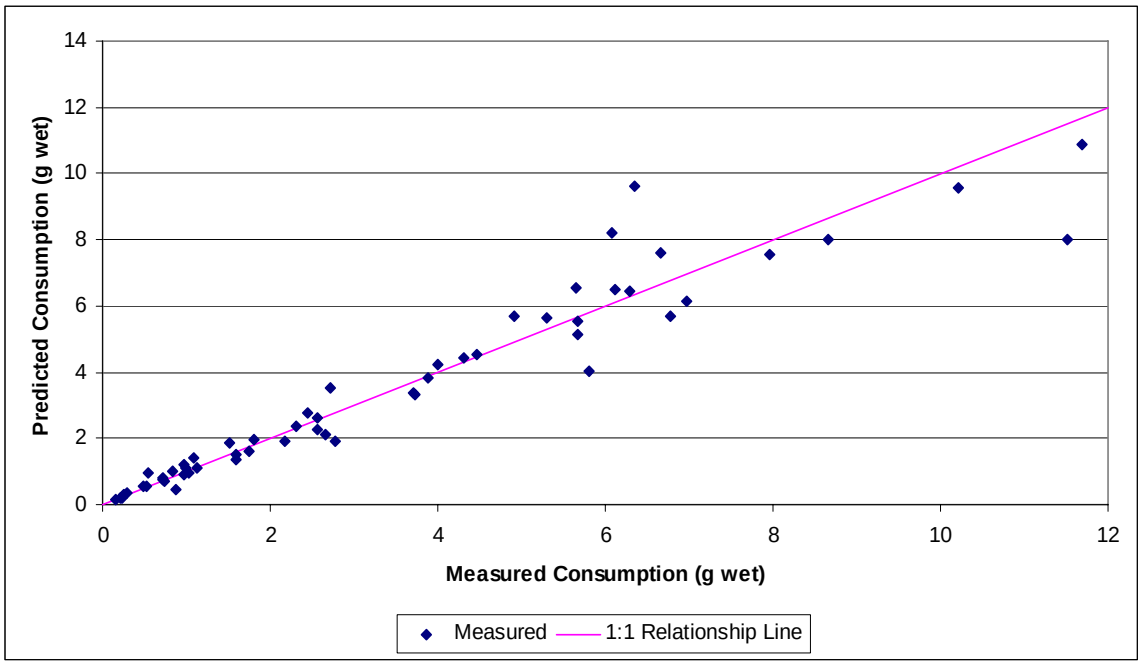

Figure 40. Comparison of new rainbow trout maximum consumption equation predictions versus measured consumption. Consumption is in grams moist pellets (0.935575 X grams moist pellets = grams chemical oxygen demand (COD))

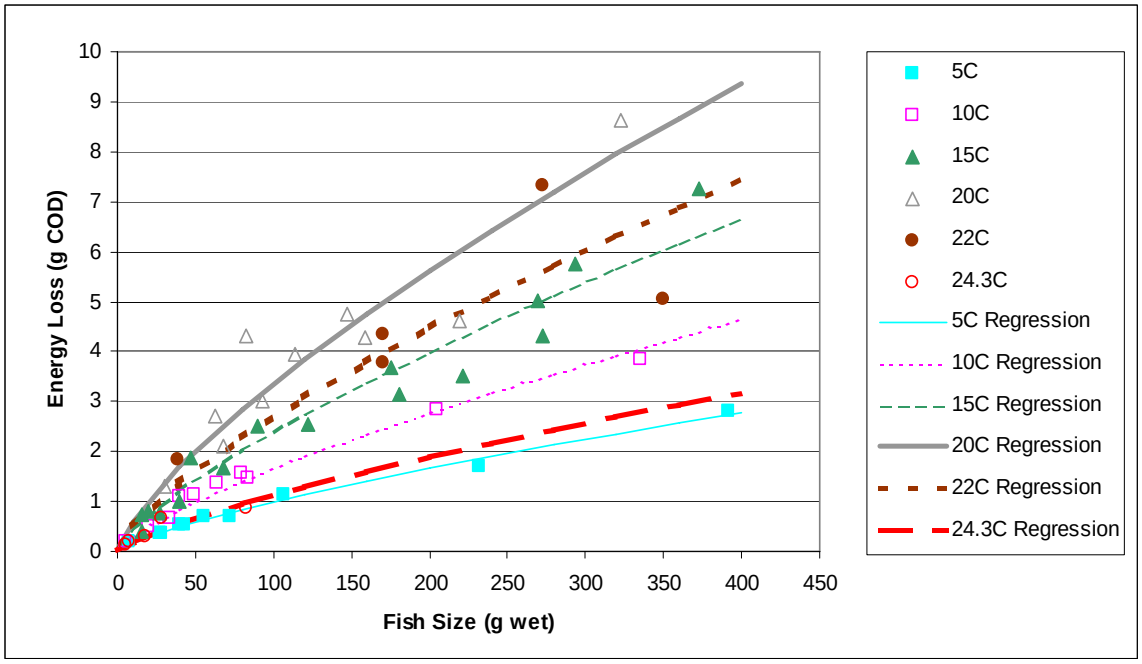

Figure 41. Comparison of losses from new rainbow trout maximum consumption losses versus fish weight equations and data from From and Rasmussen 1984.

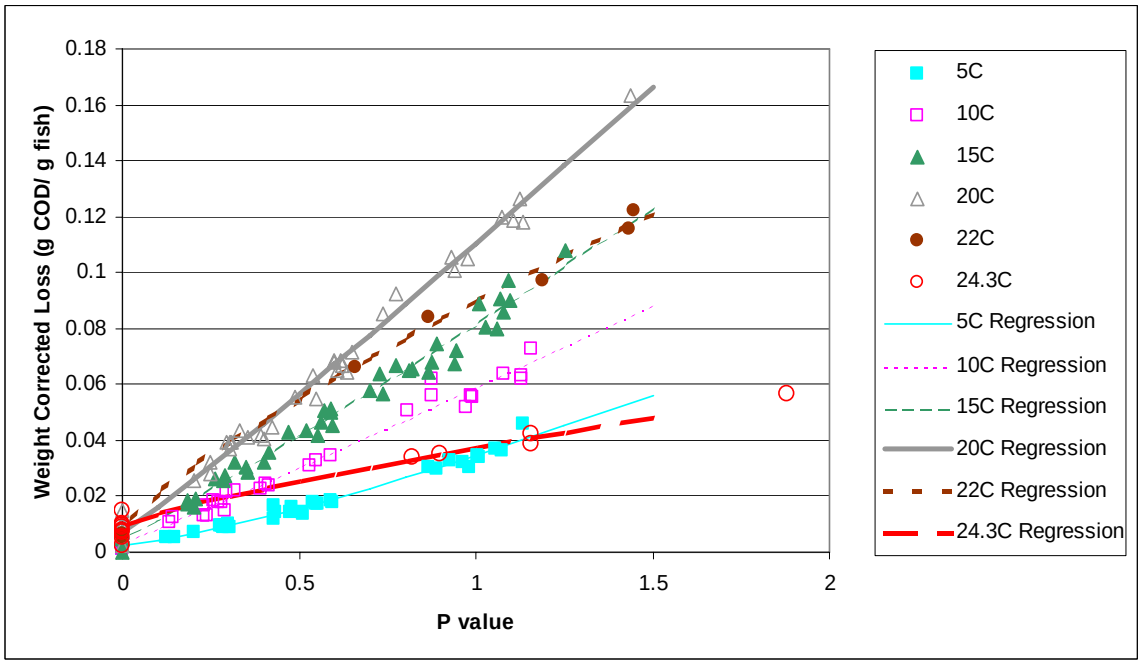

Figure 42. Comparison of losses at different food consumption levels using the new rainbow trout equations and data from From and Rasmussen 1984 for each temperature (data standardized for fish weight g COD /g fish).

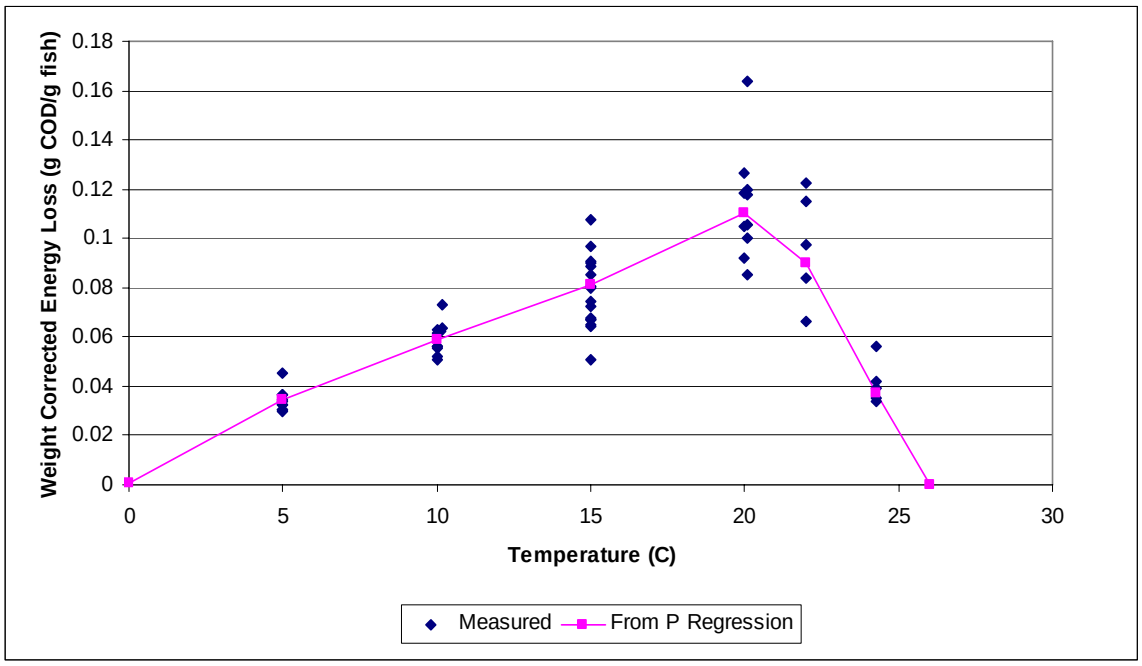

Figure 43. Comparison of new rainbow trout maximum loss versus temperature equations and data from From and Rasmussen (1984). Data standardized for fish weight (g/ g fish). Points from regression refer to the P value versus consumption regression in the following figure (see text for discussion).

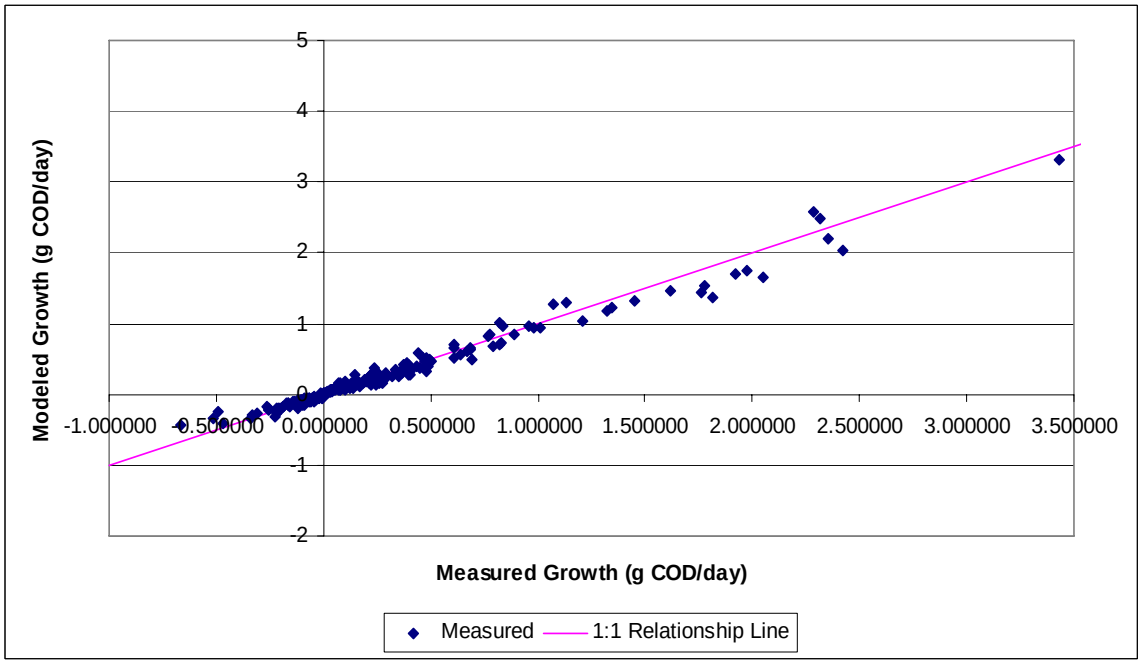

Figure 44. Comparison of new rainbow trout loss equation predictions versus measured loss (data standardized for fish weight g COD /g fish).

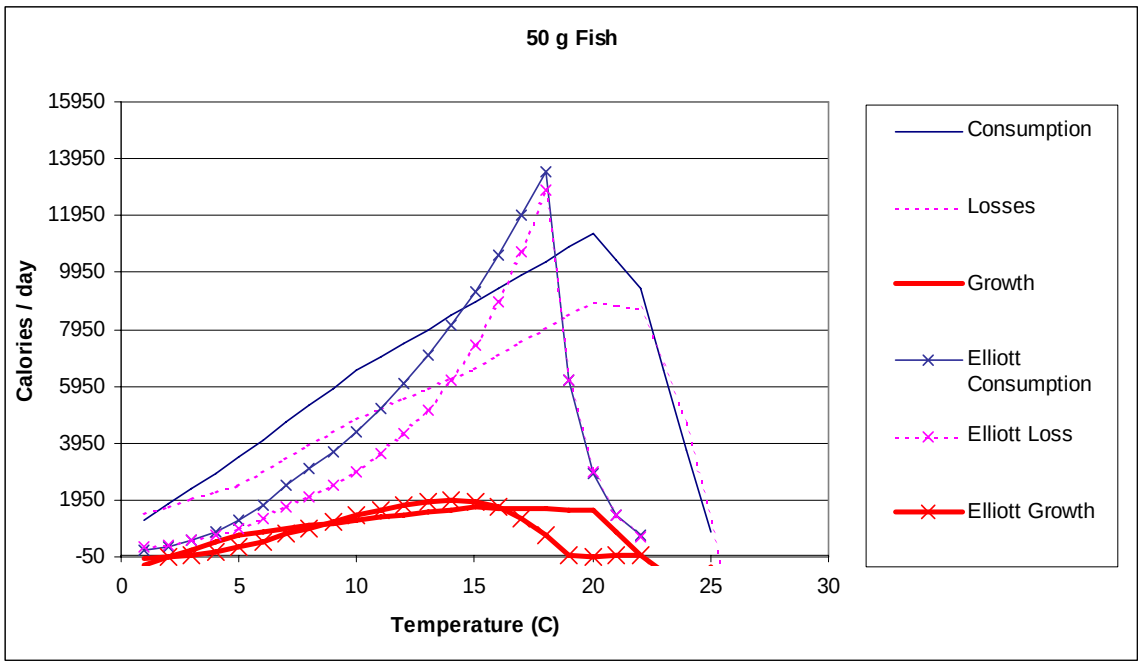

Figure 45. Comparison of new rainbow trout maximum consumption, losses (excretion, egestion, metabolism), and growth relationships (from From and Rasmussen 1984 data) versus brown trout from Elliott and Hurley (1999) for an example 50 g fish.

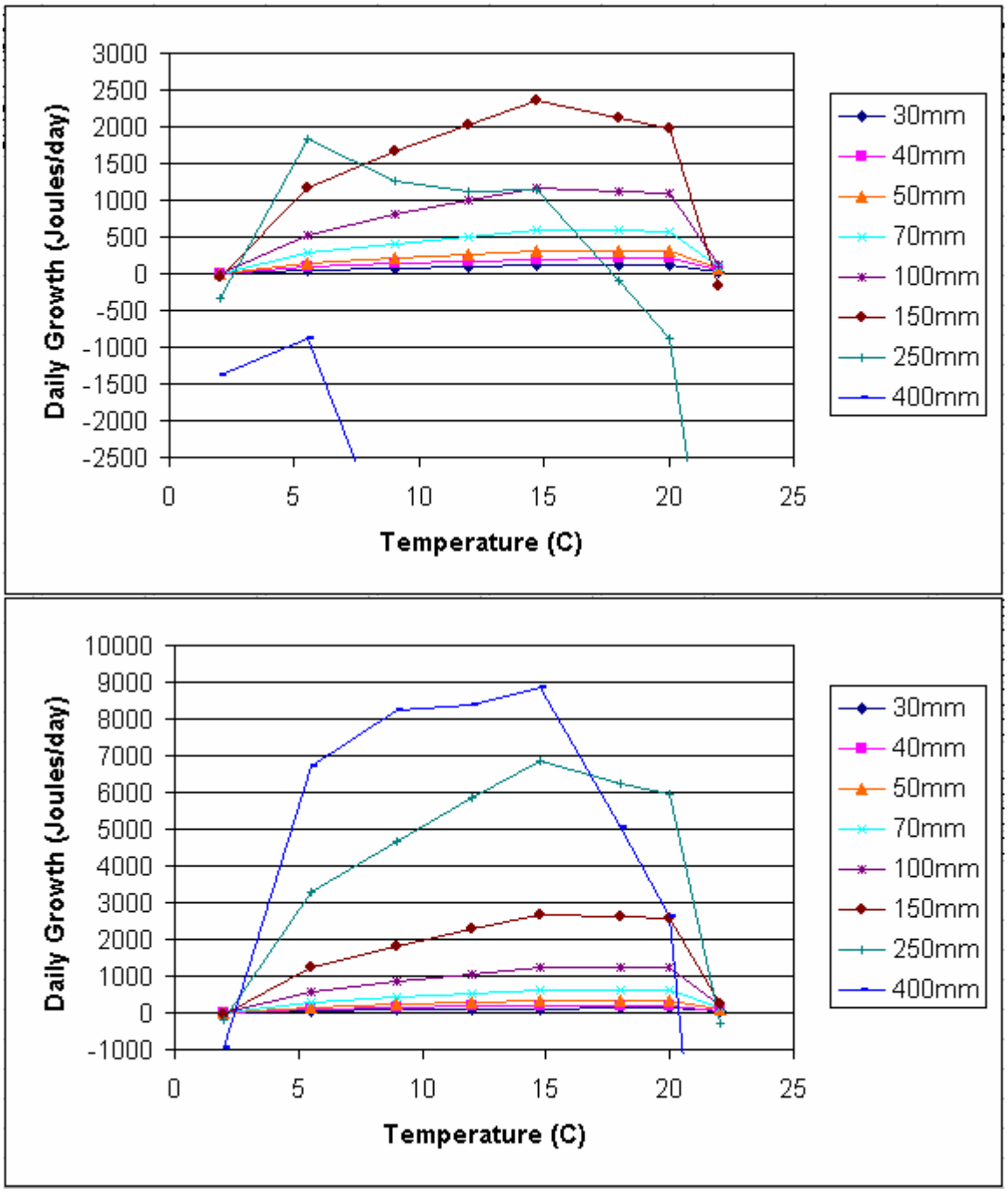

Figure 46. Daily growth potential for rainbow trout of 30, 40, 50, 70, 100, 150, 250, and 400 mm over a range of temperatures from 2 to 22 C. Calculated with a drift density of 0.02 prey/ft^3 (Top) and a drift density of 0.10 prey/ft^3. Drift densities correspond to early September and late June in the J.C. Boyle peaking reach, respectively. Note the differences in the scales.

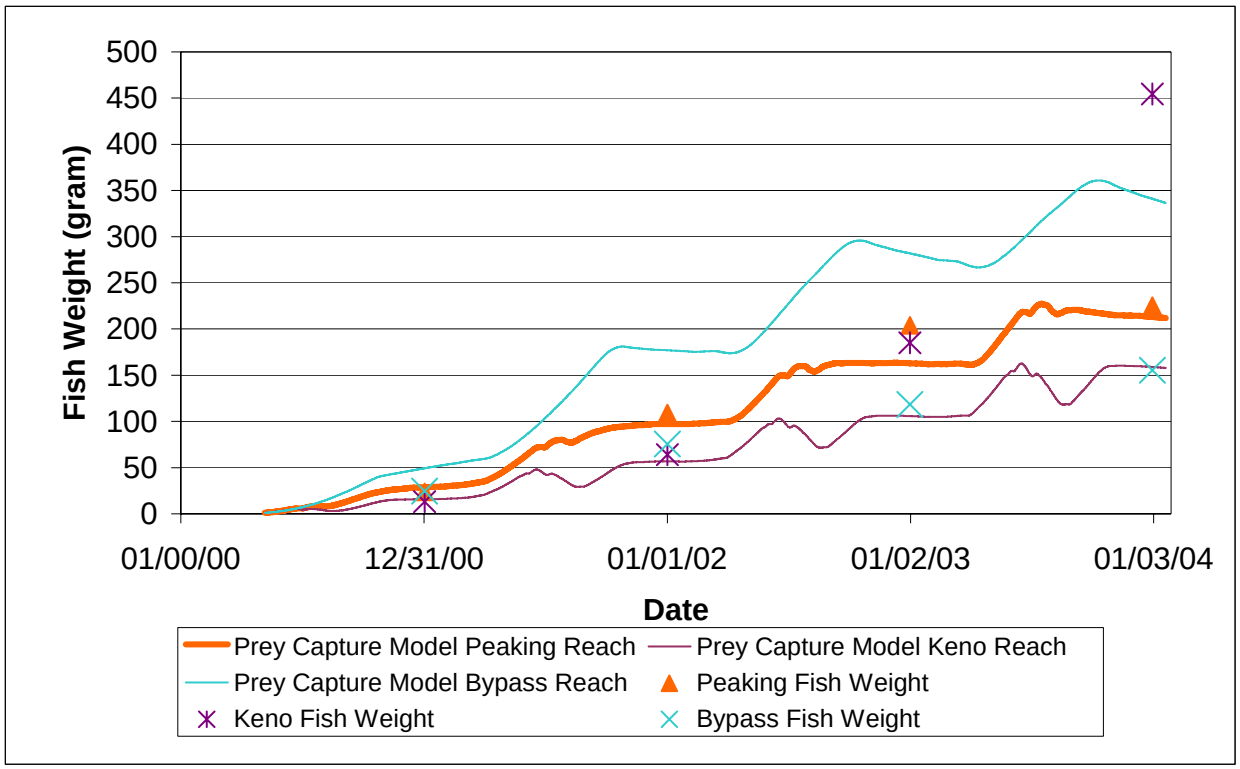

Figure 47. Foraging model growth (four years) for the Keno, J.C. Boyle peaking, and J.C. Boyle bypass reaches. Model results are compared to measured size-at-age data in the Keno, J.C. Boyle peaking, and J.C. Boyle bypass reaches.

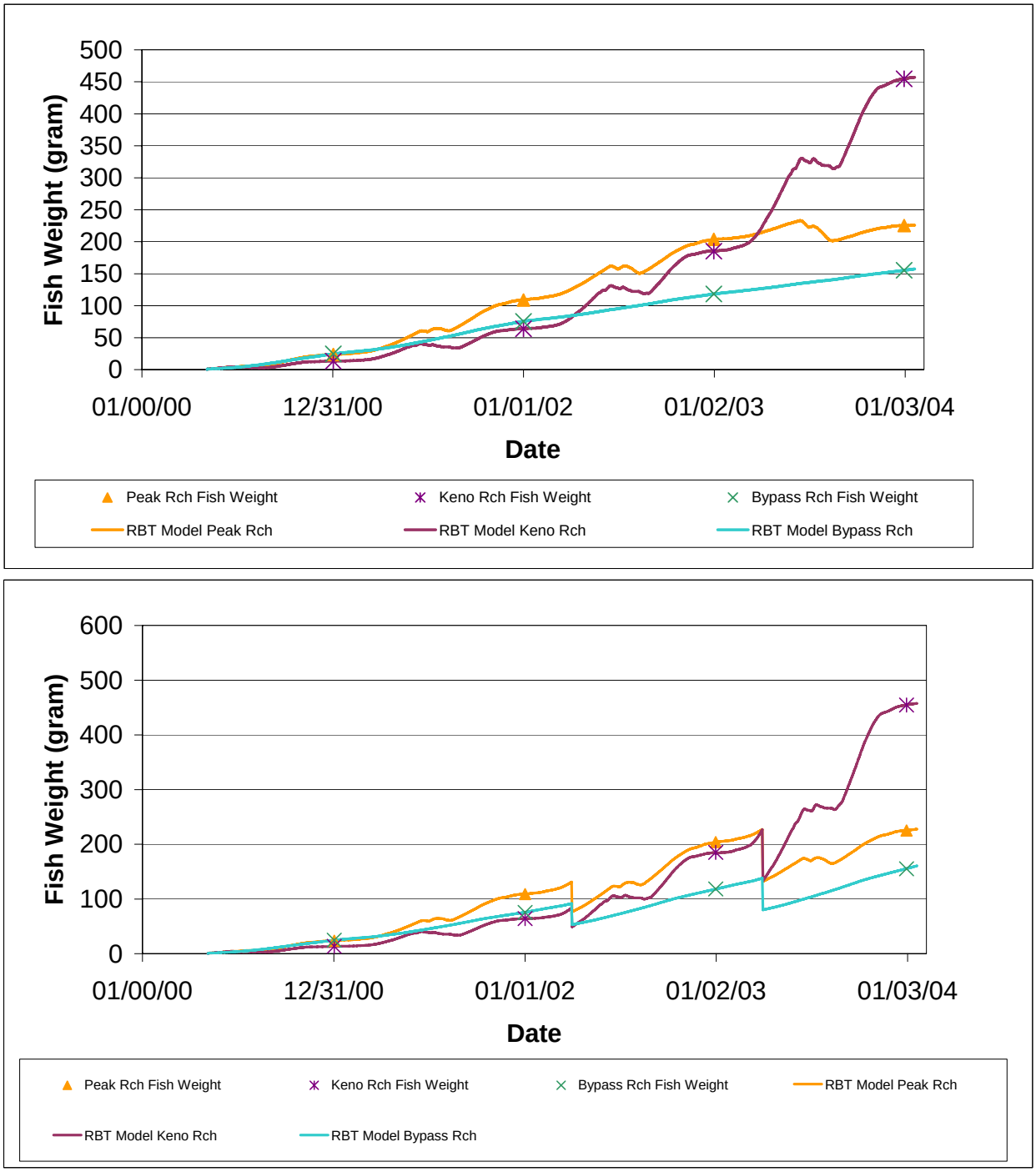

Figure 48. Growth (4 years) modeled in the Keno, J.C. Boyle peaking, and J.C. Boyle bypass reaches by fitting annual P values to the temperature-growth relationship developed from the From and Rasmussen (1984) data. P values are shown in Table 10. Model results are compared to measured size-at-age data in the Keno, J.C. Boyle peaking, and J.C. Boyle bypass reaches. The top figure assumes no spawning occurs and the bottom figure assumes spawning occurs in years 3 and 4 (46% energy loss).

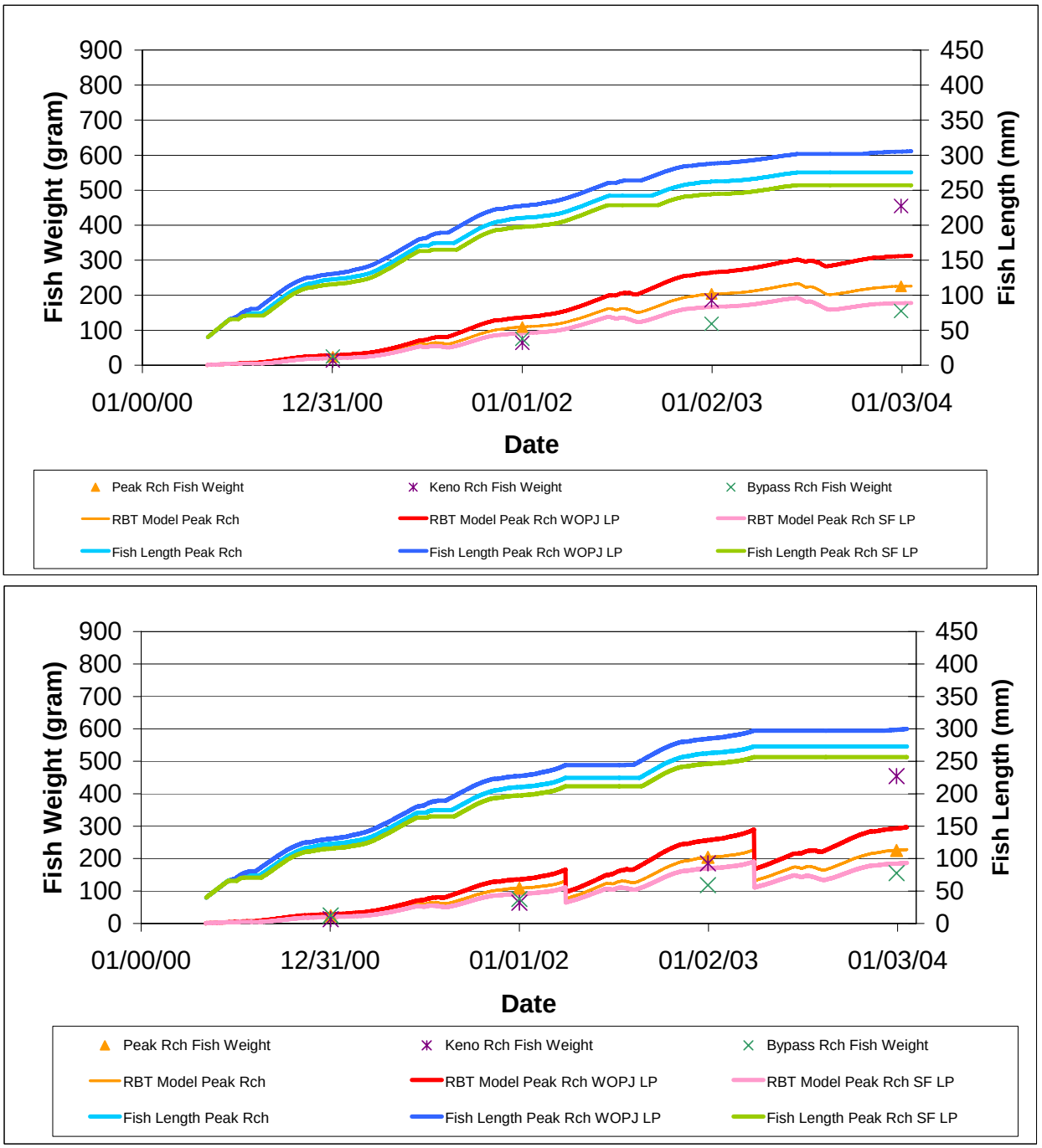

Figure 49. Growth (four years) modeled for Existing Conditions (RBT Model Peak Rch), WOP (RPB Model Peak Rch WOPJ LP) and Steady Flow scenarios (RPB Model Peak Rch SF LP) in the J.C. Boyle peaking reach by using the observed P value (Existing Conditions) and the temperature regimes of the Steady Flow and WOP scenarios. Model results are compared to measured size-at-age data in the Keno, J.C. Boyle peaking, and J.C. Boyle bypass reaches. The top figure assumes no spawning occurs and the bottom figure assumes spawning occurs in years 3 and 4 (46% energy loss).

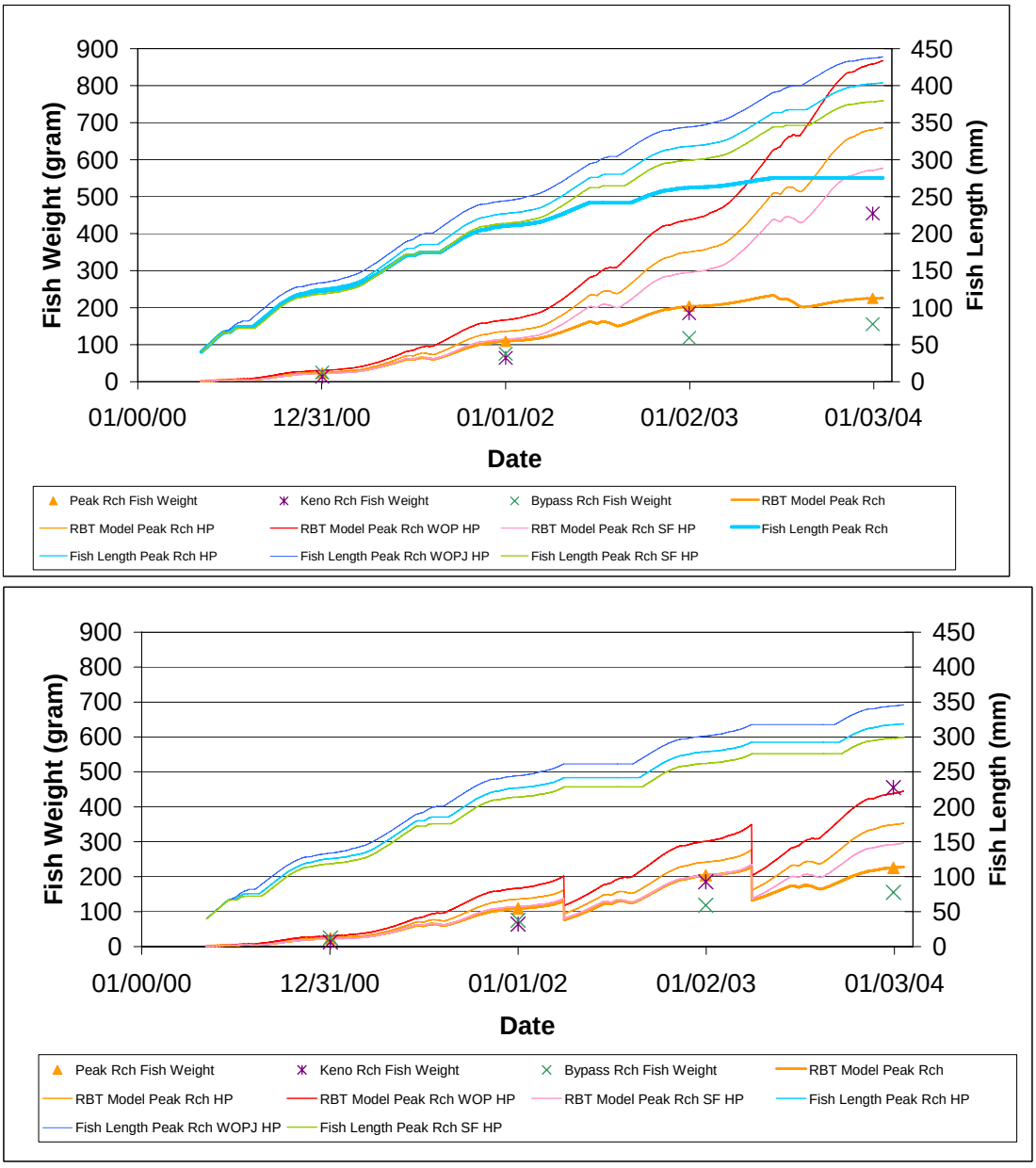

Figure 50. Growth (four years) modeled for Existing Conditions (RBT Model Peak Rch), WOP (RPB Model Peak Rch WOPJ HP) and Steady Flow scenarios (RPB Model Peak Rch SF HP) in the J.C. Boyle peaking reach by using the 0.75 P value found in the Keno reach and the temperature regimes of the Steady Flow and WOP scenarios. Model results are compared to measured size-at-age data in the Keno, J.C. Boyle peaking, and J.C. Boyle bypass reaches. The top figure assumes no spawning occurs and the bottom figure assumes spawning occurs in years 3 and 4 (46% energy loss). While this is a rational approach to modeling the changes in growth, the growth is likely overestimated. The P value is likely high because productivity may be inflated in the Keno reach due to organic material inflow from upstream Klamath Lake. Also the P value remains fixed as fish get larger, when it likely would decline for fish feeding on drift. The results are different depending on whether or not spawning is assumed.

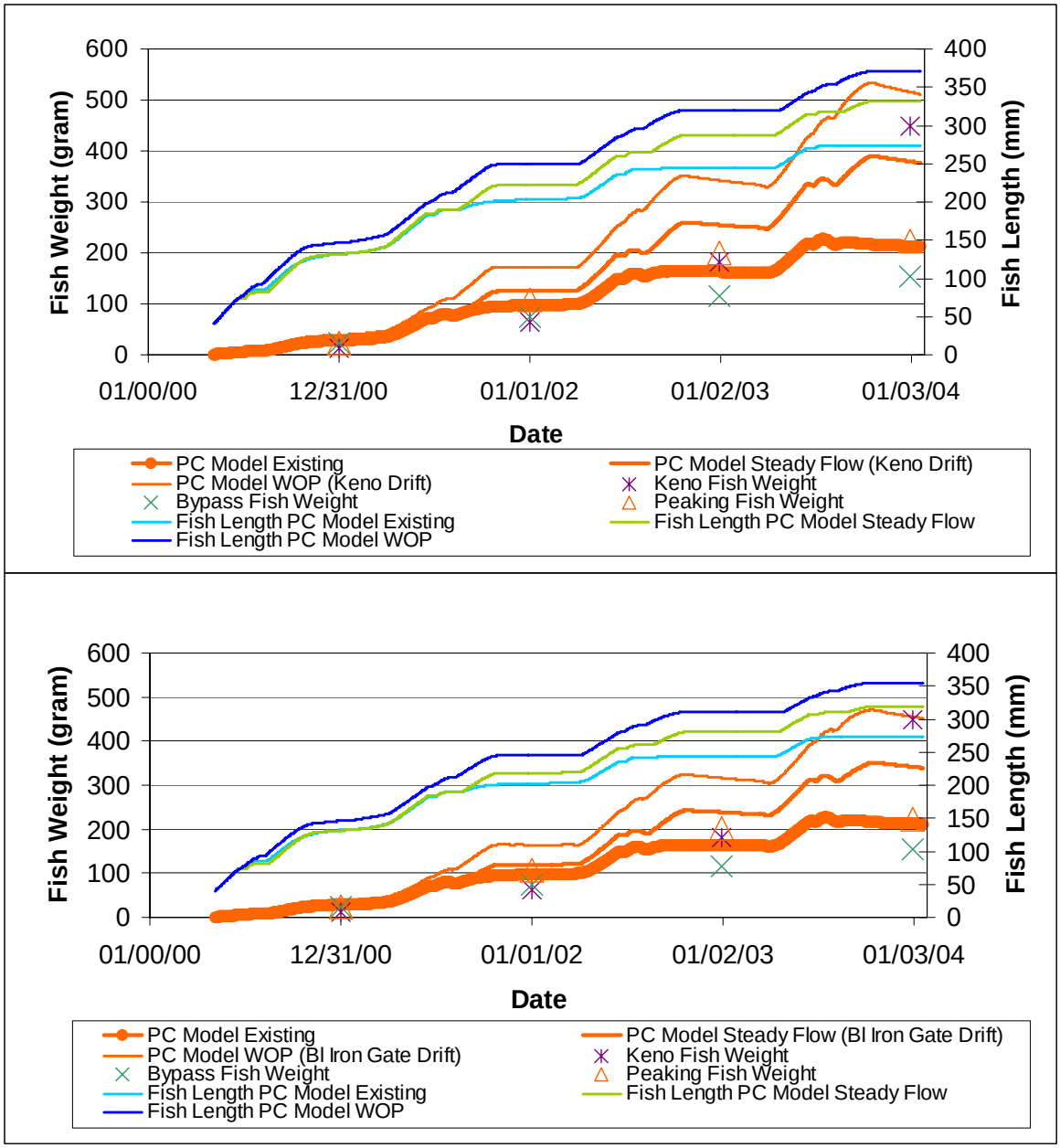

Figure 51. Growth (four years) modeled in the J.C. Boyle peaking reach for the WOP and Steady Flow scenarios using the bioenergetics foraging model with a high drift density observed in the Keno reach (top) and the drift density from the Klamath River below Iron Gate dam (bottom). Foraging model results for the J.C. Boyle peaking reach using observed drift densities and Existing Conditions (Prey Capture Model Peaking Reach) are show for comparison. Model results are also compared to measured size-at-age data in the Keno, J.C. Boyle peaking, and J.C. Boyle bypass reaches. This is our best estimate of the upper bounds for growth in the J.C. Boyle peaking reach for the Steady Flow and WOP scenarios.

Appendix A: Bioenergetics Foraging Model Description

General model description

The model evaluated in this study was derived by Addley (1993) and is similar to Hayes et al. (2001) and Hughes et al. (2003). It simulates NEI by subtracting energy losses from the gross energy intake (GEI), which is the estimated total prey energy per hour a fish can consume in a given feeding location. Energy losses consist of metabolic costs, digestive costs, and non-assimilated energy losses. Metabolic costs include routine basal metabolism while maintaining a station in the current and prey capture costs. Digestive cost is the energy required for prey digestion. Non-assimilated energy is energy egested in feces, and excreted as ammonia and urea in urine. Theoretically, NEI is

(1) $$NEI = \frac{NET\ \ ENERGY\ GAINED(J)}{TOTAL\ TIME(s)} = \frac{E}{T_s + T_f},$$

where NEI is the rate of energy intake available for growth and reproduction once costs and losses are accounted for, T_s is the time spent searching (s) and T_f is the time spent handling prey (s). For a drift feeding salmonid,

(2) $$E = \sum_{i=1}^{n} (DD_i \cdot MCA_i \cdot V_{ave_i} \cdot PC_i (E_i - CC_i) T_s) - SC \cdot T_s ,$$

where DD_i is the Drift Density of prey size class $_i$ (prey.m^{-3}) , MCA_i is the Maximum Capture Area (m^2) for prey size class $_i$ (Figure 1A), $V_{ave\,i}$ (m•s^{-1}) is the mean velocity passing through the *MCA*, PC_i is the probability of successful capture, E_i (J•prey^{-1}) is the energy available per prey item after digestive costs and assimilation losses are subtracted, CC_i is the prey capture cost (J•prey^{-1}), and *SC* (J•hr^{-1}) is the stationary swimming and basal metabolic cost.

Similarly,

(3) $$T_f = \sum_{i=1}^{n} DD_i \cdot MCA_i \cdot V_{ave_i} \cdot T_s \cdot t_{f\,i} ,$$

where $t_{f\,i}$ is the handling time per prey item (s•prey^{-1}).

Substituting the above expressions into the original equation gives:

$$NEI = \frac{\sum_{i=1}^{n} (DD_i \cdot MCA_i \cdot V_{avei} \cdot PC_i (E_i - CC_i) T_s) - SC \cdot T_s}{T_s + \sum_{i=1}^{n} DD_i \cdot MCA_i \cdot V_{avei} \cdot T_s \cdot t_{f_i}}. \quad (4)$$

Canceling T_s then results in our NEI equation, which agrees with that of Charnov 1976:

$$NEI = \frac{\sum_{i=1}^{n} (DD_i \cdot MCA_i \cdot V_{avei} \cdot PC_i (E_i - CC_i)) - SC}{1 + \sum_{i=1}^{n} DD_i \cdot MCA_i \cdot V_{avei} \cdot t_{f_i}}. \quad (5)$$

Equation 5 is essentially a formulation of the Holling disk equation (Holling 1959) that incorporates multiple prey classes and the swimming cost associated with holding a search position in the current (*SC*). Only the basic equations are included in the text. Table 1 provides a complete summary of the model equations.

The calculation of *MCA* assumes the fish maintains a holding position in the current and makes forage attempts for drifting prey (Figure 1). The *MCA* is roughly a partial-circle or partial-ellipse shaped area that is perpendicular to the fish's orientation (i.e., perpendicular to stream flow), within which the fish can capture prey before it drifts past. The shape and size of the *MCA* is determined by the maximum capture distance (*MCD* m), which is calculated in ten radial directions out from the focal position based on the combination of reaction distance, water velocity, and the potential swimming speed used by the fish during forage attempts. The 60-minute maximum sustainable velocity (*VMAX* $m \cdot s^{-1}$) is used to estimate the potential swimming speed of foraging fish.

The *MCD* is computed in all radial directions from the focal point of the fish in a plane perpendicular and transverse to the fish and the current (Figure 1). The *MCD* is generally different in each radial direction. It can be smaller vertically than laterally, for example, because of increased water velocity higher in the water column. Specifically, the *MCD* is determined by setting the time required for a prey item to pass the fish after it is spotted (reaction distance upstream) equal to the time required for the fish to intercept the prey. This process results in the following equation for *MCD*:

(6) $$MCD_i = \sqrt{\frac{RD_i^2 \cdot (VMAX^2 - V_{mean_i}^2)}{V^2_{prey_i} + VMAX^2 - V_{mean_i}^2}},$$

where *RD* is the reaction distance of the fish (cm) to the $_i$th prey size, $V_{prey\ i}$ is the velocity of the prey (m•s^{-1}), and $V_{mean\ i}$ (m•s^{-1}) is the mean water velocity along the $_i$th *MCD* radii. This equation is solved with an iterative computer program because V_{mean} is a function of *MCD.*

Reaction distance is a function of fish size, prey size, light levels, and turbidity (Dunbrack and Dill 1983; Henderson and Northcote 1985; Barrett et al. 1992). Addley (1993) derived the equation for RD shown in Table 1 from the empirical data of Dunbrack and Dill (1983).

The *MCA* is then calculated as the sum of the incremental areas associated with each *MCD* radial perpendicular to the flow and the fish (Figure 1).

(7) $$MCA_i = \sum_{j=1}^{m} \frac{d\theta}{2} \cdot MCD_{ij}^2$$

In equation 7, $d\theta$ is an incremental angle perpendicular to flow vectors and the fish that is associated with each *MCD* radial. We used m = 10 to provide a half ellipse shaped capture window with θ ranging from 0.0 to 3.14 radians and $d\theta$ = 0.314.

The velocities throughout the water column are determined from the mean velocities using the following empirical vertical velocity profile equation from Milhouse (1990) and linear interpolation (Figure 2A):

(8) $$\frac{Vp}{V} = A \cdot \left(\frac{Dp}{D}\right)^B,$$

where V is the mean velocity and D the depth at a given location in the river, Vp is the velocity at depth Dp in the water column, and A and B are empirical constants (A=0.919 and B = 0.23).

Table 1A. Equations used in the net energy intake (NEI) model (Addley 1993).

Parameter & Units	Equation/Calculation Method	Discussion and Citations
NEI_i ($J \cdot hr^{-1}$)	$NEI = \frac{\sum_{i=1}^{n} MCA_i \cdot V_{ave\,i} \cdot DD_i \cdot PC_i \cdot (E_i - CC_i) - SC}{1 + \sum_{i=1}^{n} t_{f\,i} \cdot MCA_i \cdot V_i \cdot DD_i}$	Net energy intake rate based on possible gross energy intake minus energy costs and losses for each prey class i.
MCD_{ij} (ft)	$MCD_{ij} = \sqrt{\frac{RD_i^2 (V_{\max}^2 - V_{mean_j^2})}{V_{\max}^2 + V_p - V_{mean_j^2}}}$	Maximum capture distance, calculated in the plane transverse and perpendicular to the fish by an iterative computer program where $V_{mean\,j}$ = mean velocity along MCD_{ij} (calculated within the computer program) and RD_i is the reaction distance for prey size i
V_{max} ($cm \cdot s^{-1}$)	$V_{\max} = 13.86 \left(\frac{21.42 - T}{3.92} \right)^{0.24} e^{0.24\left(1 - \left(\frac{21.42-T}{3.92}\right)\right)} TL^{0.63}$	Maximum sustained fish velocity equation derived from Brett & Glass (1973) T=temperature (°C) TL=total length (cm) .
RD_i (ft)	$PL_i = (RD_i^2 + 50\ RD_i)\left(\frac{1 + 5.8\ e^{-.034(TL)}}{1725}\right)$	Reaction distance equation derived from data of Dunbrack & Dill (1983) where PL_i = prey length (mm), RD_i = reaction distance (cm), and TL = total fish length (cm)
RD_i' (ft)	$RD_i' = \frac{RD_i(-2.27 \cdot TURB + 100)}{100}$	Reaction distance from equation above adjusted for turbidity (TURB) with equation adapted from Barrtett et al. (1992).
$V_{mean\ ij}$	Computed within computer program from velocity data.	Average velocity along MCD radian j for prey class i.
MCA_i (ft^2)	Area circumscribed by the arc created by connecting the ends of the MCD_i radians in the plane transverse and perpendicular to the fish (calculated with a computer program)	Maximum capture area at a location given water depth, water velocity, and channel morphology
$V_{ave\ i}$ ($ft \cdot s^{-1}$)	Computed within computer program from velocity data.	Average water velocity in the MCA for prey class i.
DD_i ($prey \cdot ft^3$)	Site specific emperical data	Measured daytime drift density in for each prey size i
PC_i	Assume probability of capture equals 1.0	Probability of successful prey capture
PE_i ($J \cdot prey^{-1}$)	$PE_i = 0.3818 (PL_i)^{2.46}$	Prey energy derived from Smock (1980) and Cummins and Wuycheck (1971), where PL_i = prey length (mm).
E_i ($J \cdot prey^{-1}$)	$0.58\ PE_i$	Energy assimilated (gross energy intake minus 14% for food digestion and 28% for losses due to excretion and feces) .

TC_i(s•prey^{-1})	$TC_i = \frac{2 \cdot MCD_i}{\left(VMAX^2 - V_{mean}^2\right)^{1/2}}$	Swimming time required for fish to capture a prey item 1 MCD away.
CC_i (J•prey^{-1})	$CC = \frac{6}{3600} \cdot SC(VMAX) \cdot TC$	First approximation of prey capture cost—6 times cost of steady swimming (SC) for one second at V_{max} times the capture time. This estimate falls at the lower end of the range (5-20) found empirically by Puckett and Dill (1984), at the lower end of the range (6-14) derived empirically by Bosclair and Tang (1993), and in the middle of the range (2.6-10) estimated by Hughes and Kelly (1996).
SC (J•h^{-1})	$SC = 1.4905\, W^{0.784}\, e^{0.068\,T}\, e^{(0.0259-0.0005\,T)U/30.48}$	Steady swimming cost from Stewart (1980) where W=weight (gm), T=temp (°C), and U=velocity (cm/s).
t_f(s)	Empirically approximated as 5 seconds	Estimated total time required for fish to recognize, intercept, attack and swallow prey item and then resume searching at the focal position, from Bachman (1984).

Figure 1A. Capture diagram of foraging model.

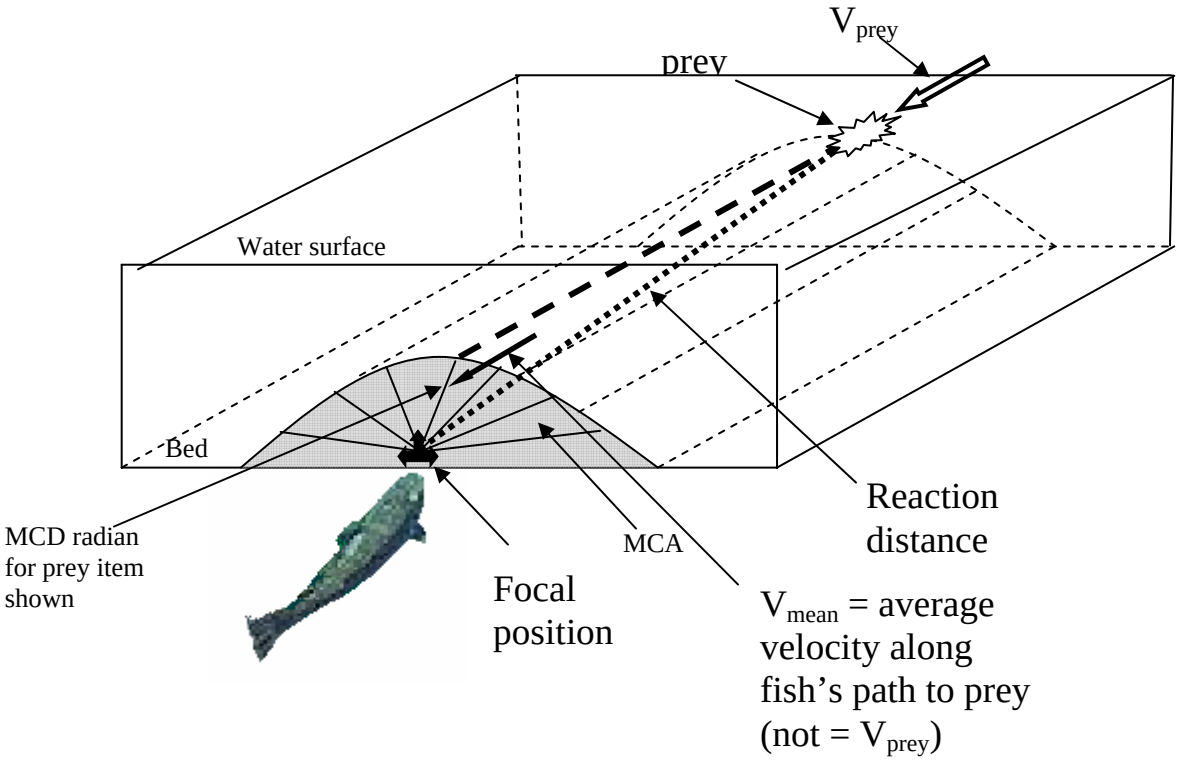

Figure 2A. Interpolated velocities (shaded contours) on a cross-section. Based on mean column velocity at 1 foot increments across the cross-section (vertical lines), empirical velocity profiles, and linear interpolation.

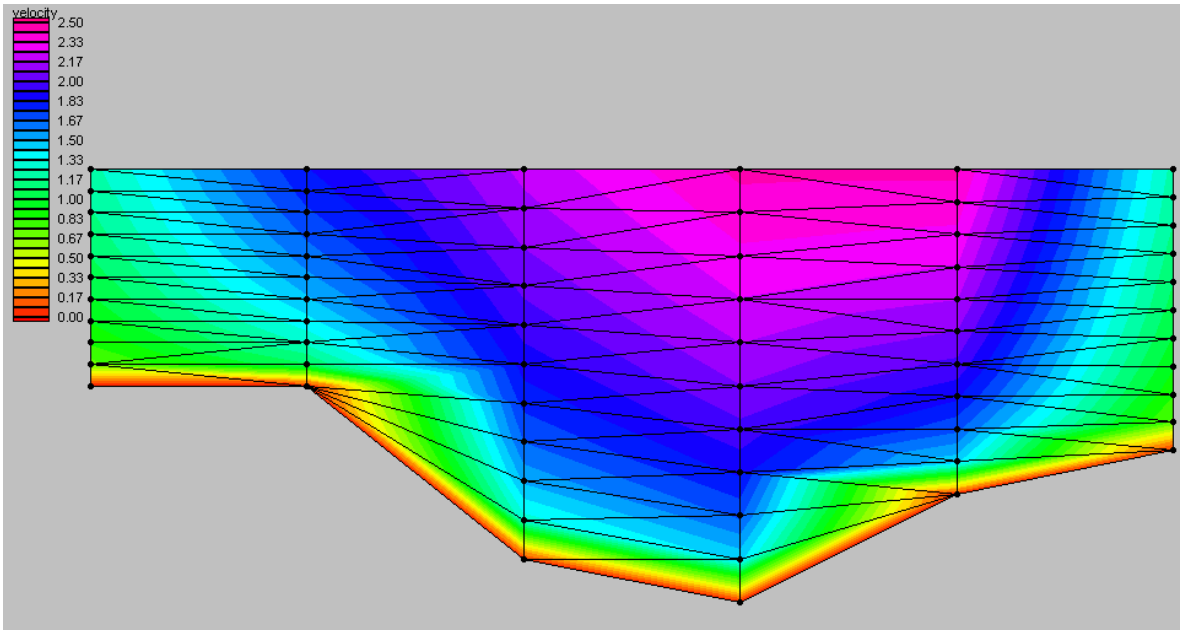

Appendix B: Gross Energy and Maximum Consumption Habitat Suitability Graphs

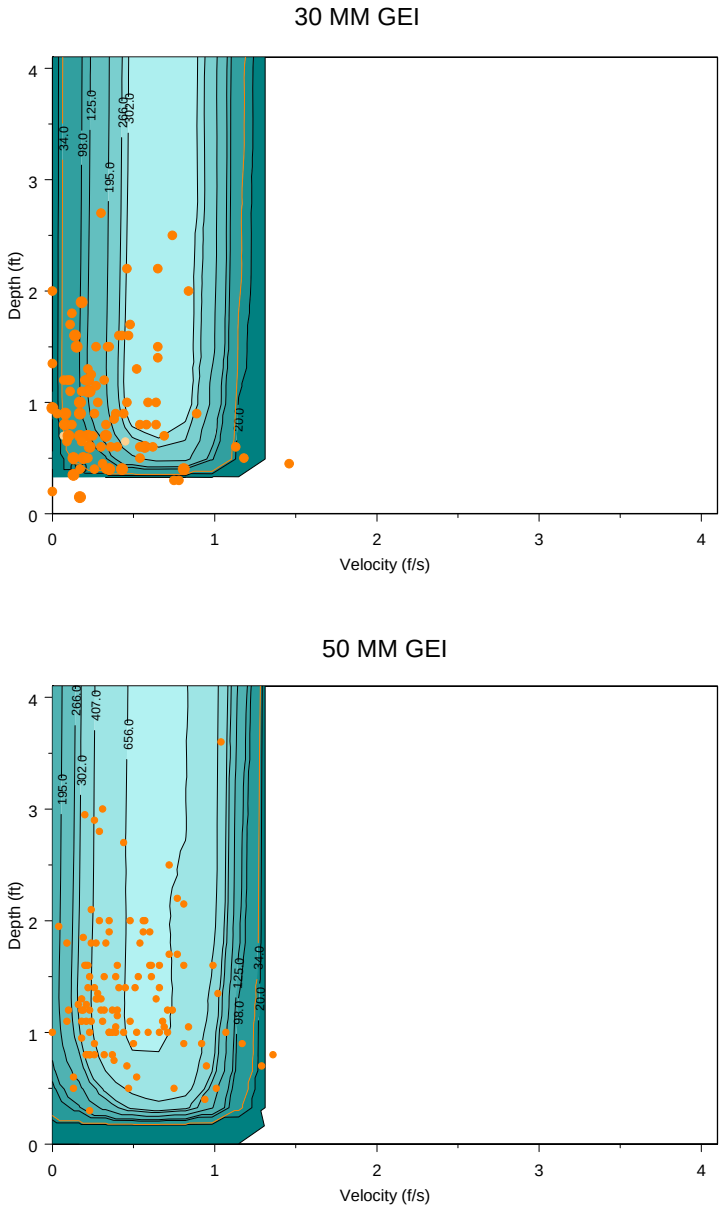

Figure 1B. Modeled gross energy intake (joules/hr) for 30 mm (top) and 50 mm (bottom) trout. Orange dots are 2002-2003 fish observations. Orange contour is the amount of hourly energy intake required to reach maximum consumption in a 13-hour day (36 and 103 joules/hr for 30 and 50 mm fish, respectively).

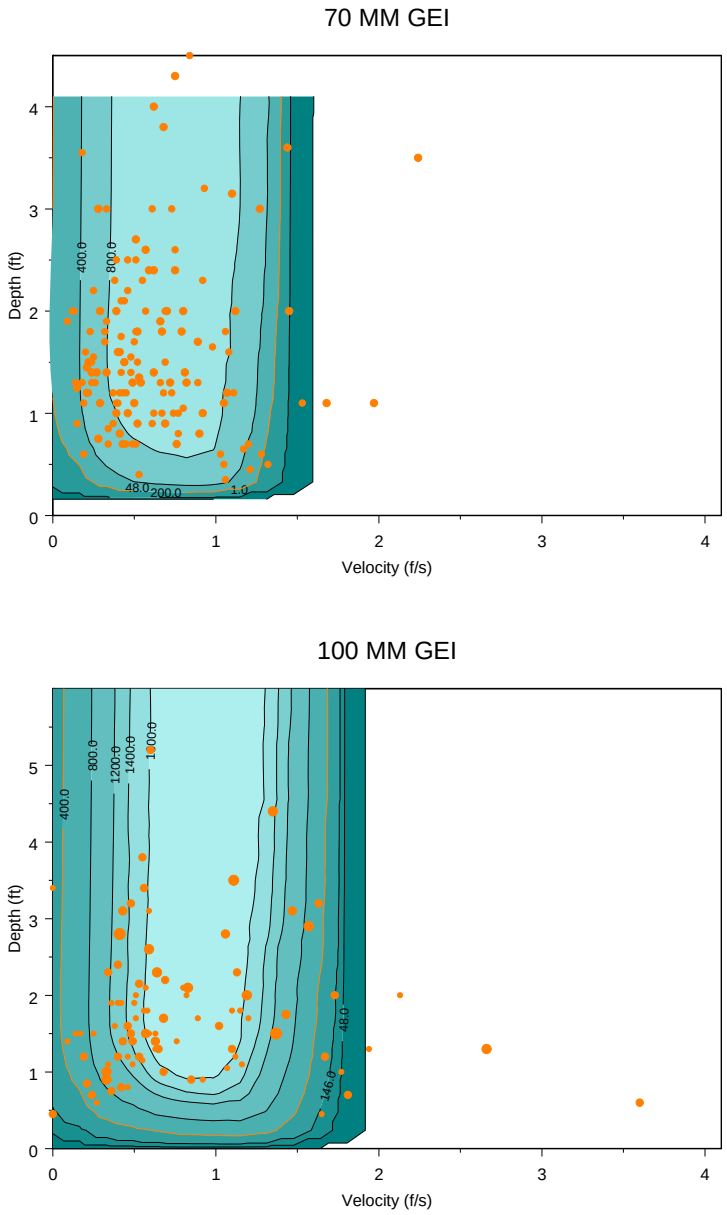

Figure 2B. Modeled gross energy intake (joules/hr) for 70 mm (top) and 100 mm (bottom) trout. Orange dots are 2002-2003 fish observations. Orange contour is the amount of hourly energy intake required to reach maximum consumption in a 13-hour day (206 and 430 joules/hr for 70 and 100 mm fish, respectively).

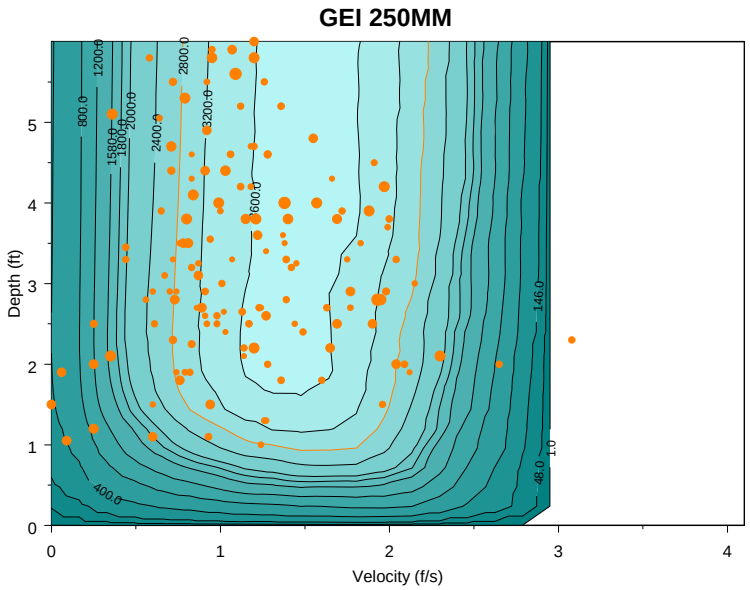

Figure 3B. Modeled gross energy intake (joules/hr) for 250 mm trout using an assumed peaking reach drift density of 0.06 prey/ft^3. Orange dots are 2002-2003 fish observations. The orange contour (bottom only) is the amount of hourly energy intake required to reach maximum consumption in a 13-hour day (2,825 joules/hr).

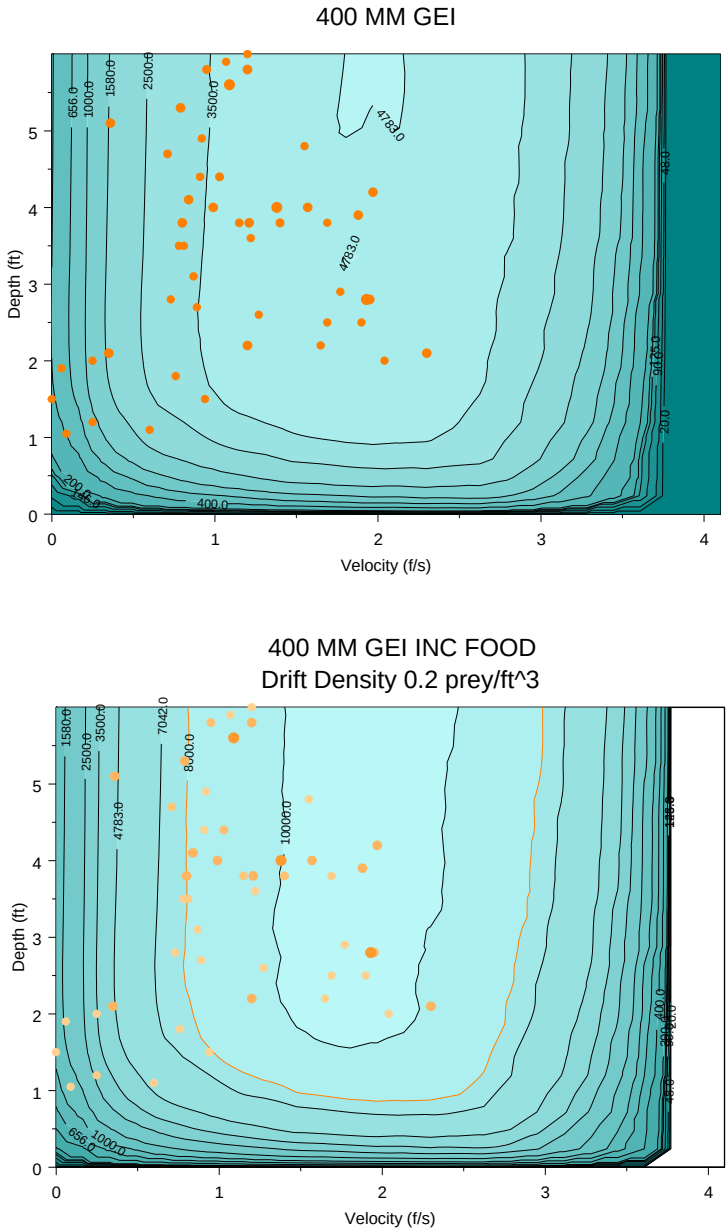

Figure 4B. Modeled gross energy intake (joules/hr) for 400 mm trout using an assumed drift density of 0.06 prey/ft^3 (top) and using a drift density of 0.20 prey/ft^3 (bottom). Orange dots are 2002-2003 fish observations. The orange contour (bottom only) is the amount of hourly energy intake required to reach maximum consumption in a 13-hour day (7,424 joules/hr). Maximum consumption cannot be achieved in the top figure.

Appendix C: Instream Flow Council Book Discussion of the Feeding Station Method

Instream Flow Council, 2002. Instream flows for riverine Resources stewardship: Instream Flow Council, 411 p. (Note: references cited below can be found in the book)

FEEDING STATION METHOD

Summary: The Feeding Station method describes a feeding habitat index based on areas of slow water adjacent to faster water that meet or exceed depth thresholds.

Objective: The method attempts to identify the discharge that maximizes the number of feeding stations for trout, using hydraulic simulation.

Type of Technique: Incremental

Description: The method serves as an alternative to conventional weighted usable area (WUA), the method relied on concepts of Bachman (1984) to provide a comparison to WUA, which in the early 1980s made intuitive sense but was unvalidated.

Appropriate Scale: Microhabitat

Riverine component(s) Addressed: Biology component is addressed by examination of hydraulic habitat.

Assumptions: The model assumes that trout select feeding stations (microhabitat) based on hydraulic habitat (i.e., consisting of slow water immediately adjacent to faster water as described above). Presence of the described feeding areas enhances salmonid production.

Level of Effort: The model requires a high level of effort in the field and in the office. In addition to hydraulic modeling requirements, the model requires manual review of each cell within a hydraulic simulation and its relation to adjacent cells at every flow of interest.

Historical Development: Snorkeling observations showed little or no use of shallow (<0.5 ft) depths by trout larger than fry. Literature and observations supported the concept (Fausch 1984; Beecher 1987; Washington Department of Fish and Wildlife and Department of Ecology 1996).

Application: This method employs hydraulic modeling from the PHABSIM system and a similar approach has been incorporated as an option in a version of a PHABSIM habitat model. Feeding areas are delineated by examination of hydraulic simulations or repeated measurements over a range of flows. Usually, habitat value (either 1 or 0) is tabulated manually for each cell, according to hydraulic conditions in the cell and the adjacent cells. A cell is considered to be a feeding station if:
Depth is at least 0.5 ft,
Velocity is less than 1 ft/sec (0.3 m/sec),
Velocity in one of adjacent (lateral) cells is at least 1 ft/sec, and
Velocity in same adjacent cell is at least 0.5 ft/sec faster than in cell.

The number of feeding stations is tabulated at each simulated flow of interest.

Strengths: None relative to alternatives available, such as PHABSIM.

Limitations and Constraints: This method is very scale dependent: distance between verticals (cell width and transect placement) must match the actual search range of the species of interest. Otherwise, you can underestimate actual feeding stations. Although the model simulates the feeding station concept that has been the subject of considerable published energetics research in field and laboratory, it is limited to lateral velocity gradients. It was originally proposed to incorporate a vertical velocity difference, but such applications require the use of three-dimensional hydraulic models and typically have not been used. It was developed when PHABSIM was relatively new and many of the assumptions, particularly that WUA incorporating depth, velocity, and substrate determine microhabitat quality, were untested for salmonids. Subsequently, more work has demonstrated a correlation between PHABSIM output and fish distributions. If feeding station analysis results match cell suitabilities at a reach level, then the feeding station method adds nothing. If it differs, then the use of PHABSIM is preferred because it has provided more successful validation.

Calibration and Validation: To date, there has been no validation demonstrating a correlation between this method of feeding station analysis and fish distributions.

To validate this method, the practitioner should (1) perform standard hydraulic model calibration to ensure that model reasonably approximates actual depths and velocities in stream at flows of interest, (2) measure fish distribution along PHABSIM transects and identify concurrent feeding stations, and (3) determine if actual fish distribution matches feeding station distribution.

Critical Opinion: This method has resulted in inadequate flow recommendations and should not be used without additional research. The main purpose of the method served as a check on WUA versus flow patterns when there were few tests of assumptions for WUA. If both methods yielded similar trends, then both were assumed to be more likely to be approximately correct. If the two methods differed, then nothing pointed to one method or the other. However, that assumption has changed. Research supports the assumptions behind WUA (Beecher et al. 1993, 1995); thus, the Washington Department of Fish and Wildlife, which developed the Feeding Station Method, now strongly prefers WUA and no longer uses the feeding station analysis. Use of this method has led to inadequate flow recommendations that were rejected by the Washington State Pollution Control Hearings Board (2000), which has initial review of water appeals.

Appendix D: Food and Space as Regulators of Fish Production

Food and Space

Food and space are two of the primary factors that control fish production (Chapman 1966; Murphy and Meehan 1991; Orth 1995). Other factors are also important (e.g., temperature, dissolved oxygen, turbidity, barriers, disease, etc.) and can limit fish populations (Bjornn and Reiser 1991). However, when these other factors are adequate, food and space will generally control fish production.

Food

In a hierarchical sense (Ryder and Kerr 1989) the productive capacity of the Klamath River is controlled by nutrients, light, temperature and allochothonous energy inputs (e.g., algae and zooplankton from upstream lakes and reservoirs). Aside from allochthonous inputs, the actual expression of the productive capacity in terms of primary productivity (e.g., algae) and secondary productivity (e.g., aquatic invertebrates), depends on the availability and characteristics of the physical habitat such as substrates (sand, cobble, etc.), stability of substrates (e.g., scouring), water velocity, water depth, and amount of time substrates are inundated. The production (primary and secondary) that is actually expressed as a result of the above conditions determines the amount of food available to fish.

In a similar hierarchical sense, the amount of food available to fish is a major determinant of the maximum fish production capacity of a river. Where other factors are not limiting, food availability has been shown to control 1) overall fish production, 2) the difference in fish abundance/biomass between rivers, 3) fish location and density within rivers, and 4) fish growth / fitness. Some example studies are listed below. While these examples are not specific to the Klamath River, they are intended to show the range of evidence suggesting that primary and secondary productivity has an affect on fisheries (except where eutrophication degrades physical variables such as dissolved oxygen).

Production

Waters (1982) found a close correlation between annual brook charr (*Salvelinus fontinalis*) populations and the natural production of their principal invertebrate food source (*Gammarus*) over a five year study period. Production of coho salmon was increased in a Vancouver Island stream during the summer when food was increased artificially (Mason 1976). The inherently greater primary productivity of open streams (more sunlight and more primary and hence secondary productivity) versus canopied streams has also been shown to increase salmonid production (e.g., Bilby and Bisson 1987).

Abundance and Biomass Between Rivers

Greater juvenile salmonid density in Alaskan streams and cutthroat trout density in the Pacific Northwest occurs in open canopy streams due to higher primary and secondary productivity (e.g., Wilzbach and Hall 1985; Murphy et. al. 1986). Hawkins et al. (1983) found a strong positive relationship between the density (and biomass) of 13 taxa of aquatic vertebrates (e.g., salmonids, dace, redside shiner, sculpins, lamprey, salamanders) and the density and biomass of aquatic invertebrates typically found in stream riffles (Northwestern USA). In the Hawkin's study there was two orders of magnitude variation in the invertebrate abundance and vertebrate abundance, and a strong positive correlation between the two. In a large multivariate study throughout New Zealand (89 study sites), Jowett (1992) found that benthic invertebrate biomass alone explained 45% of the variation in trout abundance. In artificial stream channels, Mason and Chapman (1965) observed a large positive difference in coho volitional residence (standing crop) with increased drift abundance. Warren et al. (1964) observed seven-fold higher production of cutthroat trout in experimental streams where benthic invertebrate populations had increased four-fold after enrichment with sucrose. Wilzbach (1985) found similar results. In addition, Wilzbach found that food overrode the effects of cover in determining abundance. Slaney et al. (1974) also found increased densities with increased food and an associated reduction of territory size and fry aggression.

Fish location and Density Within Rivers—Baker and Hawkins (1990) found that drift abundance entering pools was the most important descriptor of cutthroat trout abundance in a study of approximately 70 pools. Power (1984) found that algae feeding catfish densities in a Panamanian stream were strongly correlated (positively) with the rates of periphyton production on stream substrates. Habitats with low periphyton production had low numbers of catfish and vice versa.

Numerous investigators (e.g., Smith and Li 1983; Fausch 1984; Hughes and Dill 1990; Addley 1993; Hill and Grossman 1993; Genusch et al. 2001)) have shown that measures of net energy intake can accurately describe the individual habitat choice of feeding fish. These studies have found that the locations fish select in natural stream settings and/or laboratory studies are synonomous with the best locations in the stream for obtaining net energy intake. Hughes (1998) has also shown that the observed size gradient of fish along a river system is described by bioenergetics. For example, the counterintuitive gradient of larger fish upstream versus downstream found in some systems is explained simply by food abundance and fish bioenergetics.

Fish Growth and Fitness

Short-term and long-term fish growth are directly related to temperature, energy expenditure, and food availability. Cada et al. (1987) found low growth in Appalachian salmonids due to low aquatic invertebrate abundance. Fausch (1984) related short-term fish growth to modeled net energy intake. Hayes (2000) used a similar net energy approach to accurately predict the growth of brown trout in New Zealand from age 0+ through age 12. Numerous studies (many of those discussed above regarding abundance and food) have found that natural or artificial increases in food abundance increase both fish abundance and growth. Some studies have only documented increased growth. For example, after the institution of a minimum flow requirement below the Conowingo Hydroelectric Dam, Maryland, food production increased and food consumption, condition factors, and growth increased for the three abundant fish species (white perch *Morone americana*, yellow perch, and channel catfish *Ictalurus punctatus*). In another study, Johnston et al. (1990) fertilized 29-km of stream and found increased trout growth. They also found that the increased growth shortened the time required by juvenile steelhead to become smolts, reduced juvenile mortality, and increased smolt production. Ware (1982) argued that increased growth or the acquisition of net energy intake (surplus power in his paper) is a direct ecological correlate of fitness in fishes.

Fish with increased growth grow through predation windows faster (less mortality) and bigger fish are more competitive and produce more eggs (i.e., more productive). In addition, over-winter survival of fish is directly related to the size and condition of individual fish prior to the onset of winter (e.g., Smith and Griffith 1994).

Space

Physical space for fish depends in a hierarchical sense on the amount of discharge, the shape of the channel, and the channel slope. At a level lower in the hierarchy, meso-scale habitats (pools, runs, riffles, channel margins) composed of micro-scale habitats--depth, velocity, substrate, bed slope, and cover--provide space requirements for fish. In general, space needs of fish are species and lifestage specific. Some species and lifestages have very specific space needs in terms of quality and quantity (e.g., fry), whereas other species and lifestages are considered generalists and are able to utilize a broad range of habitats (e.g., adult salmonids). The physical habitats in rivers that are the most stable (least susceptible to change with changing discharge) are deep pools. At different discharges shallow margin habitats, riffles, and runs have highly variable depths, velocities, and variable locations of suitable depths and velocities (e.g., Bjornn and Reiser 1991, Aadland 1993). Species and lifestages that are dependent on these habitats are likely to be affected by the temporal pattern of the flow regime.

The temporal pattern (timing, duration) and amount of physical space (velocity, depth, substrate and cover) are important in meeting the physiological, behavioral, and life history needs of many of fishes. For example, the fish species typically spawn during short periods of time in spring or fall (cued by temperatures and streamflows) over shallow gravels or in channel margins near vegetation. Incubating eggs are non-mobile and must remain in suitable habitat until they hatch and the fry disperse. Fry and juvenile fishes occupy special rearing and nursery habitats providing protection from high water velocities and predators. These are typically shallow (slow velocity) habitats along the river margin with rock, woody debris, or vegetation cover. Small fry in particular, because of their limited swimming ability, are vulnerable to predation and downstream drift as a result of fluctuating or changing habitat conditions (larger fish for example greater than about 50 mm are less affected) (e.g., Heggenes 1988, Heggenes and Traaen 1988, Irvine 1986). The adult fish of different species have different behaviors and habitat use patterns, however, they typically choose habitats close to foraging locations and cover that are less susceptible to changing flow conditions. These habitats are typically in deeper water and/or faster water velocities than fry and juvenile habitats.

The diversity of habitats types in a river directly influences the diversity of species and lifestages. Habitat diversity begets species diversity. For example, very simple habitats (channelized rivers) have low diversity. The relationship between habitat diversity and species diversity holds true unless the habitat diversity greatly

deviates from the norm (Allan 1995) (e.g., rivers where habitat fluctuates widely on a short time scale have lower species diversity). Based on measurement of velocity, depth, and substrate diversity Gorman and Karr (1978) found a strong positive correlation between stream fish diversity in Indiana and Panama streams. Schlosser (1982) found the same relationship except that in shallow temporally variable habitats diversity was lower. Horwitz (1978) and Bain et al. (1988) also have found that temporally variable habitats have lower fish diversity.

Relevant Invertebrate Ecology

Temperature, water current (stream hydraulics) and substrate are the most fundamental physical variables defining aquatic invertebrate habitat (Allan 1995). In a river system like the Klamath River temperature is partially controlled by flow regulation. Aside from temperature, however, stream hydraulics and substrate are the main controlling variables with respect to flow. Interactions between water depth, channel slope, velocity, and substrate on the riverbed affect the space, oxygen, waste removal, and food delivery and availability to aquatic invertebrates (Hynes 1970; Allan 1995). Statzner (1986) for example considered the physical characteristics of stream hydraulics as the most important environmental factor governing the distribution (zonation) of benthos on a world-wide scale.

On a smaller scale, benthic invertebrates have a variety of habitat needs based on their feeding behavior, oxygen requirements, and morphological adaptations. In general, in rivers like the Klamath River benthic invertebrates are more abundant and diverse in intermediate sized substrates (gravels/cobbles/small boulders) and in aquatic vegetation than in simple substrates such as sand and boulder/bedrock (Keup 1988; Allan 1995). Invertebrates are also typically more abundant in riffles than pools (e.g., Allan 1995). In larger streams there is also a cross-stream distribution of benthic fauna. Benthic fauna are most abundant along the sides of the stream and least abundant in the middle of the stream (Hynes 1970, pg 248). In New Zealand river studies, the intermediate channel margins have been shown to have the highest densities (Jowett In press). The very shallow, slow habitat immediately adjacent to the channel margin (slow, depositional areas subject to natural and artificial flow fluctuations) and the center of the channel (high shear stress and disturbance rates) have relatively low invertebrate densities (Jowett, in press). In addition, in large rivers (like the Klamath River) the highest invertebrate densities are in deeper and faster water than in small streams. In part this result is due to the shape of velocity profiles in rivers. In larger rivers where water is relatively deep, higher mean column velocities are required to produce the same

near-bed velocities that produce optimum invertebrate habitats in shallower, slower water of small streams (Jowett, in press).

Statzner et al. (1988) concluded that near-bed hydraulic variables and depth, velocity and substrate models currently provided the best predictions of benthic invertebrate distribution. Velocity, for example, is a particularly important determinate of the distribution and abundance of filter feeding invertebrates, e.g., Hydropsychidae (caddis) (Eddington 1968) and Simuliidae (blackfly) larvae (Charpentier and Morin 1994). The correlation of hydraulics and substrate to benthic invertebrate density and diversity has resulted in development of habitat suitability models of depth, velocity, and substrate size to quantify physical invertebrate habitat versus flow relationships (e.g., Gore and Judy 1981; Orth and Maughan 1983; Gore 1987; Statzner 1988; Jowett and Richardson 1990; Jowett et al. 1991; Collier 1993, Quinn and Hickey 1994, Collier et al. 1995; Gore In Press).

Waters (1976), who was one of the first to use habitat suitability criteria in instream flow models, quantified food production as relatively fast (0.5 to 4.5 ft/sec) and relatively shallow water (0.2 to 7 feet) in substrates from silt to small boulder. These suitability curves are very broad and general, and have been used successfully to relate food production and trout abundance (Jowett 1992, Jowett et al. 1997) and they encompass the range of benthic invertebrate habitats quantified in the literature (Keup 1988; references above). In particular, they encompass the depths, velocities and substrates utilized by rheophilic benthic fauna in large rivers (Jowett, Pers. Comm.). These suitability criteria generally encompass faster water riffle and intermediate channel margin habitat types. These habitat types and the invertebrate community that inhabits these areas are the same taxa utilized by fish for food (Keup 1988; Rader 1997).

Flow Fluctuations

Large, frequent flow fluctuations have generally been shown to reduce fish abundance and diversity (particularly shallow-slow water fishes) and invertebrate abundance and diversity (e.g., Horwitz 1978; Schlosser 1982; Gislason 1985; Cushman 1985; Irvin 1995; Bain et al. 1988; Morgan 1991; Moog 1993) in rivers. Flow fluctuations temporally alter habitat suitability (depths, velocities, and shear) in the permanently wetted channel and create temporally and spatially variable 'varial' zones along the margins of channels. Fishes that utilize margin habitats are subjected to changing conditions (e.g., Bain et al. 1988). In addition, the substrates in the varial zone are dewatered causing a loss of benthic invertebrate

biomass in the varial zone (Fisher and LaVoy 1972; Perry and Perry 1986; Blinn et al. 1995).

Benthic Invertebrate Recolonization

Benthic invertebrate colonization dynamics govern the productivity of substrates that are affected by flow fluctuations. Colonization or recolonization of dewatered substrates (e.g., varial zone substrates) is governed by immigration and emigration rates of benthic organisms (Sheldon 1984). Immigration and emigration are primarily accomplished through the downstream movements of drifting invertebrates (e.g., Waters 1964; Townsend and Hildrew 1976). As a result, colonization is positively related to the amount of drift and water velocity and inversely correlated to the distance from a colonization source. Townsend and Hildrew (1976), Lancaster (1990), and Bird and Hynes (1981) have shown strong positive correlations between colonization and water velocity (or discharge and rainfall as surrogates of velocity). Higher velocities increase the number of drifting invertebrates available for colonization (Waters 1964; Lancaster 1990). The source of the invertebrates in the drift is benthic substrates and the distance invertebrates travel in the drift depends on the velocity (see Drift below), but is usually only a few meters. Townsend and Hildrew (1976), in a small stream with low velocities, 10 cm/s, found that the source of benthic invertebrates in the drift was from substrate only 2 meters upstream. If denuded substrates are far from source invertebrates (e.g., rewatered channels), recolonization is relatively slow and is limited by availability of invertebrates in the drift (e.g., Townsend and Hildrew 1976; Gore 1982).

The time it takes substrates to be colonized also depends on the quality of the substrate. Perry and Perry (1986) found that colonization was greatest on substrates that had periphyton (conditioned substrates) and that substrates that were barren (out of the water for some period of time) had low recolonization rates. Presumably this occurs because newly arriving benthic invertebrates (colonizers) quickly emigrate if food availability and habitat are not suitable (Bohle 1978; Walton 1978) (i.e., emigration rates of colonizers are proportional to habitat suitability). Complete colonization (density and diversity) of small patches of conditioned substrates can occur relatively rapidly, 10 – 14 days (Waters 1964). Colonization of unconditioned substrates takes from 40 to 75+ days (Gore 1982, Townsend and Hildrew 1976; Gersich and Brusven 1983) and can take much longer (3 months to many years) (Leonard 1942; Narf 1985; Blinn et al. 1995) depending on the substrates, season, and distance from the source benthic invertebrates. Blinn et al. (1995) found that two 12 hour exposure periods

(dewatering) of substrates may require >4 months for complete recovery. Gore found in a rewatered channel that a site ca. 250 m downstream took 75 days longer (nearly twice as long) to colonize than the upstream site closer to source invertebrates. Townsend and Hildrew (1976) also found large differences in colonization along a small rewatered channel.

Colonization is also potentially much lower, orders of magnitude lower, during the winter (December-March) than during the summer (Williams 1980). Williams (1980) measured colonization of substrates by various taxa over the entire year. All taxa showed marked declines in winter colonization. In addition, Williams (1980) found that colonization was dependent on lifestage. First instars were very active colonizers (termed by others as distributional drift) and some species did not colonize during various seasons likely because of mobility of various lifestages (e.g., a net spinning caddisfly only colonized as later instars, 4 and 5).

Colonization of substrates occurs relatively linearly over time. Studies that have measured colonization (Waters 1964; Gore 1982, Townsend and Hildrew 1976; Gersich and Brusven 1983) show linear (sometimes slightly curvilinear) increases in numbers of benthic invertebrates up to the point where the carrying capacity is reached or overshot.

Drift

Drift is the main source of food for many species of fish, particularly salmonids. Drifting invertebrates are derived from the benthos and spend very little time in the water column. Entry into the water column is behavioral (feeding movements, predation avoidance, better habitat seeking), accidental (accidental dislodgement), and catastrophic (erosion by high velocities such as floods) (Allan 1995). The amount of drift appears to be a constant proportion of the benthic density (although this has been widely debated). Hilderbrand (1974) found a nearly perfect linear relationship between drift and benthic density (i.e., very low benthic density equals very low drift and vise versa). Numerous investigators have found drift to be 0.01% to 0.5% of the bottom fauna (see references in Allan 1995). Propensity to drift and therefore availability to drift feeding fishes, however, is dependent on the specific invertebrate taxa, its behavior, abundance, and habitat (Allan 1995; Rader 1997). The benthic invertebrates Ephemeroptera, Chironomidae, Simuliidae, and some Plecoptera and Trichoptera, are the most common members of the drift. The Ephemeropterans *Baetis*, *Acentrella*, Heptageniidae, *Paraleptophlebia*, *Ephemerella*, and *Drunella* are very prone to drifting as well as Simulidae, free-living Chronomidae (Rader 1997).

The distance that drifting invertebrates travel in the drift (each individual trip) is also taxa specific and depends on velocity. Some species behaviorally exit the drift (i.e., swim—*Baetis* spp.) and as a result drift shorter distances than those that do not. Drift distance for taxa that do not actively regain the bottom are on average 1 and 10 meters for velocities of 5 and 50 cm/sec, respectively. For *Baetis* spp. (agile swimmers) the distances at the same velocities are approximately 0.2 to 1.2 meters (see Figure 10.3 in Allan 1995). Ciborowski (1983) found the lateral dispersion of drifting invertebrates was a function of distance traveled downstream. Lateral dispersion was roughly 30% (or less) of the longitudinal drift distance.

Where rivers, like the Klamath River, are feed from upstream lakes or reservoirs, zooplankton and phytoplankton produced in the still water habitat become a food source in the river. The availability of this food source decreases in proportion to the distance downstream as a result of settling and straining of zooplankton from the water column by vegetation (e.g., Chandler 1937). Where present, zooplankton are utilized by fishes (particularly smaller fishes) as a food source and algae and zooplankton are utilized by invertebrates as a food source (increasing benthic invertebrate densities).

Drift Density

There are a large number of papers that have reported daytime drift density, and there is a very wide range of drift densities reported. Much of the difference is due to actual differences in drift density between sites (different chemical and physical conditions), seasonal differences, and methodological differences (e.g., drift net mesh size). For example, very large drift densities can occur during the summer and the low drift densities during the winter (e.g., Alan (1978). Few of the studies report the size distribution of drift, so it is not possible to determine whether, for example, reported densities are from very small, but abundant aquatic species, or larger and possibly less abundant species.

The majority of the reported drift densities range from about 0.005 to about 0.3 per ft^3. Alan (1978) reported several studies that ranged from about 0.003 to about 0.6 per ft^3 with two studies having much higher drift densities (highest was 4.9 per ft^3). Armitage (1977) reported about 20 studies with a range from 0.006 to 0.6 per ft^3. Studies from New Zealand in numerous large rivers like the Klamath River range from about 0.01 to 0.2 per ft^3 (John Hayes, Pers. Comm.). Several studies reported by Hauer et al. (1989) including some large regulated rivers, ranged from 0.003 to 0.09 per ft^3, with one density of 0.85 per ft^3 during a

reduction in flows following a stable period of flows. The Klamath River below Iron Gate Dam had August/September drift densities of 0.02 to 0.09 per ft^3 (Hardy and Addley 2001). Streams in Idaho, Montana and Utah that we have personally sampled (St. Charles Creek, Logan River, Blacksmith Fork, Green River, Flathead River, etc.) have summer and winter (winter typically lower) drift densities in the range of 0.01 to 0.4 per ft^3 (Pers. Obser.; Filbert and Hawkins 1995). Many other papers that we have reviewed fall within the ranges listed above.

Recovery of Systems With Reduced Flow Fluctuations

We are aware of only a few studies that have assessed the recovery of river ecosystems after implementation of a flow regime designed to reduce flow fluctuations. Travnichek et al. (1995) monitored the recovery of a warmwater fishery below a hydropeaking dam after minimum flows were implemented (previously flows dropped to no running water). While the implementation of minimum flows did not reduce the frequency of fluctuating flows, it did reduce the magnitude of flow fluctuations. Travnichek et al. (1995) found that species richness doubled and that the relative abundance of species that are dependent on riverine environments (fluvial specialists) increased from less than 40% of the fish collected to over 80% after flow modification. This should not be surprising given that prior to minimum flows, no running water was present at times.

In the Lee's Ferry tailwater below Glen Canyon Dam, Arizona, McKinney et al. (2001) found that with increased minimum, higher mean, and more stable flow releases after 1991 that the abundance of wild spawned rainbow trout increased fourfold. The increase in rainbow trout was attributed to increased food production (reduction in the varial zone), stability of shallow, nearshore areas, and development of warmer nearshore area for nursery habitat with the stable flows. The condition factor of the largest size class of rainbow trout actually decreased with stabilized flows. This was attributed to density dependent effects.

Alan, J.D. 1987. Macroinvertebrate drift in a Rocky Mountain stream. Hydrobiologia 144:261-268.

Armitage, P.D. 1977. Invertebrate drift in the regulated River Tees, and an unregulated tributary Maize Bek, below Cow Green Dam. Freshwater Biology. 7:167-183.

Filbert, R.B. and C.P. Hawkins. 1995. Variation in condition of rainbow trout in relation to food, temperature, and individual length in the Green river, Utah. Trans. Am. Fish. Soc. 124:824-835.

Hauer, F.R., J.A. Stanford, and R. Steinkraus. 1989. The zoobenthos of the lower Flathead River: the effect of Kerr Dam operation. Flathead Lake Biological Station, Open File Report 108-89.

Aadland, L.P. 1993. Stream habitat types: Their fish assemblages and relationship to flow. North American Journal of Fisheries Management 13:790-806.

Addley, R.C.1993. A mechanistic approach to modeling habitat needs of drift-feeding salmonids. MS thesis. Utah State University, Logan, Utah. 141 p.

Allan, D. 1995. Stream Ecology. Chapman and Hall, Oxford London. 387 p.

Bachman, R.A. 1984. Foraging behavior of free-ranging wild and hatchery brown trout in a stream. Transactions of the American Fisheries Society 113:1-32.

Bain, M.B. 1995. L'habitat a l'echelle locale: Distribution multiparametre des poisons d'eau courante. Bull. Fr. Peche Piscic 337/338/339:165-177

Bain, M.B., J. T. Finn, and H. E. Booke. 1988. Streamflow regulation and fish community structure. Ecology 69(2):382-392.

Baker, A.D., and C.P. Hawkins. 1990. Variation in trout abundance and habitat quality: patterns at the scale of individual stream pools. Can. J. Fish. Aquat. Sci. ?.

Bartholow, J. M. 1991. A modeling assessment of the thermal regime for an urban sport fishery. Environmental Management. 15:833-845.

Bilby, R.E., P.A. Bisson. 1987. Emigration and production of hatchery coho salmon (Oncorhynchus kisutch) stocked in streams draining an old-growth and a clear-cut watershed. Can. J. Fish. Aquat. Sci. 44:1397-1407.

Bird, G.A. and H.B.N. Hynes. 1981. Movement of immature aquatic insects in a lotic habitat. Hydrobiologia, Vol. 77:103-112.

Bjornn, T.C. and D.W. Reiser. 1991. Habitat requirements of salmonids in streams. American Fisheries Society Special Publication 19:83-138.

Blinn, D.W., J.P. Shannon, L.E. Stevens, and J.P. Carder. 1995. Consequences of fluctuating discharge for lotic communities. J. N. Am. Benthol. Soc., Vol.14(2):233-248.

Bohle, C.H.W. 1978. Beziehungen zwischen dem Nahrungsangebot, der drift und der raumlichen verteilung bei larven von baetis rhodani (PICTET) (Ephemeroptera: Baetidae). Arch. Hydrobiol., Vol.84(4): 500-525.

Bovee, K.D., 1978. Probability-of-use criteria for the family salmonidae: Instream flow information paper No. 4, U.S. Fish and Wildlife, FWS/OBS-78/07, Ft. Collins, Colorado.

Bovee, K.D. 1985. Evaluation of the effects of hydropeaking on aquatic macroinvertebrates using PHABISM. Hydrologist, Western energy and land use team, U.S. Fish and Wildlife Service, Ft. Collins, Colo. Pp. 236-263.

Brown, C.J.D. 1971. Fishes of Montana. Big Sky Books, Montana State University. Bozeman, Montana. P.207.

Brown, L.C. and T. O. Barnwell. 1987. The enhanced stream water quality models Qual2E and Qual2E-UNCAS: documentation and user manual. EPA, Athens, GA.

Bustard, D.R. and D.W. Narver. 1975. Aspects of the winter ecology of juvenile coho Salmon (*Oncorhynchus kisutch*) and steelhead tour (*Salmo gairdneri*). Journal of the Fisheries Research Board of Canada 32:667-680.

Cada, G.F., J.M. Loar, and M.J. Sale. 1987. Evidence of food limitation of rainbow and brown trout in Southern Appalachian soft-water streams. Transactions of the American Fisheries Society 116:692-702.

Chandler, D.C. 1937. Fate of typical lake plankton in streams. Ecological Monographs. 7:445-479.

Chapman, D.W. 1966. Food and space as regulators of salmonid populations in streams. The American Naturalist Vol. 100(913):345-357.

Chapman, D.W. and T.C. Bjornn.1969. Distribution of salmonids in streams, with special reference to food and feeding, p.153-176. *In* T.G. Northcote (Ed.). Salmon and trout in streams. H. R. MacMillan Lectures in Fisheries, University of British Columbia, Vancouver.

Charpentiew, B., and A. Morin. 1994 Effect of current velocity on ingestion rates of black fly larvae. Can. J. Fish. Aquat. Sci. 51:1615-1619.

Ciborowski, J.J.H. 1983. Downstream and lateral transport of nymphs of two mayfly species (Ephemeroptera). Can. J. Fish. Aquat. Sci., Vol.40: 2025-2029.

Cochnauer,T. and T. Elms-Cockran. (1986). Probability-of-use curves for selected Idaho fish species. Project Performance report. Project F-71-R-10. Idaho Dept. of Fish and Game, USA.

Collier, K.J. 1993. Flow preferences of larval chironomidae (diptera) in Tongariro river, New Zealand. New Zealand Journal of Marine and Freshwater Research Vol. 27:219-226.

Collier, K.J., G.F. Croker, C.W. Hickey, J.M. Quinn, and B.S. Smith. 1995. Effects of hydraulic conditions and larval size on the microdistribution of hydrobiosidae (trichoptera) in two New Zealand rivers. New Zealand Journal of Marine and Freshwater Research Vol. 29:439-451.

Cunjak, R.A. 1996. Winter habitat of selected stream fishes and potential impacts from land-use activity. Can. J. Fish. Aquat. Sci. Vol. 53:(Supp. 1).

Cunjak, R.A., and B. Power. 1987. The feeding and energetics of stream-resident trout In winter. J. Fish Biol. 31:493-511.

Cushman, R.M. 1985. Review of ecological effects of rapidly varying flows downstream from hydroelectric facilities. N.A. J. Fish. Management, Vol.5: 330-339

Dill, L.M., R. C. Ydenberg, and A.H.G. Fraser. 1981. Food abundance and territory size in juvenile coho salmon (Onchorhynchus kisutch). Can. J. Zool. 59:1801-1809.

Dos Santos, J.M., J.E. Darling, and D. Cross. 1988. Lower Flathead River Fisheries study, executive summary, volume II, final report FY 1983-1987. BPA contract no. DE-AI79-83BP39830. Portland, OR. 102 pp.

Dos Santos, J.M., J.E. Darling, and D. Cross. 1988. Lower Flathead system fisheries study: Main river and tributaries. Volume II. Final report FY 1983-87. Bonneville Power Administration, Contract No. EE-AI79-83BP39830.

Edwards, E.A., G. Gebhart, and O.E. Maughan. (1983).Habitat Suitability Information: Smallmouth Bass. U.S. Dept. Int., Fish Wildl. Serv. FWS/OBS-82/10.36. 47 pp.

Everest, F.H., and D.W. Chapman. 1972. Habitat selection and spatial interaction by juvenile Chinook salmon and steelhead trout in two Idaho streams. J. Fish. Res. Bd. Canada 29:91-100.

Fausch, K.D. 1984. Profitable stream position for salmonids: relating specific growth rate to net energy gain. Can. J. Zool. 62:411-451.

Fisher, S.G., and A. LaVoy. 1972. Differences in littoral fauna due to fluctuating water levels below a hydroelectric dam. Journal Fisheries Research Board of Canada, Vol.29(10):1472-1477.

Fraley, J.J., and P.J. Graham. 1982. The impact of hungry horse dam on the fishery of the Flathead river- final report. Montana Department of Fish, Wildlife, and Parks.

Genusch, G.R., T.B. Hardy, and R.C. Addley. 2001. Examining feeding strategies and position choice of drift-feeding salmonids using an individual-based, mechanistic foraging model. Can. J. Fish. Aquat. Sci. 58: 446-457.

Gersich, F.M. and M.A. Brusven. 1981. Insect colonization rates in near-shore regions subjected to hydroelectric power peaking flows. Journal of Freshwater Ecology, Vol.1: 231-236.

Gibson, R.J. 1978. The behavior of juvenile Atlantic salmon (*Salmo salar*) and brook trout (*Salvelinus fontinalis*) with regard to temperature and to water velocity. Transactions of the American Fisheries Society 107:703-712.

Gislason, J.C. 1985. Aquatic insect abundance in a regulated stream under fluctuating and stable diel flow patterns. N.A. J. Fish. Management, Vol.5: 39-46.

Gore, J.A. 1982. Benthic invertebrate colonization: source distance effects on community composition. Hydrobiologia Vol.94: 183-193.

Gore, J.A. 1987. Development and applications of macroinvertebrate instream flow models for regulated flow management. Pages 99-115 in J.F. Craig and J.B. Kemper, eds., Regulate Stream. Plenum Press.

Gore, J.A., and R.D. Judy. 1981. Predictive models of benthic macroinvertebrate density for use in instream flow studies and regulated flow management. Can. J. Fish. Aquat. Sci. 38:1363-1370.

Gore, J.A., and J.M. Nestler. 1988. Instream flow studies in perspective. Regulated Rivers: Research and Management. Vol. 2:93-101.

Goreman, O.T., and J.R. Karr. 1978. Habitat structure and stream fish communities. Ecology 59(3):507-515.

Grant, J.W.A., and D.L. Kramer. 1990. Territory size as a predictor of the upper limit to population density of juvenile salmonids in streams. Can. J. Fish. Aquat. Sci. 47:1724-1737.

Griffith, J.S., and R. W. Smith. 1993. Use of winter concealment cover by juvenile cutthroat and brown trout in the south fork of the Snake river, Idaho. North American Journal of Fisheries Management 13:823-830.

Hanson, P.C., T.B. Johnson, D. E. Schindler and J. F. Kitchell. 1997. Fish bioenergetics 3.0 for Windows. University of Wisconsin Sea Grant Institute, Madison.

Harris, D.D., W.A. Hubert, and T.A. Wesche. 1992. Habitat use by young-of-year brown trout and effects on weighted usable area. Rivers Vol. 3(2):99-105.

Hawkins, C.P., M.L. Murphy, N.H. Anderson, and M.A. Wilzbach. 1983. Density of fish and salamanders in relation to riparian canopy and physical habitat in streams of the northwestern United States. Can. J. Fish. Aquat. Sci., Vol. 40:1173-1185.

Hayes, J.W., J.D. Stark, and K.A. Shearer. 2000. Development and test of a whole-lifetime foraging and bioenergetics growth model for drift-feeding brown trout. Transactions of the American Fisheries Society 129:316-332.

Heggenes, J. 1988. Physical habitat selection by brown trout (Salmo trutta) in riverine systems. Nordic J. Freshw. Res. 64:74-90.

Heggenes, J. 1988. Effects of short-term flow fluctuations on displacement of, and habitat use by, brown trout in a small stream. Transactions of the American Fisheries Society, Vol.117: 336-344.

Heggenes, J., and T. Traaen. 1988. Downstream migration and critical water velocities in stream channels for fry of four salmonid species. J. Fish. Biol., Vol.32: 717-727.

Heisey, P.G., D. Mathur , and N.C. Magnusson. 1980. Accelerated growth of smallmouth bass in a pumped storage system. Transactions of the American Fisheries Society. 109:371-377.

Hilderbrand, S.G.1974. The relation of drift to benthos density and food level in an artificial stream. Limnol., 24,1742-7.

Hill, J. 1989. The energetic significance of microhabitat use in two stream fishes. Unpublished Ph.D. Dissertation. The University of British Columbia, Vancouver, Canada, 152 p.

Hill, J., and G.D. Grossman. 1993. An energetic model of microhabitat use for rainbow trout and rosyside dace. Ecology 74(3):685-698.

Hauer, F.R., J.A. Stanford, and R. Steinkraus. 1989. The zoobenthos of the lower Flathead River: the effect of Kerr Dam operation. Flathead Lake Biological Station, University of Montana, Polson, MT.

Hobbs, H. H. 1991. Decopoda, p. 823-858. *In* J. H. Thorp and A. P. Covich (Eds). Ecology and classification of North American freshwater invertebrates. Academic Press Inc., California.

Horwitz, R.J. 1978. Temporal variability patterns and the distributional patterns of stream fishes. Ecological Monographs, Vol.48: 307-321.

Hughes, N.F. 1998. A model of habitat selection by drift-feeding stream salmonids at different scales. Ecology 79(1):281-294.

Hughes, N.F. and L.M. Dill 1990. Position choice by drift-feeding salmonids: model test for Arctic grayling (*Thymallus arcticus*) in subarctic mountain streams, interior Alaska. Can. J. Fish. Aquat. Sci. 47:2039-2048.

Hynes, H.B.N. 1970. The ecology of running waters. University of Toronto Press. Canada and America. P.555.

Irvine, J.R. 1985. Effects of Successive Flow Perturbations on Stream Invertebrates. Canadian Journal of Fisheries and Aquatic Sciences. 42:1922-1927.

Irvine, J.R. 1986. Effects of varying discharge on the downstream movement of salmon fry, Oncorhynchus tshawytscha walbaum. J. Fish Biol. Vol. 28: 17-28.

Jenkins, T.M. Jr. 1969. Social structure, position choice and micro-distribution of two trout species (*Salmo trutta* and *Salmo gairdneri*) resident in mountain streams. Anim. Behav. Monogr. 2(2) : 57-123.

Johnston, N.T., C.J. Perrin, P.A. Slaney, and B.R. Ward. 1990. Increased juvenile salmonid growth by whole-river fertilization. Can. J. Fish. Aquat. Sci. 47:862-872.

Jowett, I.G. Date? Flow management in some book? Fix this******

Jowett, I.G. 1992. Models of the abundance of large brown trout in New Zealand rivers. North American Journal of Fisheries Management 12:417-432.

Jowett, I.G., and J. Richardson. 1989. Effects of a severe flood on instream habitat and trout populations in seven New Zealand rivers. New Zealand Journal of Marine and Freshwater Research, Vol. 23: 11-17.

Jowett, I.G., and J. Richardson. 1990. Microhabitat preferences of benthic invertebrates in a New Zealand river and the development of in-stream flow-habitat models for deleatidium spp. New Zealand Journal of Marine and Freshwater Research 24:19-30.

Jowett, I.G., J. Richardson, B.J.F. Biggs, C.W. Hickey, and J.M. Quinn. 1991. Microhabitat preferences of benthic invertebrates and the development of generalized deleatidium spp. habitat suitability curves, applied to four New Zealand rivers. New Zealand Journal of Marine and Freshwater Research Vol. 25:187-199.

Keup, L.E. 1988. Invertebrate fish food resources of lotic environments. Instream Flow Information Paper No. 24. U.S. Fish Wildl. Serv. Biol. Rep. 88(13):1-96.

Kondolf, G.M., and M.G. Wolman. 1993. The sizes of salmonid spawning gravels. Water Resources Research, 29:2275-2285.

Lancaster, J. 1990. Predation and drift of lotic macroinvertebrates during colonization. Occologia, Vol.85: 48-56.

Latterell, J.J. , K. D. Fausch, C. Gowan, S. C. Riley. 1998. Relationship of trout recruitment to snowmelt runoff flows and adult trout abundance in six Colorado Mountain streams. Rivers 6(4):240-250.

Leonard, J.W. 1942. Some observations on the winter feeding habits of brook trout fingerling in relation to natural food organisms present. Transactions of Americans Fisheries Society, Vol.71: 219-227.

Mason, J.C. 1976. Response of underyearling coho salmon to supplemental feeding in a natural stream. Journal of Wildlife Management 40:775-788.

Mason, J.C. and D.W. Chapman 1965. Significance of early emergence, environmental rearing capacity, and behavioral ecology of juvenile coho salmon in stream channels. Journal of the Fisheries Research Board of Canada 22:173-190.

McKinney, T., D.W. Speas, R.S. Rogers, and W.R. Persons. Rainbow trout in a regulated river below Glen Canyon Dam, Arizona, following increased minimum flows and reduced discharge variability. North American Journal of Fisheries Management 21`:216-222.

Milhous, R.T. 1991. Instream flow needs below peaking hydroelectric projects. Pages 163-171 in D.D. David ed., Waterpower 91 Proceedings of the International Conference on Hydropower, Denver, CO. American Society of Civil Engineers.

Moog, O. 1993. Quantification of daily peak hydropower effects on aquatic fauna and management to minimize environmental impacts. Regulated rivers: Research and Management, Vol.8: 5-14.

Morgan, R.P.II, R.E. Jacobsen, S.B. Weisberg, L.A. McDowell, H.T. Wilson. 1991. Effects of flow alteration on benthos macroinvertebrate communities below the Brighton hydroelectric dam. Journal of freshwater ecology, Vol.6(4): 418-429.

Murphy, M.L., J. Heifetz, S.W. Johnson, K.V. Koski, and J.F. Thedinga. 1986. Effects of clear-cut logging with and without buffer strips on juvenile salmonids in Alaskan streams. Can. J. Fish. Aquat. Sci. 43:1521-1533.

Murphy, M.L. and W.R. Meehan 1991. Stream ecosystems. American Fisheries Society Special Publication 19:17-46.

Narf, R.P. 1985. Aquatic insect colonization and substrate changes in a relocated stream segment. Wisconsin department of natural resource, bureau of research, the great lakes entomologist, Vol.18: 84-92.

Nehring, R.B., and R.M. Anderson. 1993. Determination of population-limiting critical salmonid habitats in Colorado streams using the physical habitat simulation system. Rivers Vol. 4(1):1-19.

Neill, L. 1993. Photogrammetric heighting and accuracy. Surveying World. Sept.:42-43.

Northcote, T.G., and G.L. Ennis. 1994. Mountain whitefish biology and habitat use in relation to compensation and improvement possibilities. Reviews in Fisheries Science, 2(4):347-371.

Orth, J.D., 1995. Influence du compariment trophique dans les reponses des populations de poisons aux variations artificielles de debit. Bull. Fr. Peche Piscic. 337/338/339:317-328.

Orth, D.J., and O.E. Maughan. 1982. Evaluation of the incremental methodology for recommending instream flows for fishes. Transactions of the American Fisheries Society Vol. 111:413-445.

Ottaway, E. M. and D. R. Forrest .1983. The Influence of water velocity on the downstream movement of alevins and fry of brown trout, Salmo trutta . J. Fish Biol.; 23(2):221-227.

Perry, S.A. and W.B. Perry. 1986. Effects of experimental flow regulation on invertebrate drift and stranding in the Flathead and Kootenai rivers, Montana, USA. Hydrobiologia, Vol.134: 171-182.

Poff, N.L., J.D. Allan, M.B. Bain, J.R. Karr, K.L. Prestegaard, B.D. Richter, R.E. Sparks, and J.C. Stromberg. 1997. The natural flow regime a paradigm for river conservation and restoration. BioScience Vol. 47(11):769-784.

Power, M.E. 1984. Habitat quality and the distribution of algae-grazing catfish in a Panamanian stream. Journal of Animal Ecology 53:357-374.

Power, M. E., Matthews, W.J., and Stewart, A.J. 1985. Grazing minnows, piscivorous bass, and stream algae: Dynamics of a strong interaction. Ecology 66(5):1448-1456.

Power, M.E., A. Sun, G. Parker, W.E. Dietrich, and J.T. Wootton. 1995. Hydraulic food-chain models: an approach to the study of food-web dynamics in large rivers. Bioscience 45(3): 159-167.

Power, M.E., R.J. Stout, C.E. Cushing, P.P. Harper, F.R. Hauer, W.J. Matthews, P.B. Moyle, B. Statzner, and I.R. Wais De Badgen. 1988. Biotic and abiotic controls in river and stream communities. J. N. Am. Benthol. Soc. 7(4): 456-479.

Quinn, J.M., and C.W. Hickey. 1994. Hydraulic parameters and benthic invertebrate distribution in two gravel-bed New Zealand rivers. Freshwater Biology 32:489-500.

R2 Resource Consultants, Inc.1995. Assessment of fish habitat impacts in the Lower Flathead River from Kerr dam operations proposed by the Montana Power Company and interior 4(e) conditions. Final Report. Redmond, WA.

R2 Resource Consultants, Inc.2001. Kerr hydroelectric project Lower Flathead River ramping rate study. Draft Final Report. Redmond, WA.

Rader, R.B. 1997. A functional classification of the drift: traits that influence invertebrate availability to salmonids. Can. J. Aquat. Sci. 54:1211-1234.

Raleigh, R.F., W.J. Miller, and P.C. Nelson. 1986. Habitat suitability index models and instream flow suitability curves: Chinook salmon. U.S. Fish and Wildlife Service Biological Report 82(10.122).

Ryder, R.A., and S.R. Kerr. 1989. Environmental priorities: placing habitat in hierarchic perspective. Pages 2-12 in C.D. Levings, L.B. Holtby, and M.A. Henderson, eds., Proceedings of the National Workshop on Effects of Habitat Alteration on Salmonid Stocks. Can. Spec. Publ. Fish. Aquat. Sci. 105.

Sabo, M.J. and D. J. Orth. 1994. Temporal variation in microhabitat use by age-0 smallmouth bass in the North Anna River, Trans. Am. Fish. Soc.; 123(5):733-746. 1994.

Scheildegger, K.J., and M.B. Bain. 1995. Larval fish distribution and microhabitat use in free-flowing and regulated rivers. Copeia 1:125-135.

Schirvell, C.S., and R.G. Dungey. 1983. Microhabitats chosen by brown trout for feeding and spawning in rivers. Transactions of the America Fisheries Society 112:355-367.

Schlosser, I.J. 1982. Trophic structure, reproductive success, and growth rate of fishes in a natural and modified headwater stream. Can. J. Fish. Aquat. Sci. 39:968-978.

Schlosser, I. J. 1987. The role of predation in age-and size-related habitat use by stream fishes. Ecology 68(3):651-659.

Sheldon, Andrew. 1984. Colonization dynamics of aquatic insects. Pages 401-429 in V.H. Resh and D.M. Rosenberg, eds. Ecology of Aquatic Insects. Praeger, N.Y.

Slaney, P.A., and T.G. Northcote. 1974. Effects of prey abundance on density and territorial behavior of young rainbow trout (Salmo gairdneri) in laboratory stream channels. J. Fish. Res. Board Can. 31:1201-1209.

Smith, J.J., and H.W. Li. 1983. Energetic factors influencing foraging tactics of juvenile steelhead trout, Salmo gairdneri. Pages 173-180 in D.L.G. Noakes, eds., Predators and prey in fishes. The Hague.

Smith, R.W., and J.S. Griffith. 1994. Survival of rainbow trout during their first winter in the Henrys fork of the Snake river, Idaho. Transactions of the American Fisheries Society 123:747-756.

Statzner, B., and B. Higler. 1986. Stream hydraulics as a major determinant of benthic invertebrate zonation patterns. Freshwater Biology 16:127-139.

Statzner, B., J.A. Gore, and V.H. Resh. 1988. Hydraulic stream ecology: observed patterns and potential applications. J. N. Am. Benthol Soc. 7(4):307-360.

Thorne, C.R., R.D. Hey, and M.D. Newson. 1997. Applied Fluvial Geomorphology for River Engineering and Management. John Wiley and Sons, NY.

Travnichek, V.H., M.B. Bain, and M.J. Maceina. 1995. Recovery of a warmwater fish assemblage after the initiation of a minimum-flow release downstream from a hydroelectric dam. Transaction of the American Fisheries Society 124:836-844.

Trimble.21 Nov. 1998. Products page. http://www.trimble.com/

USFWS 1979 United States Fish and Wildlife Service, 1987. Curve file data. National Ecology Research Center, Ft. Collins, CO.

Walton Jr., O.E. 1978. Substrate attachment by drifting aquatic insect larvae. Ecology 59(5):1023-1030.

Ward, J.V. 1989. The four-dimensional nature of lotic ecosystems. J. N. Am. Benthol. Soc. 8(1):2-8.

Ware, D.M. 1982. Power and evolutionary fitness of teleosts. Can. J. Fish. Aquatic Sci. 39:3-13.

Warren, C.E., J.H. Wales, G.E. Davis, and P. Doudoroff. 1964. Trout production in an experimental stream enriched with sucrose. Journal of Wildlife Management 28:617-660.

Waters, T.F. 1964. Recolonization of denuded stream bottom areas by drift. Transactions Am. Fish. Soc. Pp.311-315.

Waters, B.F. 1976. A methodology for evaluating the effects of different streamflows on salmonid habitat. Pages 254-266 in Osburn, and J.F.B. Allman, eds., Instream Flows. American Fisheries.

Waters, T.F. 1982. Annual production by a stream brook charr population and by its principal invertebrate food. Env. Biol. Fish. Vol. 7:165-170.

Webb, P.W. 1975. Hydrodynamics and energetics of fish propulsion. Bull. Fish. Res. Board Canada, 190:1-158.

Williams, D.D. 1980. Temporal patterns in recolonization of stream benthos. Arch. Hydrobiol, Vol.90(1): 56-74.

Wilzbach, M.A. 1985. Relative roles of food abundance and cover in determining the habitat distribution of stream-dwelling cutthroat trout (Salmo clarki). Can. J. Fish. Aquat. Sci. 42:1668-1672.

Wilzback, M.A., and J.D. Hall. 1985. Prey availability and foraging behavior of cutthroat trout in an open and forested section of stream. Verh. Internat. Verein. Limnol. 22:2516-2522.

Appendix E: Map of Lower Klamath Drift Sampling Locations.